



5-2014

Fuel Economy and Greenhouse Gas Reduction Potentials of Advanced Combustion Modes in Light-Duty Vehicles: A Well-to-Wheel Analysis using Vehicle Systems Simulations with Experimental Engine Data

Scott James Curran

University of Tennessee - Knoxville, scurran@utk.edu

Follow this and additional works at: https://trace.tennessee.edu/utk_graddiss

 Part of the [Other Engineering Commons](#)

Recommended Citation

Curran, Scott James, "Fuel Economy and Greenhouse Gas Reduction Potentials of Advanced Combustion Modes in Light-Duty Vehicles: A Well-to-Wheel Analysis using Vehicle Systems Simulations with Experimental Engine Data. " PhD diss., University of Tennessee, 2014.
https://trace.tennessee.edu/utk_graddiss/2757

This Dissertation is brought to you for free and open access by the Graduate School at TRACE: Tennessee Research and Creative Exchange. It has been accepted for inclusion in Doctoral Dissertations by an authorized administrator of TRACE: Tennessee Research and Creative Exchange. For more information, please contact trace@utk.edu.

To the Graduate Council:

I am submitting herewith a dissertation written by Scott James Curran entitled "Fuel Economy and Greenhouse Gas Reduction Potentials of Advanced Combustion Modes in Light-Duty Vehicles: A Well-to-Wheel Analysis using Vehicle Systems Simulations with Experimental Engine Data." I have examined the final electronic copy of this dissertation for form and content and recommend that it be accepted in partial fulfillment of the requirements for the degree of Doctor of Philosophy, with a major in Energy Science and Engineering.

Joshua S. Fu, Major Professor

We have read this dissertation and recommend its acceptance:

Robert M. Wagner, David K. Irick, Claudia J. Rawn

Accepted for the Council:

Carolyn R. Hodges

Vice Provost and Dean of the Graduate School

(Original signatures are on file with official student records.)

**Fuel Economy and Greenhouse Gas Reduction Potentials of
Advanced Combustion Modes in Light-Duty Vehicles:
A Well-to-Wheel Analysis using Vehicle Systems Simulations
with Experimental Engine Data**

**A Dissertation Presented for the
Doctor of Philosophy
Degree
The University of Tennessee, Knoxville**

**Scott James Curran
May 2014**

ACKNOWLEDGEMENTS

Special acknowledgments to Gurpreet Singh, Ken Howden, Leo Breton, Kevin Stork and Steve Przesmitzki of the United States Department of Energy Vehicle Technologies Office for funding a significant portions of the research in this dissertation. The contributions from the researchers in the Fuels, Engines and Emissions Research Center at Oak Ridge National Laboratory include Dr. Robert Wagner, Dr. Zhiming Gao, Dr. Jim Szybist, Vitaly Prikhodko, Dr. John Storey, Dr. Derek Splitter, Dr. Jim Parks and Dr. David Smith. The contributions from the researchers in at the University of Wisconsin include Prof. Rolf Reitz, Dr. Sage Kokjohn and Dr. Reed Hanson. A special thanks to Dr. Robert Wagner and Dr. Johnney Green and ORNL management who supported this endeavor. The guidance provided by the committee, Prof. Joshua Fu, Dr. Robert Wagner, Prof. David Irick, Prof. Claudia Rawn and Prof. Lee Riedinger is also acknowledged. The Bredesen Center staff and students especially Prof. Lee Riedinger, Dr. Mike Simpson, Wanda Davis and Ben Allen have all provided a welcome and great experience. Special thanks to my supportive family, in particular the patience and encouragement of wife, Amy along with my father-in-law, Jack Clark, my mother and River.

ABSTRACT

Vehicle fuel efficiency and emissions regulations are driving a radical shift in the need for high efficiency powertrains along with control of criteria air pollutants and greenhouse gases. High efficiency powertrains including vehicle electrification, engine downsizing, and advanced combustion concepts all seek to accomplish these goals. Homogeneous charge compression ignition (HCCI) concepts have been proposed have not been able to demonstrate the controllability to operate over a sufficient engine speed and load range to make it practical for implementation in production vehicles. In-cylinder blending of gasoline and diesel to achieve reactivity controlled compression ignition (RCCI) has been shown to reduce NO_x and PM emissions while maintaining or improving brake thermal efficiency as compared to conventional diesel combustion (CDC). The RCCI concept has an advantage over many advanced combustion strategies in that the fuel reactivity can be tailored to the engine speed and load allowing stable low-temperature combustion to be extended over more of the light-duty drive cycle load range. The potential for advanced combustion concepts such as RCCI to reduce drive cycle fuel economy and emissions is not clearly understood and is explored in this research by simulating the fuel economy and emissions for a multi-mode RCCI-enabled vehicle operating over a variety of U.S. drive cycles using experimental engine maps for multi-mode RCCI, CDC and a 2009 port-fuel injected (PFI) gasoline engine. Simulations are completed assuming a conventional mid-size passenger vehicle with an automatic transmission. RCCI fuel economy simulation results are compared to the same vehicle powered by a representative 2009 PFI gasoline engine over multiple drive cycles. Engine-out drive cycle emissions are compared to CDC and observations regarding relative gasoline and diesel tank sizes needed for the various drive cycles are also summarized. The well-to-wheel energy and greenhouse gas emissions from these drive cycle simulations running various amounts of biofuels are examined and compared to the state-of-the-art in conventional, electric and hybrid powertrains.

TABLE OF CONTENTS

Introduction	1
Methodology.....	5
Laboratory Setup	5
Vehicle Systems Simulations.....	10
Well-to-wheel Modeling	11
Relevance	12
Implications	12
References	15
CHAPTER I Reactivity controlled compression ignition combustion on a multicylinder light-duty diesel engine	18
Abstract.....	19
1 Introduction.....	19
2 Experimental Setup	22
3 Fuels	23
4 Experimental Procedure	23
5 Results	25
5.1 Comparison of Peak BTE with CDC	25
5.2 Engine control parameters.....	26
5.2.1 Brake Thermal Efficiency	28
5.2.2 NO _x emissions.....	28
5.2.3 HC and CO Emissions	29
5.2.4 Filter Smoke Number	29
Conclusions.....	30
Disclaimer	31
Acknowledgments	31
References.....	32
Appendix 1	34
CHAPTER II Reactivity controlled compression ignition drive cycle emissions and fuel economy estimations using vehicle systems simulations.....	49
Abstract.....	50
1 Introduction.....	51
2 Methodology	54
2.1 Experimental Setup	54
2.2 RCCI Engine Mapping	55
3 Vehicle Systems Simulations	57
4 RESULTS.....	58
4.1 Drive Cycle Coverage.....	58
4.2 Modeled Fuel Economy	59
4.3 Modeled Emissions.....	59
4.2 Comparison to PFI Fuel Economy	59
5 SUMMARY/CONCLUSIONS.....	60
Disclaimer	60

Acknowledgments	61
References	62
Appendix 2.1	65
Appendix 2.2	84
CHAPTER III Reactivity Controlled Compression Ignition Drive Cycle Emissions and Fuel Economy Estimations Using Vehicle Systems Simulations with E30 and ULSD	88
Abstract	89
Introduction	90
Methodology	93
Experimental setup	94
RCCI Engine Mapping Results	95
Vehicle Systems Simulations	96
Drive cycles	97
Results	98
0-60 mph Performance	98
Modeled PFI Fuel Economy for Mid-Size Passenger Sedans	98
Drive Cycle Fuel Use for RCCI/CDC	98
Fuel Economy Comparisons	99
Modeled Drive Cycle Engine-Out Emissions Trends	99
Summary	99
Conclusions	100
References	101
Disclaimer	103
Acknowledgments	103
Appendix 3.1	104
Appendix 3.2	116
CHAPTER IV Well-to-wheel comparison of multi-mode advanced combustion strategies and other advanced light-duty vehicle technologies	120
Abstract	121
1. Introduction	122
2. Methodology	126
3.1 RCCI experiments leading to map	126
3.2 Vehicle Systems simulations leading to RCCI fuel economy estimates	127
3.3 Benchmarking simulations to actual data	128
3.4 GREET modeling using fuel economy simulation results	129
3.5 Electricity generation in GREET including future CO ₂ regulations	130
3.6 Modifying GREET for dual fuel operation	131
4. Results	131
5. Discussion	132
6. Conclusions	133
7. Disclaimer	133
8. Acknowledgments	133
References	135

Appendix 4.1	139
Appendix 4.2	149
Conclusion and Future Studies.....	153
VITA.....	155

LIST OF TABLES

Table 1. Engine specifications	8
Table 2. Diesel injector specifications	8
Table 3. Engine specifications	8
Table 4. Engine specifications	34
Table 5. Fuel Properties.....	34
Table 6. Comparison of RCCI and CDC at 2600rev/min, 6.9bar BMEP	35
Table 7. Experimental engine specifications.....	65
Table 8. Experimental diesel injector specifications.....	65
Table 9. Experimental PFI injector specifications	65
Table 10. Experimental fuel properties	66
Table 11. Multi-mode RCCI drive cycle performance.....	66
Table 12. Drive cycle fuel improvements with multi-mode RCCI operation.....	67
Table 13. Modeled emissions reductions compared with CDC operation (number with a plus sign in red indicates increases).....	67
Table 14. Multi-mode RCCI fuel economy compared with downsized PFI	68
Table 15. B20 Map Performance	84
Table 16 B20 Map Emissions	86
Table 17 GM 1.9 L CIDI Base Configuration for E30 RCCI Experiments.....	104
Table 18 Diesel injector specifications for E30 RCCI Experiments	104
Table 19 Port-fuel injector specifications for E30 RCCI Experiments	104
Table 20 Fuel specification for E30 and ULSD	105
Table 21 0-60 MPH Acceleration Modeling.....	105
Table 22 RCCI drive cycle coverage and amount of diesel fuel consumption over the drive cycle simulations.....	106
Table 23 Fuel economy improvements for RCCI/CDC operation as compared to CDC and PFI baselines	106
Table 24 RCCI/CDC missions results compared to CDC baseline	106
Table 25. E30 Map - Performance	116
Table 26 E30 Map Emissions	118
Table 27 IPCC GWP potentials [24].....	139
Table 28 E30/ULD RCCI Multi-Mode Results	139
Table 29 Gasoline/B20 RCCI Multi-mode Results	139
Table 30. Benchmarking UDDS and HWFET fuel economy	140
Table 31 Vehicle Systems simulation fuel economies used for WTW analysis.....	140
Table 32 Dual fuel PFI and DI fuel economies used in GREET for analysis.....	141
Table 33. Nissan Leaf Modeling Results.....	150

LIST OF FIGURES

Figure 1. Dual-Fuel RCCI Injection Strategy.....	2
Figure 2. Modified RCCI pistons (schematic right, pictures left).....	6
Figure 3. Modified intake manifold allowing PFI gasoline injection	7
Figure 4. Experimental schematic.....	7
Figure 5. Modified intake manifold allowing PFI gasoline injection	9
Figure 6. Multi-mode strategy for various drive cycles.	11
Figure 7. Conceptual layout of well-to-wheels analysis from experimental data.	12
Figure 8. Experimental schematic.....	36
Figure 9. Systematic procedure for obtaining RCCI operating points	37
Figure 10. Speed and load range of RCCI operation examined	38
Figure 11. Cylinder pressure traces for RCCI and CDC at 2600 rev/min.....	39
Figure 12. Heat release traces for RCCI and CDC at 2600 rev/min.....	40
Figure 13. Diesel SOI and premixed ratio as a function of BMEP.....	41
Figure 14. Exhaust temperatures for RCCI and CDC at 2000 rev/min over a load sweep from 2.0bar to 6.0bar BMEP.....	42
Figure 15. BTE premixed ratio, diesel SOI timing, and combustion phasing (MFB50) vs. BMEP for 2000 rev/min	43
Figure 16. BTE vs. BMEP for RCCI and CDC for 1500, 2000 and 2600 rev/min	44
Figure 17. NO _x as a function of BMEP for CDC and RCCI for maximum BTE operation (various engine speeds for maximum BTE)	45
Figure 18. NO _x vs. BTE for RCCI and CDC for all engine speed and loads	46
Figure 19. HC emissions for RCCI and CDC vs. BMEP for all engine speeds and loads	47
Figure 20. CO emissions for RCCI and CDC vs. BMEP	48
Figure 21. Dual-fuel RCCI injection strategy for experiments.	69
Figure 22. Experimental ORNL multi-cylinder RCCI engine.	70
Figure 23. Experimental RCCI map with UDDS drive cycle point overlain.....	71
Figure 24. Experimental CDC map with stock pistons	72
Figure 25. Difference in RCCI and CDC BTE.	73
Figure 26. Experimental RCCI NO _x	74
Figure 27. RCCI engine out NO _x compared with CDC (grey circles).....	75
Figure 28. Experimental RCCI HC emissions.	76
Figure 29. Experimental RCCI exhaust temperature.	77
Figure 30. Experimental RCCI premixed ratio.	78
Figure 31. RCCI coverage of various drive cycles investigated with 1 HZ engine speed and load points overlain.	79
Figure 32. Drive cycle fuel economy for PFI, CDC, and multi-mode RCCI operation.....	80
Figure 33. Modeled exhaust temperatures for CDC and RCCI over the UDDS.....	81
Figure 34. FTP (UDDS) fuel economy for PFI engines of various displacement with the modeled RCCI (red star) and modeled PFI data (yellow star).....	82

Figure 35. HWFET fuel economy for PFI engines of various displacement with the modeled RCCI (red star) and modeled PFI data (yellow star).	83
Figure 36 Dual-Fuel RCCI Injection Strategy for E30 RCCI Experiments.....	107
Figure 37 ORNL Multi-Cylinder RCCI Engine for E30 RCCI Experiments	107
Figure 38 RCCI Map with E30 and ULSD with 32 data points	108
Figure 39 RCCI premixed ratio as a function of engine speed and load for E30 RCCI Experiments	108
Figure 40 RCCI BTE as a function of engine speed and load for E30 RCCI Experiments.....	109
Figure 41 . CDC BTE as a function of engine speed and load for E30 RCCI Experiments.....	109
Figure 42 . RCCI NOX with ppm labeled contours.....	110
Figure 43 . CDC NOX with areas over 105 ppm not colored with ppm labeled contours	110
Figure 44. E30 Multi-mode RCCI/CDC map	111
Figure 45. Multi-mode E30 RCCI/CDC map coverage regulatory drive cycles used for the drive cycle simulations	111
Figure 46 . Simulated time for 0-60 mph acceleration.....	112
Figure 47 Modeled fuel economy results for 2009 PFI engines with transmissions optimized for fuel economy as a function of displacement.....	112
Figure 48 Fuel consumption modeling over the UDDS	113
Figure 49 Engine efficiency as a function of power demand over the UDDS....	113
Figure 50. Fuel economy results for all PFI engines, CDC only operation with the base CIDI engine and RCCI/CDC multi-mode operation	114
Figure 51. Modeled fuel economy results compared to actual vehicle dynamometer data using EPA and ORNL data.	114
Figure 52. Modeled RCCI/CDC exhaust temperatures compared to CDC operation under the hot-start UDDS cycle.	115
Figure 53. US EPA light-duty dynamometer driving cycles.....	142
Figure 54. WTW fuel pathway.....	142
Figure 55. Drive cycle coverage in terms of engine speed and load plots for RCCI multi-mode map	143
Figure 56. Vehicle Systems simulations for PFI, CDC and RCCI multi-mode...	144
Figure 57. Fuel economy penalty for vehicle mass using a 2.2L SIDI engine conventional gasoline baseline.....	145
Figure 58. US Electrical Generation Mix	145
Figure 59. Total and vehicle energy use	146
Figure 60. Total and vehicle petroleum use	146
Figure 61. Total and vehicle GHG emissions.....	147
Figure 62. Petroleum energy use, with and without biofuels.....	147
Figure 63 GHG emissions, with and without biofuels.....	148
Figure 64 Nissan Leaf Model	149

List of Abbreviations

AFR.....	Air to Fuel Ratio
AKI.....	Anti-Knock Index
BEV.....	Battery Electric Vehicle
BMEP.....	Brake Mean Effective Pressure
bsXX.....	Brake Specific Emissions (XX = species)
BTE.....	Brake Thermal Efficiency
BXX.....	Biodiesel blend (XX = % biodiesel)
CAD.....	Crank Angle Degrees
CAFÉ.....	Corporate Average Fuel Economy
CCS.....	Carbon Capture and Storage
CFD.....	Computational Fluid Dynamics
CIDI.....	Compression Ignition Direct Injection
CLD.....	Chemiluminescence Detector
CN.....	Cetane Number
COV.....	Coefficient of Variance
DBTDC.....	Degrees Before Top Dead Center
DCAT.....	Drivven Combustion Analysis Toolkit
DI.....	Direct Injection
DOE.....	Department of Energy
DPF.....	Diesel Particulate Filter
EGR.....	Exhaust Gas Recirculation
EPA.....	Environmental Protection Agency
EXX.....	Biodiesel blend (XX = % biodiesel)
FID.....	Flame Ionization Detector
FSN.....	Filter Smoke Number
FTP.....	Federal Test Procedure
GGE.....	Gasoline Gallon Equivalent
GHG.....	Greenhouse Gas
REET	Greenhouse Emissions and Energy Use in Transportation
GTE.....	Gross Thermal Efficiency
GWP	Global Warming Potential
HCCI.....	Homogenous Charge Compression Ignition
HECC.....	High Efficiency Clean Combustion
HWFET.....	Highway Fuel Economy Test
IMEP.....	Indicated Mean Effective Pressure
IPCC.....	Intergovernmental Panel on Climate Change
ITE.....	Indicated Thermal Efficiency
LHV.....	Lower Heating Value
LNT.....	Lean NO _x Trap
LTC.....	Low Temperature Combustion
MCE.....	Multi-Cylinder Engine
MFB50.....	Mass Fraction Burned, 50%

MON.....	Motor Octane Number
MPRR.....	Maximum Pressure Rise Rate
N.....	Rotational Speed
N _r	Number of Crank Revolutions Per Stroke
NETL	National Energy Technology Laboratory
NHTSA.....	National highway Safety Administration
NMOG.....	Non-Methane Organic Gases
NYC.....	New York City Cycle
OEM.....	Original Equipment Manufacturer
ORNL.....	Oak Ridge National Laboratory
P.....	Pressure
PCCI.....	Premixed Charge Compression Ignition
PFI.....	Port Fuel Injection
PMD.....	Paramagnetic Detector
PRR.....	Pressure Rise Rate
PTW.....	Pump-to-Wheel
QLHV.....	Lower Heating Value
RCCI.....	Reactivity Controlled Compression Ignition
R _p	Premixed Ratio
RON.....	Research Octane Number
SCE.....	Single Cylinder Engine
SCOTE.....	Caterpillar Single Cylinder Oil Test Engine
SCR.....	Selective Catalytic Reduction
SMPS.....	Scanning Mobility Particle Sizer
SOI.....	Start of Injection
STEM.....	Science Engineering Technology and Mathematics
T&D.....	Transmission and Distribution
UDDS	Urban Dynamometer Driving Schedule
ULSD.....	Ultra-Low Sulfur Diesel
UTG.....	Unleaded Test Gasoline
UTK.....	University of Tennessee, Knoxville
UW.....	University of Wisconsin
VGT.....	Variable Geometry Turbocharger
VSA.....	Variable Swirl Actuator
WTP.....	Well-to-Pump
WTW.....	Well-to-Wheels
VTO.....	Vehicle Technologies Office

INTRODUCTION

The United States Department of Energy (DOE), Vehicle Technologies Office's (VTO) mission is to develop more energy-efficient and environmentally friendly highway transportation technologies that will enable the United States to use significantly less petroleum and reduce greenhouse gas emissions and criteria air pollutants [1]. Fuel efficiency improvements and petroleum displacement are the overarching goals of the VTO and within these research activities, resolving the interdependent emissions challenges from high efficiency engines is important not only due to a regulatory and market barrier standpoint, but also in terms of total engine system efficiency.

Engine system efficiency includes not only the fuel energy required for the production of motive or shaft power, but also the fuel penalties associated with exhaust aftertreatments. For diesel engines, these fuel penalties include fuel regeneration of diesel particulate filters (DPF) as well as fuel regeneration of lean NO_x traps (LNT), or reductant addition for selective catalytic reduction (SCR) systems. The DOE VTO Advanced Combustion Engine research and development program's strategic goals are to reduce petroleum dependence by removing critical technical barriers to mass commercialization of high-efficiency, emissions-compliant internal combustion engine powertrains in passenger and commercial vehicles [2].

Improvements in engine efficiency and engine systems efficiency through advanced combustion strategies is an important pathway to this goal. For advanced combustion strategies to be able to meet these goals, their effectiveness over driving cycles [3] will have to be determined.

In-cylinder blending of gasoline and diesel to achieve reactivity controlled compression ignition (RCCI) has been shown to reduce NO_x and PM emissions while maintaining or improving brake thermal efficiency as compared to conventional diesel combustion (CDC). The ability to control the percent premixed low reactivity fuel along with the timing and number of injections of the direct injected high reactivity fuel allows for not only reactivity stratification but also temperature and equivalence ratio stratification in the cylinder providing further control of combustion phasing and cylinder pressure rise rate. The RCCI concept as shown in Fig 1. has an advantage over many advanced combustion strategies [4 – 11] in that the fuel reactivity can be tailored to the engine speed and load allowing stable low-temperature combustion to be extended over more of the light-duty drive cycle load range [12].

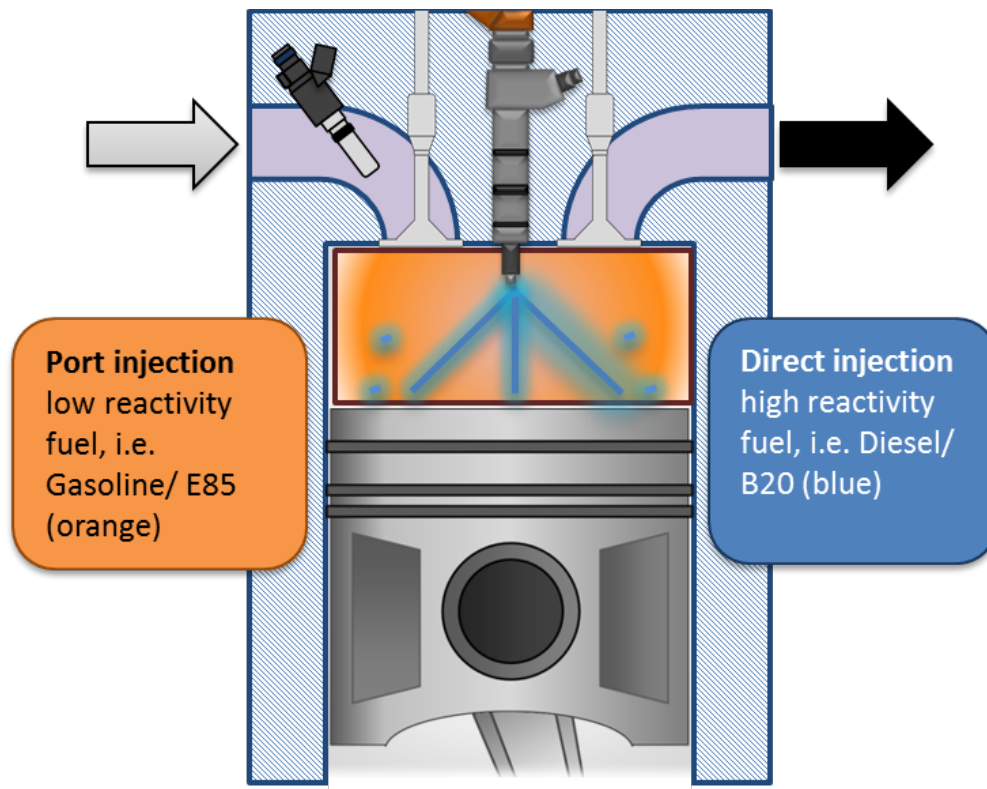


Figure 1. Dual-Fuel RCCI Injection Strategy

Previous computational fluid dynamics (CFD) modeling and single cylinder engine (SCE) results have demonstrated high gross thermal efficiencies (GTE) with ultra-low NO_x and soot emissions. Thorough reviews of RCCI SCE experiments and CFD modeling advances can be found in papers by Kokjohn, Splitter, Hanson and Reitz [12-16].

Previous experiments have investigated the translational effects of taking CFD modeling and single cylinder engine experiments to multi-cylinder engines (MCE) on efficiency, emissions, and controls [17-23]. These effects include the behavior of real turbomachinery, effects of real EGR, cylinder to cylinder imbalances and swirl. Despite the translational effects, MCE RCCI has been shown to be capable of diesel like efficiency at lower engine loads and greater than diesel efficiency at higher engine loads with an order of magnitude reduction in engine-out NO_x as compared to CDC. Previous experiments have shown the benefits of increased control over the combustion process allowed by RCCI operation on extending the operating range of low temperature combustion (LTC) compared to diesel premixed charge compression ignition (PCCI) on a multi-cylinder light-duty compression ignition engine [19, 20].

To date there have not been any published studies that investigate the potential vehicle fuel economy improvements that RCCI could allow. Previous studies by Curran et al. [19, 20] looked at using the Fuels Working group's ad-hoc modal points [7] to estimate drive cycle emissions with RCCI as compared to conventional diesel combustion. These modal points are representative of key areas of the federal drive testing protocol (FTP) and have weighting factors attached to them linked to the amount of drive cycle spent at similar conditions. That work showed that the ability to obtain noise constrained RCCI operation over all of the ad-hoc modal points was dependent on the fuels used. The light-duty MCE experiments showed that the hard acceleration modal point of 2600 RPM, 8.8 bar BMEP was not obtainable with a 46 Cetane ULSD and certification gasoline with an RON of 96 (UTG-96) [20] while adhering to a cylinder pressure rise rate limit of 10bar/deg. A follow-up study showed that the 2600 RPM, 8.8 bar BMEP point was achievable with RCCI using E85 and ULSD [19]. The results of the RCCI modal point studies showed significant weighted composite NO_x reductions (~66%) were made possible with RCCI operation as compared to CDC. The results also showed significant increases in engine out HC and CO emissions resulted from RCCI operation. The RCCI modal point studies only examined estimated drive cycle emissions and did not attempt to apply the weighting factors to fuel economy improvements.

In the United States, the U.S. Environmental Protection Agency (EPA) regulates emissions based on federal drive cycle compliance [3]. There are a number of EPA dynamometer driving cycles which attempt to take into account the real world driving conditions seen with light-duty passenger vehicles. If the engine cannot be operated in an advanced combustion over the entire speed and load range demanded by the drive-cycle in question, then the engine would have to operate in a multi-mode strategy in which the engine would switch to conventional combustion when engine power demands cause the engine to operate outside of the advanced combustion speed and load operating range. There have been a number of studies examining the potential for multi-mode operation with diesel engine baselines [24, 25]. For LTC/CDC multi-mode operation, the engine switches to CDC for areas of the engine map that fell outside LTC region. The need for multi-mode operation has implications for the needs of the aftertreatment system to be able to meet stringent federal emissions standards over the prescribed drive cycles, namely for NO_x control if the engine has to switch to CDC mode for higher loads in regions of the map that produce high amounts of NO_x.

It is difficult to draw conclusions on drive cycle fuel economy and emissions performance for combustion strategies in the development stage which only have demonstrated a limited number of steady state operating points. Vehicle systems simulation tools such as Autonomie developed by Argonne National Laboratory for the Department of Energy can be used to simulate

vehicle operation using model based simulations [26]. The simulations use performance based measurements including fuel consumption and exhaust properties such as emissions and temperature which are tabulated allowing for the generation of interpolated response surfaces over the entire operating range of the engine maps. Previous work by Gao et al. has demonstrated the use of steady state engine maps in transient drive cycle simulations [27, 28]. Previous work by Gao has examined this type of simulation with multi-mode advanced combustion steady state engine data for engine performance and emissions modeling [28].

Initial drive cycle performance modeling using vehicle systems simulations using engine maps derived from experimental data in Curran and Gao [29] showed multi-mode operation RCCI/CDC had the potential to offer greater than 15% fuel economy improvement over representative 2009 gasoline PFI baselines over many light-duty driving cycles [30]. RCCI fuel economy improvements were observed despite lack of complete drive cycle coverage. These simulations were performed on the same engine being investigated in this study using certification grade gasoline and B20 (20% biodiesel, 80% diesel) for the DI fuel. The results showed how much of an effect multi-mode operation can have on engine out NO_x emissions depending on the amount of the drive cycle coverage that RCCI operation can allow. Modeled drive cycle emissions results showed between a 17% and 21% reduction in NO_x with multi-mode RCCI as compared to diesel only operation. If an engine has to switch to CDC operation during high engine loads, the engine out NO_x will be very high and quickly can degrade the NO_x reduction potential of RCCI. Fuel usage over the drive cycles showed that nearly equal amounts of gasoline and diesel fuel would most likely needed be carried on board for RCCI multi-mode operation. During RCCI only operation fuel usage was found to be between 57% and 69% gasoline.

The ultimate goals of developing high efficiency, low emissions combustion concepts are to improve fuel economy and to reduce total greenhouse gas emissions and life-cycle energy use on a well-to-wheels basis (WTW). A WTW energy and emissions analysis was used to make a direct comparison between the total energy costs and emissions of the different vehicle technologies taking into account fuel cycle aspects. This study takes advantage of the WTW analysis tool known as the Greenhouse Gases, Regulated Emissions and Energy Use in Transportation (GREET) model developed for the U.S. Department of Energy by Argonne National Laboratory. The total energy for each scenario by type as well as GHG emissions and criteria air pollutants are estimated to make a complete comparison which is important for evaluating the total energy and emissions of powertrains that use energy produced off-board such as electric vehicles which have zero tailpipe emissions.

The GREET model used for this proposed study is designed for WTW analysis for transportation systems and as such has a backbone of stationary power calculations to accurately account for electricity's role in transportation, including upstream emissions for electrical power generation as well as assumptions and data for the fossil and biofuel pathways. GREET [32] is a Microsoft Excel-based calculation tool that has simulation values for emissions factors and energy use for stationary power generation to more accurately determine life-cycle criteria and GHG emissions and energy use for mobile applications. For both stationary and transportation use there are default electricity generation mixes for the US regions as well as user-defined mixes. The mixes allow inputs for percent of electricity generated by residual oil, natural gas, coal, nuclear, biomass, and others [33]. The latter category is broken down into: hydroelectric, wind, solar photovoltaic, and undefined others.

Though previous studies have compared the WTW energy use and GHG emissions of both conventional advanced vehicle powertrains such as fuel cells, hybrid, plug-in hybrid and electric vehicles, no studies have examined the potential for advanced combustion concepts with either conventional or biofuels. To be able to complete a well-to-wheel analysis for advanced combustion concepts, emissions factors and fuel economy will need to be first determined through actual vehicle data or from drive cycle simulations as proposed here.

Methodology

Laboratory Setup

The engine used for this study is a modified 2007 General Motors 4 cylinder 1.9L turbocharged diesel engine. The base engine has a rated power of 110 kW and a rated torque of 315 Nm. The original equipment manufacturer (OEM) pistons were replaced with pistons modified for RCCI. The RCCI modified piston bowl geometry was designed for RCCI using CFD modeling by UW as shown in Fig. 2. The piston design is based on a heavy duty piston and minimizes the surface area of the piston to minimize heat transfer losses and also results in a lowered compression from 17.1 in the OEM configuration to 15.1 to allow for higher load operation while maintaining reasonable pressure rise rate limits. More information about the piston design can be found in the paper by Hanson et al [23].

The diesel injection system and variable geometry turbo charger (VGT) were left in production form. The intake manifold was modified to incorporate extended tip narrow spray angle PFI injectors for the gasoline supply. The intake manifold was modified to allow the PFI injectors to spray directly into the non-swirl actuated intake port of the engine. The gasoline PFI injectors at cylinders 2, 3 and 4 were positioned similarly to traditional PFI installations, however, the

position of the cam driven high pressure fuel pump necessitated the installation location of the PFI injector for cylinder 1 to be on top of the intake manifold and aimed at the intake port as shown in Fig. 3. This was preferred rather than modifying the high-pressure fuel pump for the diesel fuel injection system since cylinder 1 is located at the end of the intake manifold and the PFI injector has a narrow spray angle such that the fuel should get into the port without much mass transfer to the other cylinders. To help ensure fuel spray into the cylinder, an extended tip narrow spray angle Multec® 3.5 PFI injector from Delphi Automotive Systems was used. The fuel supply pressure for the gasoline injectors was 380 kPa. The original equipment manufacturer (OEM) DI diesel injectors were used for this study. The specifications for the DI diesel injectors and the PFI gasoline injectors are provided in Tables 2 and 3, respectively. Figure 4 shows the overall fuel system layout for RCCI operation. Table 2 shows engine specifications for the base engine with a picture shown in Fig 5. Additionally the current configuration shows the ability for a dual fuel system to be retrofitted to a production engine for a clear pathway to production ready systems in the future.

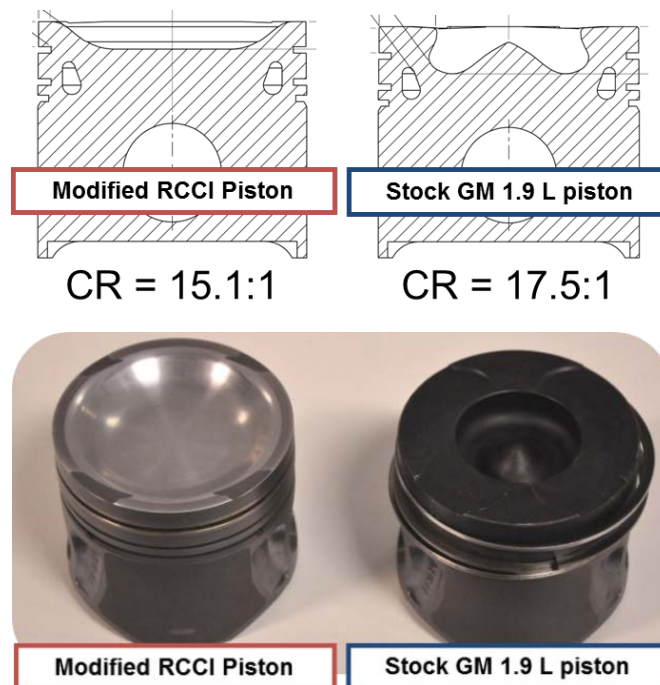


Figure 2. Modified RCCI pistons (schematic right, pictures left)



Figure 3. Modified intake manifold allowing PFI gasoline injection

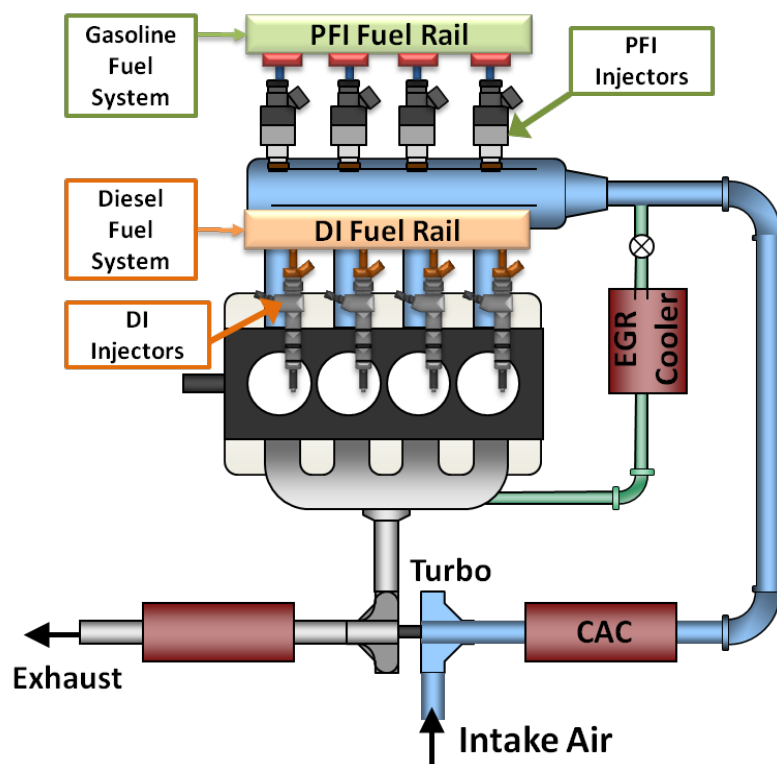


Figure 4. Experimental schematic

Table 1. Engine specifications

Specification	Value
Displacement, liters	1.9
Number of Cylinders	4
Bore, mm	82.0
Stroke, mm	90.4
Compression Ratio	17.5
Rated Power, kW	110
Rated Torque, Nm	315

Table 2. Diesel injector specifications

Specification	Value
Number of nozzle holes	7
Included spray angle, °	148

Table 3. PFI specifications

Specification	Value
Number of nozzle holes	4
Cone angle, °	15
Separation angle, °	22

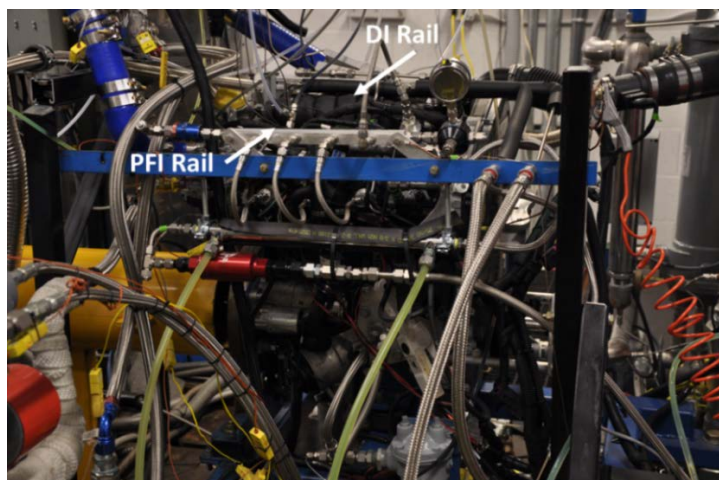


Figure 5. Modified intake manifold allowing PFI gasoline injection

The stock ECU was replaced with a full-pass DRIVEN control system which allowed simultaneous control of the PFI and DI fuel systems and all other engine parameters. Engine torque was measured using an absorbing eddy-current dynamometer. The DI fuel flowrate was measured with a Micro Motion Coriolis fuel meter, while the PFI fuel flowrate was measured using a Max Machinery 710-213 positive displacement volumetric flow measurement system. The intake air flowrate was measured using a laminar flow element and the stock intake mass-airflow sensor.

Engine-out emissions were measured using standard analysis techniques. A heated flame ionization detector (FID) was used to measure total unburned hydrocarbons. A chemiluminescence (CLD) instrument was used to measure NO_x . CO and CO_2 were measured using non-dispersive infrared (NDIR) instruments. Intake and exhaust O_2 was measured using a paramagnetic detector (PMD). Both intake and exhaust CO_2 were measured to provide the EGR rate. Sampled emissions were chilled prior to measurement by PMD and NDIR instruments. Both intake and exhaust sample streams were conveyed from heated filters to the instruments through heated lines maintained at 190°C . Conditioned air was supplied to the engine at a constant temperature of 25°C and a relative humidity of 58%. An AVL 415S smoke meter was used to measure filter smoke number (FSN). A limitation to using a smoke meter based on the blackening of filter paper (reflectivity) is that it may not accurately account for condensable organic hydrocarbons in the PM, which have been shown to be the primary PM mode with RCCI. Previous studies have compared the results of FSN and PM filter mass measurements from RCCI operation and have shown that the RCCI PM is mostly organic carbon with almost no elemental carbon [31].

Engine emissions as well as important temperatures, pressures, flowrates as well as engine speed and torque were sampled for 180 seconds after 120 seconds of stable operation had been attained.

High speed combustion data was acquired using Kistler model 6058A pressure sensors installed in the glow plug ports of all 4 cylinders. Individual Kistler type 5010 Dual-Mode Amplifiers were used to process the pressure signals and the built in combustion package from Drivven was used to process the data. Combustion metrics were monitored and recorded using the DRIVEN combustion analysis toolkit (DCAT). All brake thermal efficiencies presented here are calculated using the lower heating value (LHV) of the fuels used and brake power as measured from the dynamometer.

Vehicle Systems Simulations

Vehicle drive cycle simulations were performed using steady-state experimental engine maps on the same base vehicle available in Autonomie. In addition to standard Autonomie features, a previously published methodology was also utilized to account for fuel consumption, emissions and temperature transients under drive cycle conditions [27, 28]. This approach assumes that transient fuel consumption and exhaust properties can be estimated by applying dynamic correction factors to steady-state engine maps. The previous studies have shown that the transient exhaust properties predicted by the updated Autonomie agree well with experimental chassis dynamometer measurements.

The base vehicle used for all drive cycle simulations is a conventional 1,580 kg mid-size passenger vehicle with an automatic transmission available in Autonomie. The engine maps were changed to conduct the comparative simulations for the vehicle operating in CDC, multi-mode RCCI, and PFI modes. The engine mapping experiments revealed that for the majority of the driving schedules examined here, it will be possible to utilize RCCI. However, when those engine conditions are out of the RCCI operating range, the engine must shift back to CDC. To simulate such multi-mode operation, two sets of steady-state engine maps and transient correction parameters were combined for the relevant speed and load operating regions, as is similar to the literature [27]. The engine controller model is not calibrated for transient operation however. Mode switching behavior is not accounted for in this study (perfect step change). A limitation of this simulation is that the multi-mode map uses an RCCI map with modified pistons while the CDC map was created using the stock pistons.

The fuel economy and emissions from the simulated conventional vehicle over multiple urban and highway driving cycles were evaluated. Hot-start cycle simulations were performed in which standard transmission controls are applied, and the engine switches from CDC into RCCI when speed and load fall in the allowed RCCI range depicted in the RCCI enabled zone as shown in Fig 6. No

warm-up portion or cold start emissions were considered. The multi-mode RCCI and CDC fuel economy simulation results are compared to the same vehicle powered by a representative 2009 port-fuel injected gasoline engine over these multiple standard EPA driving cycles.

Well-to-wheel Modeling

This study will estimate the WTW energy and GHG emissions from a light-duty vehicle using a multi-mode CDC/RCCI combustion strategy with the various fuel combinations that have been mapped. The upstream transportation fuel pathways (well-to-tank) and the downstream energy and emissions (tank-to-wheels) will be compared the results to conventional and advanced powertrain vehicles. Calculations are performed using the GREET model (GREET1_2012 rev 1) [32].

The RCCI multi-mode maps used for the vehicle system simulations in Autonomie were generated using experimental engine data. The two maps explored here are an E30/ULSD engine map and an UTG-96/ B20 map. In both cases the CDC portion of the map is assumed to use the base fuel.

Simulated fuel economy of multi-mode RCCI operation using vehicle systems simulations with experimental steady-state engine maps compared to a representative 2009 gasoline PFI engine as baseline for comparison using diesel fuel and E30 (30% ethanol, 70% gasoline). Experimental steady-state RCCI operating points on modified multi-cylinder GM 1.9-L engine using an in-house methodology for RCCI combustion were used to develop an RCCI speed/load map consistent with a light-duty drive-cycle with sufficient detail to support vehicle simulations. The RCCI map developed as part of this study represents an increase in RCCI operation over previous low temperature combustion operation maps [30], but was still not able to cover the engine speed and load required to meet all power demands over the light-duty drive cycles with the self-imposed constraints imposed on the engine experiments leading to the RCCI engine map.

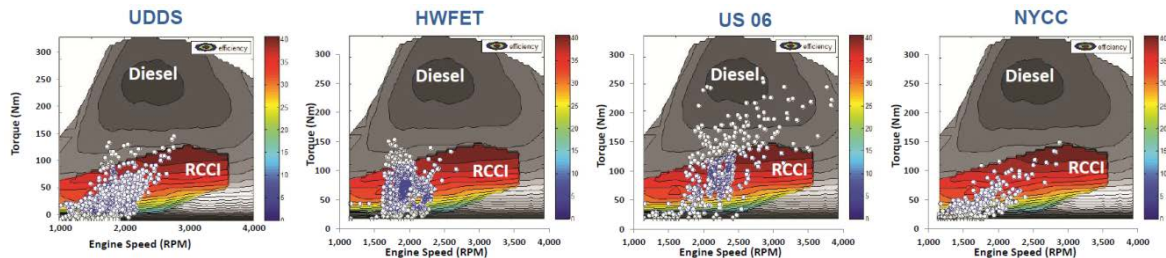


Figure 6. Multi-mode strategy for various drive cycles.

Relevance

The need to better understand the implications that high efficiency combustion concepts can ultimately have on fuel economy are of vital importance to industry and research institutions. Since prototype combustion concepts are quite difficult to put into vehicles to run experiments, these types of vehicle systems simulations can provide valuable information. Though previous studies have compared the WTW energy use and GHG emissions of both conventional and advanced powertrains including various HEV architectures they have not specifically addressed the use of an advanced combustion enabled vehicle in an apples-to-apples comparison of currently available technologies.

Implications

The implications on the WTW energy use and GHG results will help guide future advanced combustion research in terms of focus areas needed from the current state-of-the-art in advanced combustion research. A baseline of where the current advanced combustion research is will help determine what else is needed to meet the proposed. Furthermore the experimental engine maps and vehicle systems models will provide valuable resources to the research community.

The potential for advanced combustion concepts to reduce well-to-wheel energy use and GHG emissions compared to other state-of-the-art powertrains is still unknown. This study uses a combination of vehicle system simulations to model drive cycle fuel use and emissions and well-to-wheel analysis to estimate the potential for WTW energy use and GHG reductions for two multi-mode RCC/CDC vehicles with fuel economy results from vehicle systems simulations compared to other powertrains. Vehicle systems simulations are performed in Autonomie.

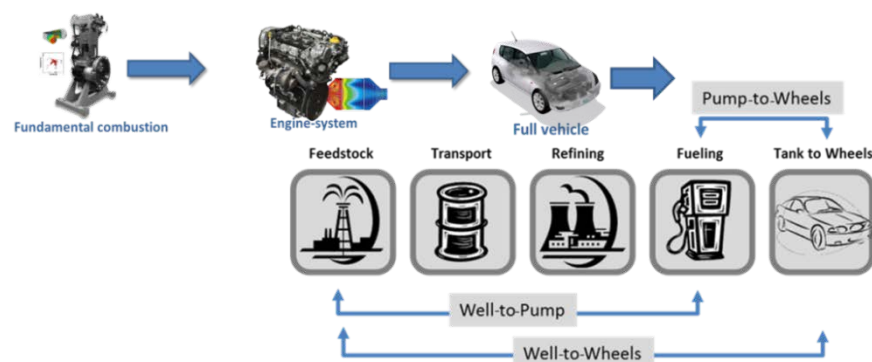


Figure 7. Conceptual layout of well-to-wheels analysis from experimental data

The high brake thermal efficiency and potential for low engine-out emissions of NO_x and PM make RCCI a promising approach to meet regulatory goals of increased fuel economy and lower GHG emissions with concurrent regulations on criteria air pollutants from on-road light-duty vehicles. This research evaluates this potential through the use of the GREET Model, a well-to-wheels analysis toolset, using drive cycle results from vehicle systems simulations based on experimental engine maps. The engine maps and drive cycle simulations were conducted as part of DOE funded research conducted at the Fuels, Engines and Emissions Research Center at Oak Ridge National Lab (ORNL) with the life-cycle-analysis being the main focus of the dissertation proposed here. The conceptual layout of the research is shown in Fig. 7.

What follows is a bundled set of four journal papers that cover the ability for RCCI to be mapped, the mapping and drive cycle simulations with RCCI and finally the well-to-wheel analysis of the RCCI concept. The sequential nature of the papers logically follows the progression of building the framework for being able to conduct the well-to-wheel analysis of RCCI in a light-duty vehicle.

- **Paper 1:** Reactivity controlled compression ignition combustion on a multi-cylinder light-duty diesel engine. Published in International J of Engine Research 13(3) 216–225.
 - Focus on demonstrated the ability of RCCI combustion to be implemented on multi-cylinder engines without direct model guidance and the development of a systematic procedure for mapping RCCI engine operating points for highest efficiency and lowest possible emissions.
- **Paper 2:** Reactivity controlled compression ignition drive cycle emissions and fuel economy estimations using vehicle systems simulations. To be submitted in International J of Engine Research [submitted]
 - Focus on mapping RCCI operation and using those maps in vehicle systems simulations to model fuel economy and drive-cycle emissions with B20/UTG-96.
- **Paper 3:** “Reactivity Controlled Compression Ignition Drive Cycle Emissions and Fuel Economy Estimations Using Vehicle Systems Simulations with E30 and ULSD”, SAE Int. J. Engines
- Number: V123-3EJ; Published: 2014-07-20
 - Focus on mapping RCCI operation and using those maps in vehicle systems simulations to model fuel economy and drive-cycle emissions with ULSD/E30.
- **Paper 4:** Well-to-wheels analysis of Reactivity Controlled Compression Ignition based on Vehicle Systems Simulation Drive Cycle Results using Experimental Engine Data [to be submitted].
 - Focus on taking vehicle systems simulation results and performing well-to-wheels energy and GHG analysis with comparison to

state-of-the-art powertrains using fuel economy estimates using RCCI maps in papers 3 and 4 which were developed using the procedure in paper 1.

For each presented paper, the figures and tables appear separately in a section following the references and have been renumbering sequentially through the paper. The equations and reference numbers specific to each paper have the original numbering maintained. The references at the end of this section are for the introduction only.

REFERENCES

1. U.S. Department of Energy, Office of Vehicle Technologies Multi-Year Program Plan 2011-2015, 2010, http://www1.eere.energy.gov/vehiclesandfuels/pdfs/program/vt_mypp_2011-2015.pdf.
2. Vehicle Technologies Program. Advanced Combustion Engines. <http://www1.eere.energy.gov/vehiclesandfuels/technologies/engines/index.html>.
3. U.S. Environmental Protection Agency, Testing and Measuring Emissions, <http://www.epa.gov/nvfe/testing/dynamometer.htm>.
4. C Sluder, R Wagner, J Storey, S Lewis (2005) "Implications of Particulate and Precursor Compounds Formed During High-Efficiency Clean Combustion in a Diesel Engine," SAE Paper 2005-01-3844, 2005.
5. R Wagner, J Green, T Dam, K Edwards, J Storey (2003) "Simultaneous Low Engine-Out NOX and Particulate Matter with Highly Diluted Diesel Combustion," SAE Paper 2003-01-0262, 2003.
6. C Sluder, R Wagner, S Lewis, J Storey (2006) "Fuel Property Effects on Emissions from High Efficiency Clean Combustion in a Diesel Engine," SAE Paper 2006-01-0080, 2006.
7. C Sluder, R Wagner (2006) "An Estimate of Diesel High-Efficiency Clean Combustion Impacts on FTP-75 Aftertreatment Requirements". SAE Paper 2006-01-3311, 2006.
8. K Cho, M Han, R Wagner, C Sluder (2008), "Mixed-Source EGR for Enabling High-Efficiency Clean Combustion Modes in a Light-Duty Diesel Engine," SAE 2008-01-0645, 2008.
9. K Inagaki, T Fuyuto, K Nishikawa, K Nakakita (2006) "Dual-Fuel PCCI Combustion Controlled by In-Cylinder Stratification of Ignitability," SAE paper 2006-01-0028, 2006.
10. C Chadwell, T Alger, C Roberts, S Arnold (2011) "Boosting Simulation of High Efficiency Alternative Combustion Mode Engines," SAE 04-12-2011, 2011.
11. V Manente, B Johansson, P Tunestal (2009) "Partially Premixed Combustion at High Load using Gasoline and Ethanol, a Comparison with Diesel," SAE Paper 2009-01-0944, 2009.
12. S Kokjohn, R Hanson, D Splitter, R Reitz (2009) "Experiments and Modeling of Dual-Fuel HCCI and PCCI Combustion Using In-Cylinder Fuel Blending," SAE Paper 2009-01-2647, 2009.
13. D Splitter, R Hanson, S Kokjohn, R. Reitz (2011) "Reactivity Controlled Compression Ignition (RCCI) Heavy-Duty Engine Operation at Mid-and High-Loads with Conventional and Alternative Fuels," SAE Paper 2011-01-0363, 2011.
14. R Hanson, S Kokjohn, D Splitter, R Reitz (2010) "An Experimental Investigation of Fuel Reactivity Controlled PCCI Combustion in a Heavy-Duty Engine," SAE Paper 2010-01-0864, 2010.

15. S Kokjohn, R Reitz, D Splitter, M Musculus (2012) "Investigation of Fuel Reactivity Stratification for Controlling PCI Heat-Release Rates Using High-Speed Chemiluminescence Imaging and Fuel Tracer Fluorescence," SAE Paper 2012-01-0375, 2012.
16. S Kokjohn, R Hanson, D Splitter, J Kaddatz, R Reitz (2011) "Fuel Reactivity Controlled Compression Ignition (RCCI) Combustion in Light- and Heavy-Duty Engines," SAE Paper 2011-01-0357, 2011.
17. S Curran, V Prikhodko, K Cho, C Sluder, J Parks, R Wagner, S Kokjohn (2010) "In-Cylinder Fuel Blending of Gasoline/Diesel for Improved Efficiency and Lowest Possible Emissions on a Multi-Cylinder Light-Duty Diesel Engine," SAE Paper 2010-01-2206, 2010.
18. S Curran, K Cho, T Briggs, R Wagner (2011) "Drive Cycle Efficiency and Emissions Estimates for Reactivity Controlled Compression Ignition in a Multi-Cylinder Light-Duty Diesel Engine". Proceedings of the 2011 Internal Combustion Engine Division Fall Technical Conference, ICEF2011, Morgantown Wv.
19. S Curran, R Hanson, R. Wagner (2012) "Effect of E85 on RCCI Performance and Emissions on a Multi-Cylinder Light-Duty Diesel Engine," SAE Paper 2012-01-0376, 2012.
20. S. Curran, R. Hanson, R. Wagner (2012) "Reactivity controlled compression ignition (RCCI) combustion on a multi-cylinder light-duty diesel engine", International Journal of Engine Research, 13(3), 216-225, 2012.
21. R Hanson, S Curran, R Reitz, and R Wagner (2012) "Piston optimization for RCCI in Light-Duty Multi-Cylinder Engine," SAE Paper 2012-01-0380, 2012.
22. S Curran, J Szybist, R Wagner (2012) "Reactivity Controlled Compression Ignition Performance with Renewable Fuels," ICEF2012-92192, Proceedings of the ASME 2012 Internal Combustion Engine Division Fall Technical Conference, ICEF2012, September 23-26, 2012, Vancouver, BC, Canada, 2012.
23. R Hanson, S Curran, R. Wagner, R Reitz (2013) "Effects of Biofuel Blends on RCCI combustion in a Light-Duty, Multi-Cylinder Diesel Engine," SAE Int. J. Engines 6(1):488-503, 2013, doi:10.4271/2013-01-1653.
24. V Prikhodko, J Parks (2009) "Implications of Low Particulate Matter Emissions on System Fuel Efficiency for High Efficiency Clean Combustion," SAE Paper 2009-01-2709, 2009.
25. C Sluder, R Wagner, J Storey, S Lewis (2005) "Implications of Particulate and Precursor Compounds Formed During High-Efficiency Clean Combustion in a Diesel Engine," SAE Paper 2005-01-3844, 2005.
26. R Gopal, A Rousseau (2011) "System Analysis Using Multiple Expert Tools," SAE Paper 2011-01-0754, 2011.
27. Z Gao, J Conklin, C Daw, and V Chakravarthy (2010) "A proposed methodology for estimating transient engine-out temperature and emissions from steady-state maps," International Journal of Engine Research, 11(2), 137-151, 2010.

28. Z Gao, C Daw, R Wagner, K Edwards, D Smith (2013) "Simulating the impact of premixed charge compression ignition on light-duty diesel fuel economy and emissions of particulates and NOx," Proceedings of the Institution of Mechanical Engineers, Part D: Journal of Automobile Engineering 227(1), 31-51, 2013.
29. S Curran, R Hanson, R Reitz, R Wagner (2013) "Efficiency and Emissions Mapping of RCCI in a Light-Duty Diesel Engine", SAE Paper 2013-01-0289.
30. S Curran, Z Gao, R Wagner, "Reactivity controlled compression ignition drive cycle emissions and fuel economy estimations using vehicle systems simulations" IJER, Submitted, 2013.
31. V Prikhodko, S Curran, T Barone, S Lewis, J Storey, C Cho, R Wagner, J Parks (2010) "Emission Characteristics of a Diesel Engine Operating With In-Cylinder Gasoline and Diesel Fuel Blending," SAE Paper 2010-01-2266, 2010.
32. Curran, S., Bunce, M., and Theiss, T., "Greenhouse Gas Reduction Potential with Combined Heat and Power with Distributed Generation Prime Movers, ESFuelCell2012-91045, ESFuelCell2012 July 23–26, 2012, San Diego, California, USA.
33. Wu, Y., Wang, M., Sharer, P., and Rousseau, A., "Well-to-Wheels Results of Energy Use, Greenhouse Gas Emissions, and Criteria Air Pollutant Emissions of Selected Vehicle/Fuel Systems," SAE Technical Paper 2006-01-0377, 2007.

CHAPTER I
REACTIVITY CONTROLLED COMPRESSION IGNITION
COMBUSTION ON A MULTICYLINDER LIGHT-DUTY DIESEL
ENGINE

A version of this chapter was originally published by Scott Curran, Reed Hanson and Robert Wagner:

S. J. Curran, R. M. Wagner, and R. M. Hanson, "Reactivity Controlled Compression Ignition (RCCI) Combustion on a Multi-Cylinder Light-Duty Diesel Engine", *International Journal of Engine Research*, Vol. 13, No. 3, pp. 216-225 (2012).

The article is presented in its original form, formatted for this dissertation including renumbering tables and figures. Author was lead author and lead investigator on study. Coauthor Reed Hanson was a visiting student working at ORNL during parts of the study, and coauthor Robert Wagner's guidance and revisions were instrumental in its publication.

Abstract

Reactivity controlled compression ignition is a low-temperature combustion technique that has been shown, both in computational fluid dynamics modeling and single-cylinder experiments, to obtain diesel-like efficiency or better with ultra-low nitrogen oxide and soot emissions, while operating primarily on gasoline-like fuels. This paper investigates reactivity controlled compression ignition operation on a four-cylinder light-duty diesel engine with production-viable hardware using conventional gasoline and diesel fuel. Experimental results are presented over a wide speed and load range using a systematic approach for achieving successful steady-state reactivity controlled compression ignition combustion. The results demonstrated diesel-like efficiency or better over the operating range explored with low engine-out nitrogen oxide and soot emissions. A peak brake thermal efficiency of 39.0% was demonstrated for 2600 r/min and 6.9 bar brake mean effective pressure with nitrogen oxide emissions reduced by an order of magnitude compared to conventional diesel combustion operation. Reactivity controlled compression ignition emissions and efficiency results are compared to conventional diesel combustion operation on the same engine.

1 Introduction

Low-temperature combustion (LTC) techniques, often categorized as High-Efficiency Clean Combustion (HECC), traditionally have a limited operating range determined by the compression ratio of the engine and the reactivity of the fuel [1-7]. RCCI has the potential for greatly extending the HECC operating range by varying the reactivity of the fuel in-cylinder by stratifying a highly-premixed low reactivity fuel such as gasoline, with a highly reactive fuel such as diesel fuel. Using a port-fuel injection (PFI) of gasoline and direct injection (DI) of diesel fuel, not only is reactivity stratification produced, but temperature and equivalence ratio gradients are also produced in-cylinder. Initial research with RCCI was motivated by a need to extend the LTC operating range using fuels that had properties in between those of gasoline, which are best for high loads, and diesel

fuel, which are desirable at lower loads [8]. The ability to adjust fuel reactivity in-cylinder addresses the lack of control of the combustion process with some other LTC techniques namely combustion phasing and pressure rise rate at higher loads and combustion stability at lower loads. A thorough examination of the RCCI combustion process can be found in the papers by Kokjohn et al. [9] and Hanson et al. [10].

More recently RCCI combustion has advanced due to extensive CFD modeling and single cylinder experiments by Reitz, Kokjohn, Hanson, and Splitter [9-13]. These efforts have been primarily focused on heavy duty engines and results have demonstrated high indicated efficiencies with ultra-low NO_x and soot as measured using a filter smoke number (FSN) technique. An early study by Kokjohn et al. compared dual-fuel RCCI with homogenous charge compression ignition (HCCI) using an ideal fuel reactivity and found the stratification of fuel reactivity was needed to control rate of heat release while the global fuel reactivity was important for controlling combustion phasing [11]. A study by Kokjohn et al. [8] investigated RCCI operation on both a heavy-duty 2.4L single cylinder Caterpillar Single Cylinder Oil Test engine (SCOTE), and single cylinder engine (SCE) version of a GM 1.9L diesel engine with a compression ratio 15.2:1. For the SCE experiments, port-fuel injection of gasoline and a split diesel injection of ULSD was used. The first injection was delivered between 80 and 50 degrees before top dead center (DBTDC) with the second injection between 45 and 30 DBTDC. With a split injection strategy, the first injection acts to control the reactivity in the squish region while the second injection targets the piston bowl creating a region of high reactivity which acts as an ignition source. The study made comparisons between the light and heavy duty engine operating in RCCI mode with a focus on identifying heat transfer losses. The SCE experiments focused on 9 bar indicated mean effective pressure (IMEP) with 41% EGR. Light-duty SCE experimental results showed gross indicated thermal efficiencies ($\text{ITE}_{\text{GROSS}}$) of around 50% with NO_x emissions of less than 0.1 g/kW-hr and soot emissions of less than 0.01 g/kw-hr, both based on indicated power. Numerical studies showed heat transfer losses decreased with increasing engine speed, decreasing swirl ratio and decreasing surface to volume ratio of the piston. The numerical study also identified unreacted and partially reacted fuel in the ring-pack and near liner regions to be major contributors to high HC and CO emissions.

Initial light-duty multi-cylinder engine (MCE) RCCI experiments performed at Oak Ridge National Laboratory (ORNL) were guided by CFD and chemical kinetics modeling performed at the University of Wisconsin-Madison (UW) [15]. These initial MCE RCCI experiments by Curran et al. focused on the operating point of 2,300 rev/min, 4.4 bar brake mean effective pressure (BMEP) which is representative of a moderate road load or light acceleration in a light-duty passenger vehicle. These experiments focused on the real-world challenges of

implementing RCCI on a multi-cylinder engine including the importance of cylinder-to-cylinder balancing, sensitivity of pressure rise rate on intake temperature and sensitivity of brake thermal efficiency (BTE) to boost pressure with real turbomachinery. The study showed a strong dependence of BTE on swirl ratio with higher swirl ratios leading to higher BTE with RCCI in direct contradiction to the numerical studies in [8]. The dependence on BTE with higher swirl ratios shown in the MCE experiments in [15] may indicate a benefit from increased in-cylinder mixing despite the tendency to increase heat transfer. Results showed greater than diesel efficiency with significant reductions of NO_x and FSN with increased HC and CO emissions with RCCI compared to CDC operation. Results from diesel start of injection (SOI) sweeps indicated good agreement of trends predicted by the CFD model. A follow-up MCE study by Prikhodko et al. [16] compared engine out emissions of aldehydes, ketones and PM of RCCI with CDC and diesel Premixed Charge Compression Ignition (PCCI) at the 2,300 rev/min, 4.4 bar BMEP point and found RCCI increased both aldehydes and ketones. Furthermore, the increase in carbonyl species from RCCI indicated the combustion chemistry is quite different than that of CDC or PCCI. The study investigated particle geometric mean diameter (μ_g), number-size distribution and total number concentration (C_{tot}) as measured by a scanning mobility particle sizer (SMPS). The RCCI particle number concentration was less than CDC or PCCI for 10 to 470 nm particles with a shift of RCCI particles to a smaller geometric mean diameter. Particle mass measurements were collected on Teflon-coated quartz-fiber filters and measured gravimetrically and showed RCCI particulate matter (PM) emissions were ~40% less than CDC but almost twice that of PCCI. The near zero FSN readings and very slight color change of PM collected on the filters suggested semi-volatile organics present in the gas phase may have condensed on the filter. The study also investigated the effectiveness of a diesel oxidation catalyst (DOC) on the destruction of CO, HC and formaldehyde as well as the reduction of PM, and found that the DOC was effective at reducing all four even at the lower exhaust temperatures resulting from RCCI operation. Further MCE investigations by Curran et al. [17] looked at estimating the drive-cycle performance of RCCI using the ad-hoc modal points which loosely approximate the federal light duty drive cycle [18-20] and compared RCCI emissions and efficiency to CDC and diesel PCCI. The study found that low load operation of RCCI was possible, but a mismatch of turbomachinery at the lower engine speed/load points (due to lower exhaust enthalpy) and high fraction of diesel fuel needed to maintain stable combustion offered little reduction in NO_x emissions compared to CDC which uses a high EGR fraction during those points. Weighting factors applied to the emissions results were used to estimate the drive-cycle emissions performance of RCCI operating with gasoline and diesel fuel and showed a 50% reduction in engine out NO_x compared to CDC and 17% compared to PCCI however, some level of NO_x aftertreatment would most likely still be needed.

This work examines a broader range of RCCI operation with gasoline and diesel fuel across the light-duty speed and load range on a light-duty MCE. Current experience and insight from simulation and experiments has led to directions in optimization without need to model each engine operating point directly.

2 Experimental Setup

For this study, a 4-cylinder light-duty GM 1.9 L turbo-diesel engine was modified to allow for port fuel injection of gasoline. The only other modifications made to the stock engine setup were the use of a high-heat capacity exhaust gas recirculation (EGR) cooler allowing for greater control over heat rejection within the high pressure EGR loop, and the removal of the alternator and water pump which were replaced with electrified components. The variable-geometry turbocharger, diesel injection system, and reentrant bowl pistons were all left in stock form. The experimental setup is shown in Figure 8 and engine specifications are presented in Table 4.

The stock ECU was replaced with a full-pass DRIVEN control system which allowed simultaneous control of the PFI and DI fuel systems and all other engine parameters. Engine torque was measured using an absorbing eddy-current dynamometer. The DI fuel flowrate was measured with Micro Motion Coriolis fuel meter, while the PFI fuel flowrate was measured using a Max Machinery 710-213 positive displacement volumetric flow measurement system. The intake air flowrate was measured using a laminar flow element and the stock intake mass-airflow sensor.

Engine-out emissions were measured using standard analysis techniques. A heated flame ionization detector (FID) was used to measure total unburned hydrocarbons. A chemiluminescence (CLD) instrument was used to measure NO_x . CO and CO_2 were measured using non-dispersive infrared (NDIR) instruments. Intake and exhaust O_2 was measured using a paramagnetic detector (PMD). Both intake and exhaust CO_2 were measured to provide the EGR rate. Sampled emissions were chilled prior to measurement by PMD and NDIR instruments. Both intake and exhaust sample streams were conveyed from heated filters to the instruments through heated lines maintained at 190°C. Conditioned air was supplied to the engine at a constant temperature of 25°C and a relative humidity of 58%.

An AVL 415S smoke meter was used to measure FSN. A limitation to using a smoke meter based on opacity is that it may not accurately account for condensable organic hydrocarbons in the PM, which have been shown to be the primary PM mode with RCCI. Previous studies have compared the results of FSN and PM filter mass measurements from RCCI operation [15, 20]. Engine

emissions as well as important temperatures, pressures and flowrates were sampled for 180 seconds after 120 seconds of stable operation had been attained.

High speed combustion data was acquired using Kistler model 6058A pressure sensors installed in the glow plug ports of all 4 cylinders. Individual Kistler type 5010 Dual-Mode Amplifiers were used to process the pressure signals and the built in combustion package from Drivven was used to process the data. Combustion metrics were monitored and recorded using the DRIVEN combustion analysis toolkit (DCAT). Cylinder pressure was pegged to the intake manifold pressure near the end of the intake stroke and sampled at 0.2 crank angle resolve. The high resolution is important to ensure the capture of important phenomena with advanced combustion. Ensemble-averaged cylinder pressure and heat release rate curves presented here result from 300 cycles based on a forward and reverse IIR filtered cylinder pressure signal.

3 Fuels

The high reactivity fuel used in this study was a 2007 certification grade ultra low sulfur diesel (ULSD) fuel with a cetane number of 45.7, the low reactivity fuel was an unleaded test gasoline (UTG-96) with a pump octane number ((RON+MON)/2) of 92.1. The properties of the fuels used in this study are similar to the certification-grade ULSD and UTG-96 used in previous MCE studies at ORNL [15-17]. Fuel specifications are presented in Table 8.

4 Experimental Procedure

The initial MCE RCCI experiments performed at ORNL were guided by the UW CFD modeling in order to narrow down the extensive parameter space needed to obtain stable combustion. Further MCE experiments were performed without the direct use of modeling for obtaining stable RCCI operation at a given engine speed and load, but instead through the use of a systematic approach based on the previous MCE experimental results and modeling. A separate startup procedure was followed to transition combustion from CDC to RCCI at low engine loads by gradually increasing the premixed ratio and advancing diesel start of injection (SOI) at a low engine load. Premixed ratio (r_p) is defined as the ratio of the energy of the premixed fuel to the total fuels as shown in Equation 1, where the premixed fuel and direct injected fuel are identified with the subscripts p and d respectively.

$$r_p = \frac{Q_p}{Q_p + Q_d} = \frac{m_p \times LHV_p}{m_p \times LHV_p + m_d \times LHV_d} \quad (1)$$

A procedure for obtaining successful RCCI operation is shown in Figure 9 assuming the transition step at low engine load had already been completed with cylinder-to-cylinder balancing of both IMEP and combustion phasing (i.e., 50% of fuel mass fraction burned (MFB50)) being implicit with each step of the approach. For this study the primary control parameters are diesel SOI and premixed ratio which must be balanced for the best control of combustion phasing and cylinder pressure rise rate while minimizing NO_x emissions as well as HC and CO emissions.

The MCE RCCI experiments were focused on the speed range of 1,500 to 2,600 rev/min. The upper BMEP range of operation was limited by a self-imposed 10bar/deg cylinder pressure rise rate (PRR) limit and the lower load range was limited by a self-imposed CO emissions limit of 5,000 ppm due to limitations of the CO analyzer used. This engine speed and load range covers a large portion of the light-duty drive cycle as shown previously [17] and is a significant expansion of the engine operating range studied for MCE RCCI operation. The engine speed and load range of RCCI operation explored in this study is shown in Figure 10. The lowest engine speed investigated in this study was 1,500 rev/min however, RCCI operation down to 1,000 rev/min was achieved with no observable limits for further decreasing engine speed. RCCI operation has also been demonstrated on the experimental platform for speeds up to approximately 4,000 rev/min.

All experimental results reported in this study were completed on the same engine in the same configuration allowing for direct comparisons of BTE and emissions between RCCI and CDC operation. CDC operation was carried out using the automatic maps in DRIVEN based on a Euro IV calibration supplied by GM Europe using ULSD. CDC emissions reported in this study are engine-out emissions. RCCI operation was carried out on the same engine using the aforementioned systematic approach with an early, single pulse injection strategy with the same ULSD and premixed UTG-96. A split injection similar to that used in the study by Kokjohn et al.[8] was not found to produce higher thermal efficiencies or reduce emissions in the speed and load range investigated. This may indicate less of a need for conditioning of the squish area in an MCE than previous modeling has shown. PFI fuel injection pressure was set to the manufacturer's recommended injector specification of 3.8 bar for all points. DI rail pressure varied somewhat with load, with most points operating at 500 bar rail pressure and rail pressure as low as 360 bar for some of the lowest engine loads.

5 Results

5.1 Comparison of Peak BTE with CDC

The peak BTE demonstrated with RCCI with UTG-96 and ULSD in this study was 39.0.% at 2,600 rev/min, 6.9 bar BMEP. The maximum load achievable was 7.21 bar BMEP at the same engine speed, but higher boost levels needed to maintain stable combustion at this point resulted in a small decrease in BTE to 38.9 % BTE. The cylinder pressure and heat release rate traces for the 2600 rev/min, 6.9 bar BMEP point for CDC and RCCI are shown in Figure 11 and Figure 12 respectively. A table of the key results of the comparison is presented in Table 9.

At the peak RCCI BTE condition, RCCI showed a 7% relative increase in BTE over CDC (39.0 from 36.4% BTE). RCCI shows a higher net indicated thermal efficiency (ITE_{NET}) than CDC most likely due to the reduction in pumping losses associated with the use of EGR and higher boost levels with CDC. ITE_{GROSS} values are very similar between RCCI and CDC operation. RCCI operation resulted in an 87% reduction in NO_x without the use of EGR. As compared to CDC which used 15% EGR. Brake specific NO_x emissions were 0.61 and 4.9 g/kw-hr for RCCI and CDC respectively. There were substantial increases with HC and CO with RCCI operation along with 36° C decrease in exhaust temperature. The decrease in exhaust temperature was seen across the range of RCCI operation in this study. Combustion stability of RCCI was examined using the coefficient of variance (COV) of indicated mean effective pressure (IMEP) and MFB 50. COV of IMEP is under 3% for both cases but the higher COV of combustion phasing as measured through MFB 50 with RCCI may prove challenging for implementing feed-back control of combustion phasing. Also of note is the lower rail pressure used for RCCI operation of 500 bar compared to 1,100 bar used for CDC operation. Net and gross thermal efficiencies were calculated using the definition of mean effective pressure from Heywood [21] to convert MEP to power as shown in Equations 2-4. Indicated mean effective pressure was averaged over the sample and calculated using DRIVEN's DCAT.

$$\eta = \frac{P}{\dot{m}_f Q_{LHV}} \quad (2)$$

$$P = MEP \times V_d \times \frac{N}{n_R} \quad (3)$$

$$ITE = \frac{IMEP \times V_d \times N}{n_R \times \dot{m}_f \times Q_{LHV}} \quad (4)$$

The above equations have terms representing thermal efficiency (η), power (P), fuel mass flow (\dot{m}_f) lower heating value of fuel (Q_{LHV}), indicated thermal efficiency (ITE), mean effective pressure (MEP), displaced volume (V_d), crankshaft rotational speed (N), and number of crank revolutions per stroke (n_R), which for this engine is 0.5.

5.2 Engine control parameters

With multi-cylinder RCCI operation, the real-world issues from going to a MCE from a SCE using production grade hardware can be significant. The previous section examined a single RCCI operating point compared the same engine speed and load with CDC operation. The following sections provide a summary of trends observed over a wider speed and load range of RCCI operation.

The two most powerful controls over combustion phasing are the diesel SOI timing and premixed ratio. There was a balancing act with controlling NO_x and PRR using the premixed ratio and diesel SOI timing. Figure 13 shows the trends of diesel SOI timing and premixed ratio with increasing BMEP for RCCI operation at 2,000 rev/min without the use of EGR, with similar trends observed at other engine speeds. At lower loads, the premixed ratio can be as low 20% with diesel SOI around 30 DBTDC. If the premixed ratio is lowered, or if the diesel SOI is retarded decreasing the time available for mixing, NO_x emissions can increase due to lowering the degree of homogeneity. At the higher loads, the premixed ratio can be as high as 85% with diesel SOI timing close to 65 DBTDC. If diesel SOI is advanced further, combustion can become unstable as the diesel mixture becomes too premixed. If the premixed ratio is increased past ~85%, HC and CO emissions increase and PRR becomes too weak to sustain stable combustion.

Ideally, it is assumed that for optimum BTE, the lowest possible swirl setting would be advantageous to use in terms of minimizing pumping losses and maximizing volumetric efficiency and minimizing heat loss. However, with the engine configuration used in this study it was found that there was in fact an ideal swirl for best BTE and lowest emissions and furthermore the idle swirl ratio depends on speed and load. This effect of higher swirl ratios needed to obtain maximum BTE and lowest emissions was shown in previous work [15]. Small swirl ratio sweeps are an important part of the systematic procedure as described earlier.

It was found that lower boost levels were needed for maximizing BTE as compared to a similar operating point for CDC operation. Most engine operating points explored here used significant amounts of EGR. This means for a given engine operating point under RCCI operation without EGR, the equivalence ratio

is already lower than with CDC operation and increasing boost will result in an even leaner charge. At the lower loads this could result in nearing or surpassing the lean limit of the premixed gasoline, potentially reducing combustion efficiency. Higher levels of boost were however found to be helpful in controlling PRR at higher engine load points namely by adding trapped mass and adding fine control over combustion phasing. RCCI has been shown to have a lower exhaust temperature than CDC which is important not only in terms of exhaust energy availability for turbomachinery needs, but also for any exhaust aftertreatments. Figure 14 shows the comparison of exhaust temperatures as measure at the outlet of the turbocharger for RCCI and CDC at 2,000 rev/min over a load sweep from 2.0 bar to 6 bar BMEP. Over the load range shown at 2,000 rev/min, RCCI had between a 26% to 43% drop in exhaust temperature which represents a temperature reduction 68 °C at the lowest load to 181 °C at 5.0 bar BMEP. RCCI had similarly lower exhaust temperatures than CDC over the speed and load range investigated.

Cooled high-pressure EGR was found to help control PRR and NO_x at the higher loads with RCCI, but at the expense of lowering BTE. EGR was not found to be able to provide a significant load expansion due the EGR raising intake temperatures, negating any combustion phasing delay from dilution. Cooling the EGR to levels needed for stable RCCI operation (40-50 °C) risked severe condensation of water and HC in the EGR cooler.

EGR was found to enable a small expansion in load when EGR outlet temperature was matched to the intake manifold temperature. Figure 15 shows a RCCI load sweep at 2,000 rev/min through 6.0 bar BMEP. The highest load attainable with RCCI without the use of EGR while keeping under the self-imposed 10bar/ deg PRR limit and maintaining stable combustion at an engine speed of 2,000 rev/min was approximately 5.0 bar BMEP. Figure 15 shows the decrease in BTE with increasing EGR used to increase load to 6.0bar BMEP. Even with the use of EGR, it was not possible to increase engine load beyond 6.0bar BMEP while observing the PRR limit. It was also not possible to increase load at an engine speed of 2,600 rev/min with the use of EGR due to need of low intake temperatures.

It was observed that RCCI exhaust temperatures were somewhat higher with the use of EGR. At the RCCI operating point of 2,000 rev/min and 5.0 bar BMEP, there was a 20 °C increase in exhaust temperature when an EGR rate of 25% was used to control PRR. In this case, premixed ratios were similar and diesel SOI timing was adjusted to keep PRR constant. BTE was reduced from 36.5% to 33.6% with the use of EGR keeping while keeping NO_x emissions fixed at 10 ppm. The air-to-fuel ratio (AFR) decreased from 39.6 to 29.3 with the addition of 25% EGR. MFB50 without EGR was 6.9 DBTDC and 7.7 DBTDC with EGR. HC emissions were the same however, CO emissions increased from 1,690 ppm to 1,870 with the use of EGR. The reduction in AFR at lower loads

which, with stock turbomachinery and un-throttled operation could be as high as 70:1, was beneficial to achieving stable operation and was explored in a previous study [17].

5.2.1 Brake Thermal Efficiency

The maximum BMEP achievable with RCCI while observing the self-imposed limit on cylinder pressure rise rate goes up as engine speed is increased. Also, as engine speed increases, airflow increases and could help the stock VGT operate in a more efficient area than with lower engine speeds. It was observed that for each engine load, there is a significant variation in BTE, as much as four points in BTE at certain loads. These are the effects of varying diesel SOI and EGR on allowing premixed ratio to vary at a given BMEP depending on speed and intake temperature.

To provide perspective on the efficiency performance of RCCI it is necessary to compare BTE with RCCI operation to that of CDC operation with the same engine as shown in Figure 16 for engine speeds of 1,500, 2,000 and 2,600 rev/min. From Figure 16 it is observed as engine speed is increased, the BTE of RCCI goes from diesel like efficiency at 1500 rev/min to up to 7% higher at 2,600 rev/min. The cross over at 1,500 and 2,000 rev/min where CDC has a higher BTE than RCCI at the lower loads could be in part attributed to the mismatch in turbomachinery for RCCI operation. The study by Kokjohn et al. also discuss the reduced heat transfer losses at higher engine speeds with RCCI [8].

5.2.2 NO_x emissions

RCCI operation has been shown to produce very low NO_x emissions. The general trend in RCCI NO_x emissions was found to be parabolic with higher NO_x at the lower loads due to the need for a lower premixed ratio and retarded diesel SOI to maintain stable combustion with reasonable CO and HC levels, and higher NO_x at the higher loads due to higher pressure rise rates. NO_x generally trended downwards with increasing boost due to the higher trapped mass. Figure 17 shows a comparison of NO_x with RCCI and CDC as a function of BMEP for the maximum BTE cases at a given load.

Another way to compare the NO_x reductions with RCCI over CDC is to plot NO_x as a function of BTE as shown in Figure 18. NO_x with CDC combustion raises exponential with load with an increase at the higher loads where no EGR is used. The bs-NO_x emissions from CDC operation quickly rise to 4.0 g/kw-hr as BTE approaches 37% for all engine speeds and loads and increases sharply from there. NO_x from RCCI operation remains relatively flat through the operating range explored in this study with an average bs-NO_x emission rate of 0.24 g/kw-hr and a maximum of 0.74 g/kw-hr.

5.2.3 HC and CO Emissions

In previous light-duty multi-cylinder studies the HC emissions for RCCI operation have been shown to be relatively high compared to CDC operation. The large speed and load range with this study allows a more in-depth study into the high HC levels with RCCI. In general it was found that brake specific hydrocarbon (bsHC) emissions were reduced as BMEP increased. Figure 19 shows the general trend with bs-HC trending down with BMEP as compared to CDC operation. The ranges of bs-HC for each load are the result of variations in DI-SOI, stability, engine speed and intake temperature. The lower limit for bs-HC emissions from RCCI operation in this study was just under 10g/kw-hr at ~ 7.0 bar BMEP.

Despite the downward trend in bsHC emissions with increasing load, the HC emissions on a volumetric basis did not trend as such. HC emissions averaged around 3000 ppm across the entire speed and load range investigated with the lowest volumetric HC emissions of an operating point of 1,820 ppm at 2,600 rev/min, 3.5 bar BMEP. In general, HC emissions were seen to somewhat reduce with advancing SOI, increased AFR, retarding combustion phasing and increasing stability as measured by COV of PRR. There were not however, clear overall trends indicating the consistently high HC emissions with RCCI operation may be resulting from trapped unburned fuel in the crevice volume.

Bs-CO emissions from RCCI track similarly to HC emissions and are shown in Figure 20 compared to CDC operation. The lower bs-CO performance from RCCI operation in this study was approximately 7 g/kw-hr at 7.0 bar BMEP. Volumetric CO emissions for RCCI operation averaged approximately 2,500 ppm across the entire speed and load range with the lowest observed CO emissions of 1,244 ppm at the operating point of 2,600 rev/min, 6.9 bar BMEP. CO emissions were not as constant overall operating conditions as HC emissions with volumetric CO emission clearly decreasing with engine load. This indicates that while there may be high systematic HC levels with RCCI operation, CO emissions are more clearly reduced with increasing load (and decreasing premixed ratio) and decreasing AFR.

5.2.4 Filter Smoke Number

The filter smoke number for all the RCCI experimental points averaged around 0.03. This shows the low-soot capabilities of RCCI operation, but does not capture the total PM performance of RCCI. Previous comparisons of RCCI PM to CDC and PCCI have shown that despite the near zero FSN, RCCI had higher PM mass emissions composed of primarily semi-volatile organics [16, 22].

Conclusions

RCCI operation with production viable hardware was shown to achieve diesel-like efficiency or better with ultra-low NO_x emissions over a wide speed and load range on a multi-cylinder light-duty diesel engine. Stable RCCI operation was demonstrated using a systematic approach to optimizing combustion for high efficiency with the lowest possible emissions without direct CFD modeling guidance for each operating point. This approach was based on general trends explored by previous modeling efforts along with the results of previous experimental work performed on a multi-cylinder light-duty diesel engine. The extra degree of freedom that dual-fuel RCCI allows in controlling the combustion process is very powerful in helping to meet pressure rise rate limits and controlling combustion phasing over a wide engine operating range.

The relatively high HC and CO emissions across the speed and load range explored in this study show a downward trend in brake specific emissions as load is increased. The high levels of CO and HC resulting from RCCI operation led to a subsequent study in which the piston bowl design was changed from a typical light-duty re-entrant bowl to a more heavy-duty shallow dish bowl design in an attempt to reduce squish area and reduce surface area available for heat transfer [23]. The results of that study are not presented here but did show similar results.

The ability to achieve stable RCCI combustion across such a wide speed and load range without the need for direct CFD modeling guidance demonstrates the potential of the combustion mode to be controlled in a vehicle. Combustion controls based on some metric such as combustion phasing or PRR would depend on some form of pressure rise feedback.

Hardware challenges still exist limiting the potential for RCCI combustion on a light-duty multi-cylinder engine for achieving higher BTE with lower HC and CO emissions including mismatch of turbomachinery for LTC operation and limitations of high-pressure EGR when intake temperature is a critical combustion control parameter. The engine load limit of 7.2 bar BMEP at 2600 rev/min using the certification grade ULSD and UTG-96 in this study is not the absolute limits for MCE RCCI operation. Other MCE studies have shown the effectiveness of using E85 [24], as well as reducing the compression ratio [23] at increasing the maximum load attainable with RCCI.

The following key conclusions can be made:

1. RCCI can achieve diesel like efficiency in a light-duty multi-cylinder diesel engine with production viable hardware and in the case of this study stock piston geometry, compression ratio, diesel injection system, and turbomachinery.

2. Peak RCCI BTE in this study was 39% for the 2600 rev/min, 6.9 bar BMEP operating point which was ~ a 7% improvement from CDC. Gross thermal efficiencies for CDC and RCCI were similar.
3. NO_x emissions reductions with RCCI range from ~ 50% reductions at the lowest loads to ~90% at higher loads as compared to CDC operation.
4. HC and CO emissions were much higher with RCCI operation than with CDC operation (over an order of magnitude increase) with volumetric HC and CO emissions being somewhat constant across the speed and load range but falling with load as measured on a brake specific basis.
5. The robustness of RCCI allows rapid speed and load exploration/optimization without direct model guidance.
6. Increased mixing time with the diesel SOI timings with RCCI allows for lower rail pressures (<500bar) to be used as compared to CDC operation without an increase in soot emissions.
7. RCCI produces lower exhaust temperatures than CDC operation across the speed and load investigated meaning lower quality exhaust for turbomachinery and lower temperatures for aftertreatment, which is concern for high HC and CO emissions.

Disclaimer

This manuscript has been authored by a contractor for the U.S. Government under contract number DE-AC05-000R22725. Accordingly, the U.S. Government retains a nonexclusive, royalty-free license to publish or reproduce the published form of this contribution, or allow others to do so, for the U.S. Government.

Acknowledgments

This work was supported by the U.S. Department of Energy (DOE), Office of Vehicle Technologies. The authors gratefully acknowledge the support and guidance of Gurpreet Singh, Ken Howden and Kevin Stork at DOE. The authors would like to acknowledge the input from their colleagues at the University of Wisconsin, Professor Rolf Reitz and Sage Kokjohn, and support from General Motors and Delphi.

References

1. Sluder, C., Wagner, M., Storey, J., and Lewis, S. Implications of Particulate and Precursor Compounds Formed During High-Efficiency Clean Combustion in a Diesel Engine. SAE paper 2005-01-3844, 2005.
2. Wagner, R., Green, J., Dam, T., Edwards, K., and Storey, J. Simultaneous Low Engine-Out NOX and Particulate Matter with Highly Diluted Diesel Combustion. SAE paper 2003-01-0262, 2003.
3. Sluder, C., Wagner, R., Lewis, S., and Storey, J. Fuel Property Effects on Emissions From High Efficiency Clean Combustion in a Diesel Engine. SAE paper 2006-01-0080, 2006.
5. Manente, V., Johansson, B., and Tunestal, P. Partially Premixed Combustion at High Load using Gasoline and Ethanol, a Comparison with Diesel. SAE paper 2004-20-2009, 2009.
6. Chadwell, C., Alger, T., Roberts, C., and Arnold, S. Boosting Simulation of High Efficiency Alternative Combustion Mode Engines. SAE paper 04-12-2011, 2011.
7. Sluder, C.S., and Wagner, R.M. An Estimate of Diesel High-Efficiency Clean Combustion Impacts on FTP-75 Aftertreatment Requirements. SAE paper 2006-01-3311, 2006.
8. Kokjohn, S., Hanson, R., Splitter, D., Kaddatz, J., and Reitz, R. Fuel Reactivity Controlled Compression Ignition (RCCI) Combustion in Light- and Heavy-Duty Engines. SAE Paper 2011-01-0357
9. Hanson, R., Kokjohn, S., Splitter, D., and Reitz, R. An Experimental Investigation of Fuel Reactivity Controlled PCCI Combustion in a Heavy-Duty Engine. SAE paper 2010-01-0864, 2010.
10. Inagaki, K., Fuyuto, T., Nishikawa, K., and Nakakita, K. Dual-Fuel PCCI Combustion Controlled by In-Cylinder Stratification of Ignitability. SAE paper 2006-01-0028, 2006.
11. Kokjohn, S., Hanson, R., Splitter, D., and Reitz, R. Experiments and Modeling of Dual-Fuel HCCI and PCCI Combustion Using In-Cylinder Fuel Blending. SAE paper 2009-01-2647, 2009.
12. Kokjohn, S., Hanson, R., Splitter, D., and Reitz, R. (2009) Experiments and Modeling of Dual-Fuel HCCI and PCCI Combustion Using In-Cylinder Fuel Blending. SAE paper 2009-01-26478, 2009.
13. Splitter, D., Hanson, R., Kokjohn, S., Rein, K., Sanders, S., and Reitz, R. An Optical Investigation of Ignition Processes in Fuel Reactivity Controlled PCCI Combustion. SAE paper 2010-01-0345, 2010.
14. Splitter, D., Hanson, R., Kokjohn, S., and Reitz, R. Reactivity Controlled Compression Ignition (RCCI) Heavy-Duty Engine Operation at Mid-and High-Loads with Conventional and Alternative Fuels. SAE paper 2011-01-0363, 2011.
15. Curran, S., Prikhodko, V., Cho, K., Sluder, C., Parks, J., Wagner, R., Kokjohn, S., and Reitz, R. In-Cylinder Fuel Blending of Gasoline/Diesel for

Improved Efficiency and Lowest Possible Emissions on a Multi-Cylinder Light-Duty Diesel Engine. SAE paper 2010-01-2206, 2010.

16. Prikhodko, V., Curran, S., Barone, T., Lewis, S., Storey, J., Cho, C., Wagner, R., and Parks, J. Emission Characteristics of a Diesel Engine Operating With In-Cylinder Gasoline and Diesel Fuel Blending. SAE 2010-01-2266, 2010.

17. Curran, S., Cho, C., Briggs, T., and Wagner, R. Drive Cycle Efficiency and Emissions Estimates for Reactivity Controlled Compression Ignition in a Multi-Cylinder Light-Duty Diesel Engine. ICEF2011-60227, Proceedings of the 2011 Internal Combustion Engine Division Fall Technical Conference ICEF2011 October 2-5, 2011, Morgantown, Wv.

18. Szymkowicz, P., French, D., and Crellin, C. Effects of Advanced Fuels on the Particulate and NOx Emissions from an Optimized Light-Duty CIDI Engine. SAE paper 2001-01-0148, 2001.

19. Kenney, T., Gardner, T., Low, S., Eckstrom, J., Wolf, L., Korn, S., and Szymkowicz, P. Overall Results: Phase 1 Ad Hoc Diesel Fuel Test Program. SAE paper 2001-01-0151, 2001.

20. Gonzalez, M., Clark, W., Wolf, L., Garbak, J., Wright, K., Natarajan, M., Yost, D., Frame, E., Kenney, T., Ball, J., Wallace, J., Hilden, D., and Eng, K. Impact of Engine Operating Conditions on Low-NOX Emissions in a Light-Duty CIDI Engine Using Advanced Fuels. SAE Paper Number 2002-01-2884, 2002.

21. Heywood, J. *Internal Combustion Engine Fundamentals*, 1988 (McGraw-Hill, New York)

22. Barone, T., Storey, J., Prikhodko, V., Curran, S., Parks, J., and Wagner, R. Particle Emissions Reduction by In-Cylinder Blending of Gasoline and Diesel Fuel. 21st CRC Real World Emissions Workshop, San Diego Ca.

23. Hanson R., Curran S., Reitz, R., and Wagner R. Piston optimization for RCCI in Light-Duty Multi-Cylinder Engine. SAE Paper 2012-01-0380, 2012.

24. Curran S., Hanson R., and Wagner R. Effect of E85 on RCCI Performance and Emissions on a Multi-Cylinder Light-Duty Diesel Engine. SAE Paper 2012-01-0376, 2012.

Appendix 1

Table 4. Engine specifications

Specification	Value
Displacement (liters)	1.9
Number of Cylinders	4
Bore (mm)	82.0
Stroke (mm)	90.4
Compression Ratio	17.5
Rated Power (kW)	110
Rated Torque (Nm)	315
Rated BMEP (bar)	20.7
Max Engine Speed (rev/min)	4500

Table 5. Fuel Properties

Specification	Gasoline	Diesel
Lower Heating Value (kJ/kg)	43124	42912
Specific Gravity	0.7389	0.8452
H (weight %)	13.9	13.2
C (weight %)	86.1	86.8
Aromatics (weight %)	32.7	29.3
Sulfur (ppm)	29.6	9.9
Initial Boiling Point (°C)	34	189
Final Boiling Point (°C)	185	344
Research Octane Number (RON)	96.1	NA
Motor Octane Number (MON)	88.2	NA
(RON + MON)/2	92.1	NA
Cetane Number	NA	45.7

Table 6. Comparison of RCCI and CDC at 2600rev/min, 6.9bar BMEP

	CDC	RCCI
Premixed Ratio	NA	88%
Boost (bar)	1.58	1.22
EGR Rate (%)	15.3	0
Diesel SOI (°BTDC)	7	65
Rail Pressure (bar)	1100	500
BTE (%)	36.4	39.0
MFB50 (°BTDC)	11.8	8.5
ITE _{NET} (%)	41.7	43.4
ITE _{GROSS} (%)	44.5	44.8
NO _x (ppm)	417	53
HC (ppm)	251	3207
CO (ppm)	140	1099
FSN (-)	1.51	0.01
COV IMEP (%)	2.26	1.58
COV MB50 (%)	3.56	14.3
Exhaust Temp (C)	370	334

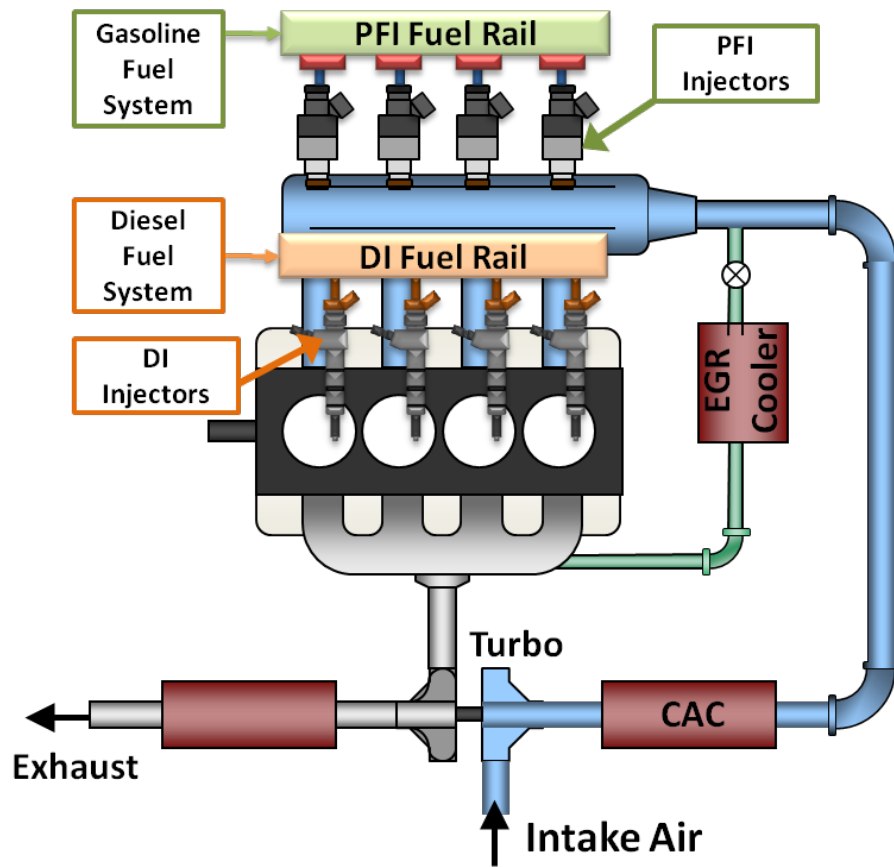


Figure 8. Experimental schematic

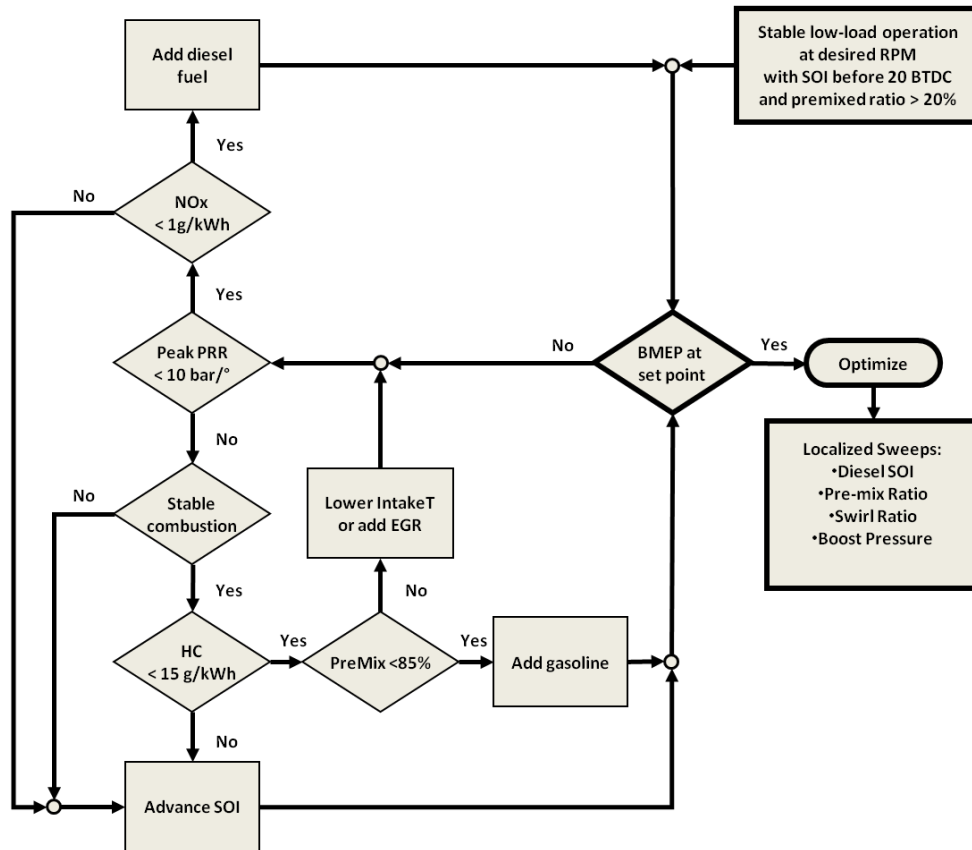


Figure 9. Systematic procedure for obtaining RCCI operating points

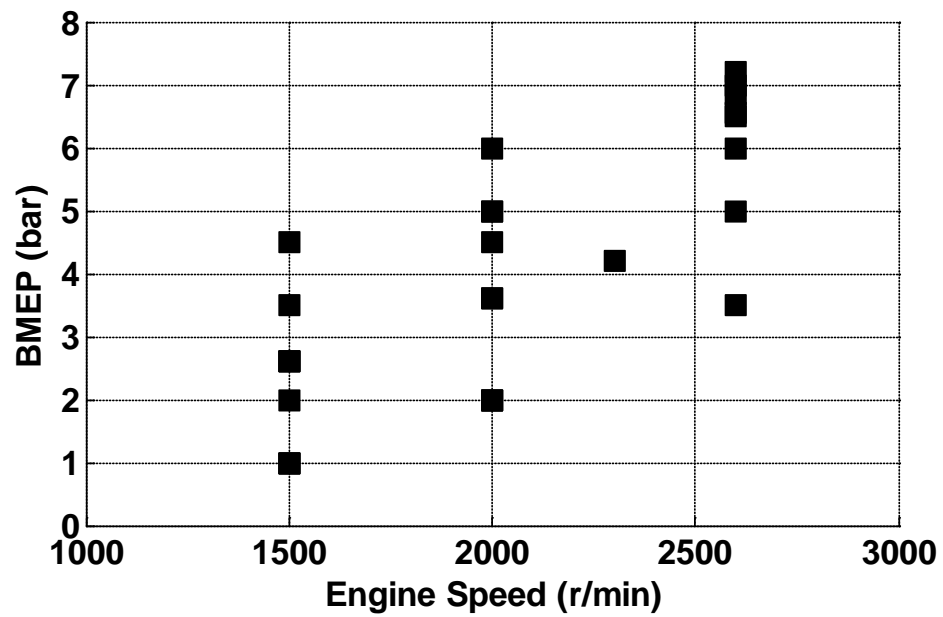


Figure 10. Speed and load range of RCCI operation examined

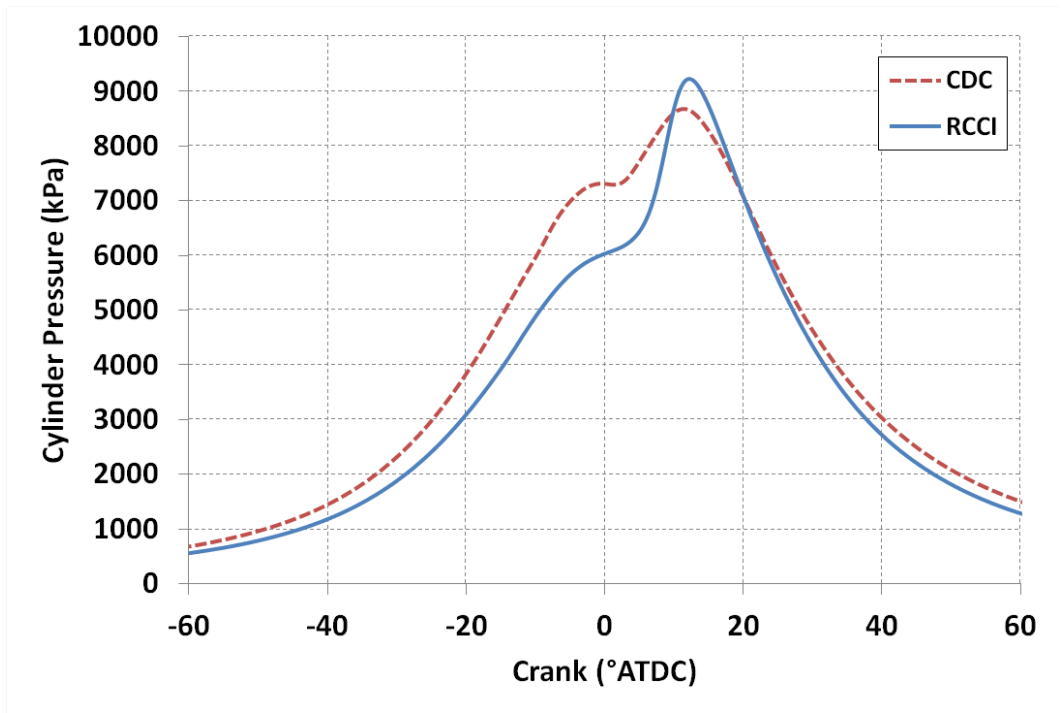


Figure 11. Cylinder pressure traces for RCCI and CDC at 2600 rev/min, 6.9 bar BMEP

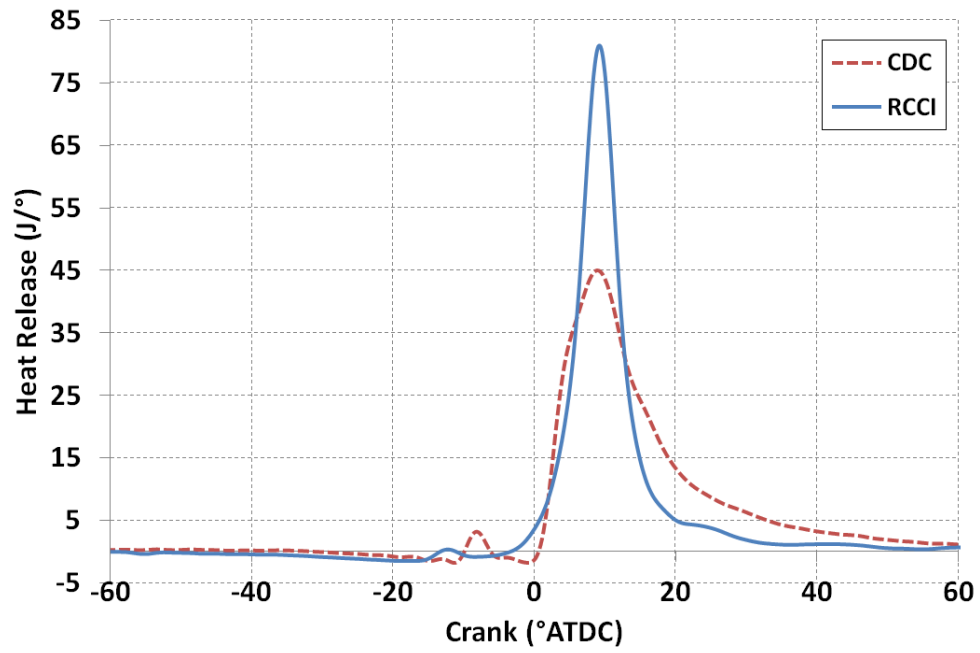


Figure 12. Heat release traces for RCCI and CDC at 2600 rev/min, 6.9 bar BMEP

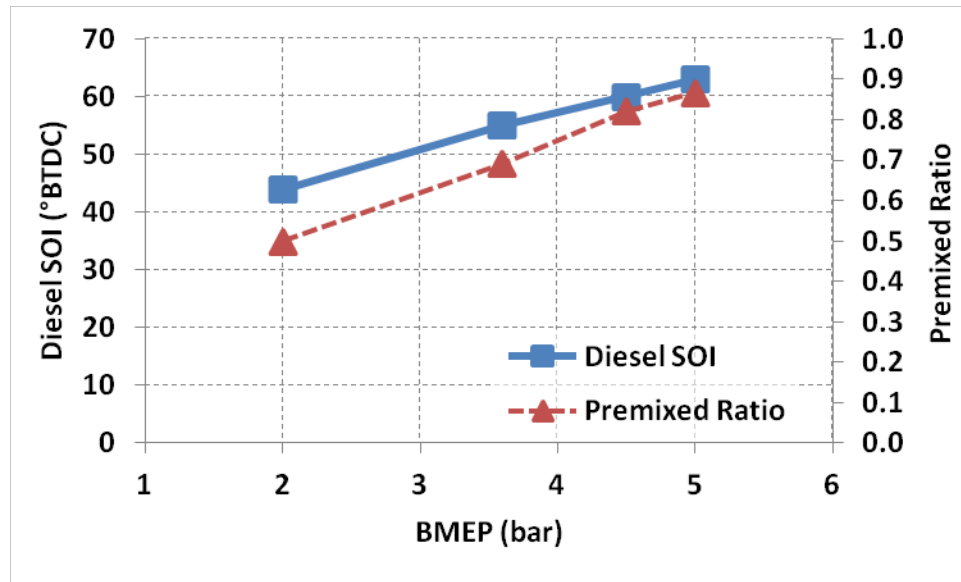


Figure 13. Diesel SOI and premixed ratio as a function of BMEP at 2000 rev/min

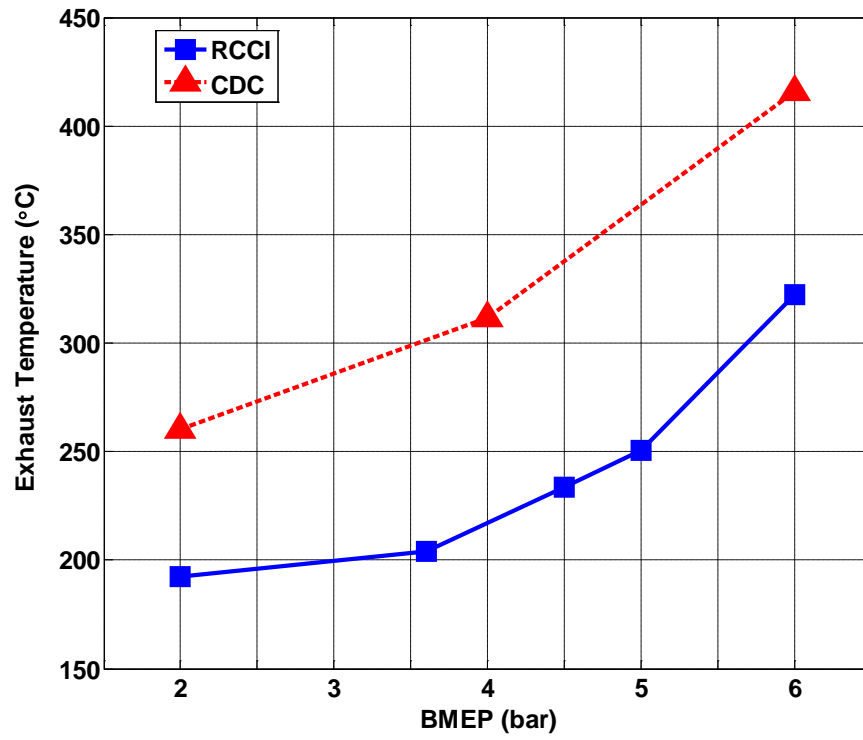


Figure 14. Exhaust temperatures for RCCI and CDC at 2000 rev/min over a load sweep from 2.0bar to 6.0bar BMEP.

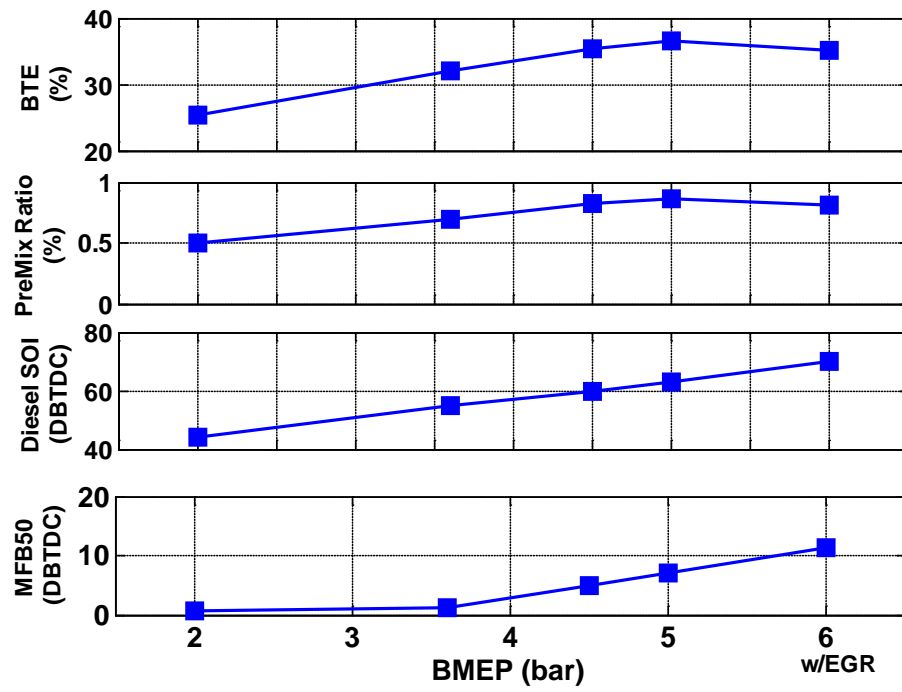


Figure 15. BTE premixed ratio, diesel SOI timing, and combustion phasing (MFB50) vs. BMEP for 2000 rev/min

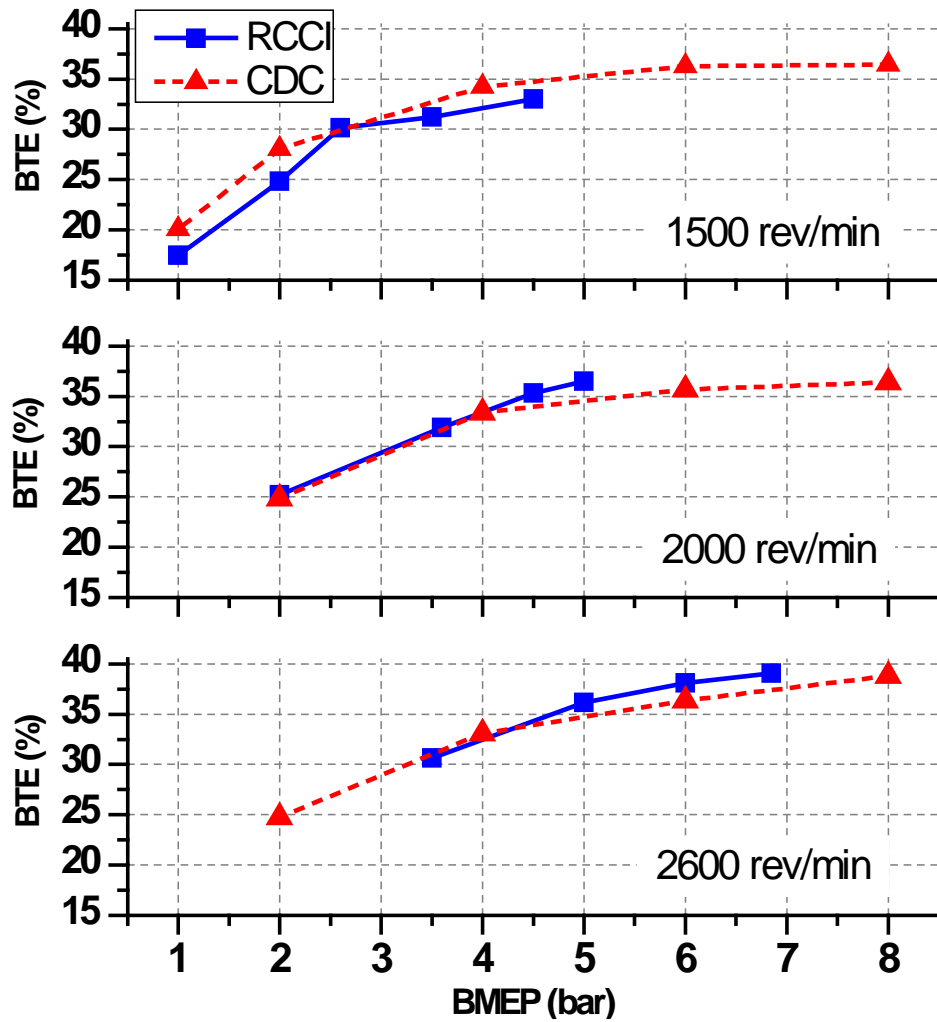


Figure 16. BTE vs. BMEP for RCCI and CDC for 1500, 2000 and 2600 rev/min

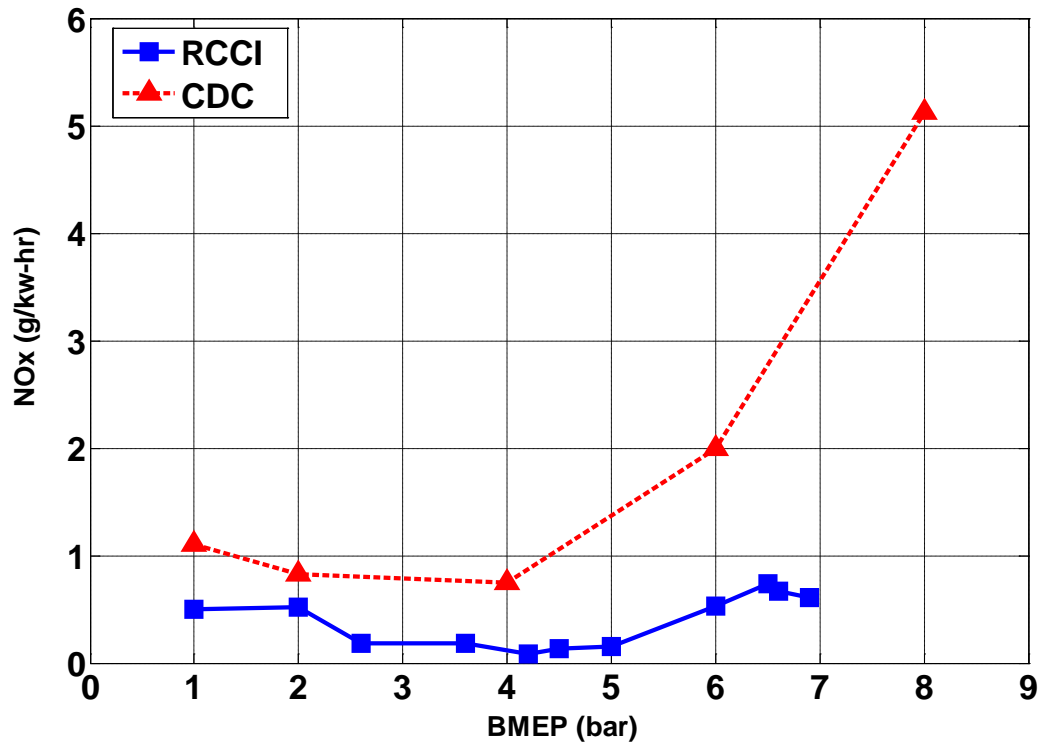


Figure 17. NO_x as a function of BMEP for CDC and RCCI for maximum BTE operation (various engine speeds for maximum BTE)

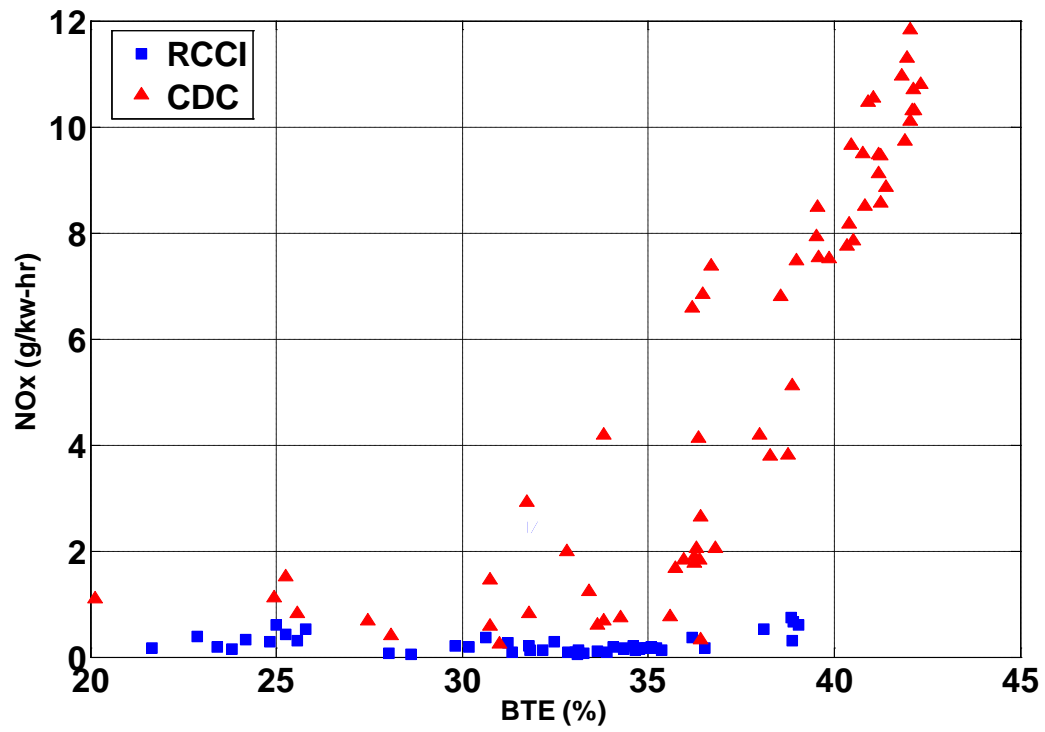


Figure 18. NO_x vs. BTE for RCCI and CDC for all engine speed and loads

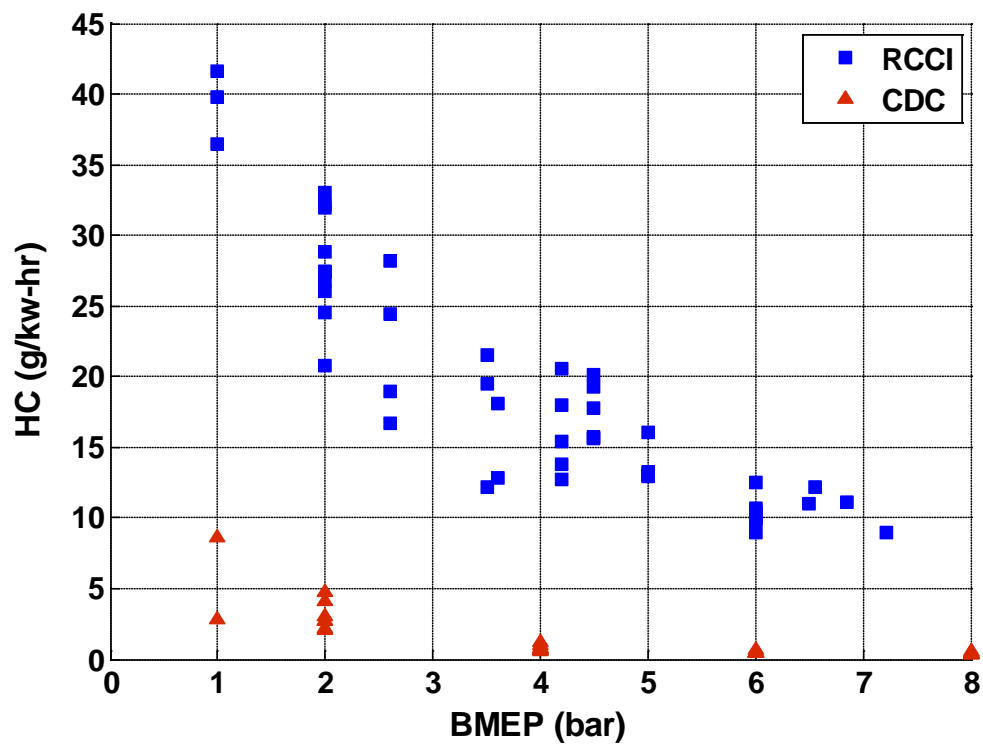


Figure 19. HC emissions for RCCI and CDC vs. BMEP for all engine speeds and loads

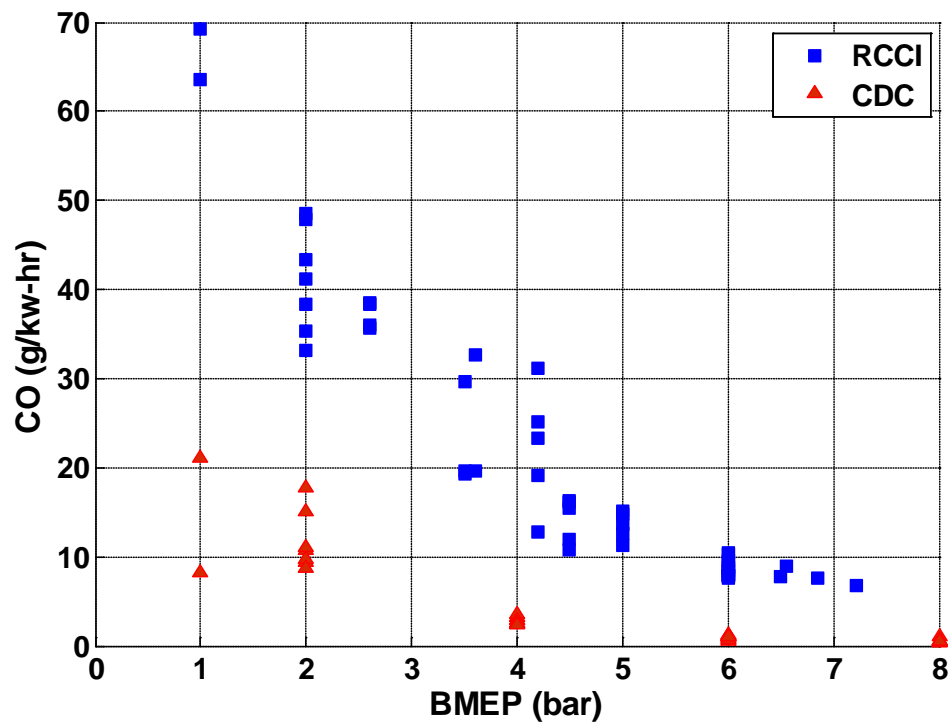


Figure 20. CO emissions for RCCI and CDC vs. BMEP for all engine speeds and loads

CHAPTER II
REACTIVITY CONTROLLED COMPRESSION IGNITION DRIVE
CYCLE EMISSIONS AND FUEL ECONOMY ESTIMATIONS USING
VEHICLE SYSTEMS SIMULATIONS

A version of this chapter was originally submitted to the *International Journal of Engine Research* by Scott Curran, Zhiming Gao and Robert Wagner: S. J. Curran, R. M. Wagner, and R. M. Hanson, "Reactivity controlled compression ignition drive cycle emissions and fuel economy estimations using vehicle systems simulations". This article is currently under review and has not been published anywhere, nor will it be before I turn in the final version of my ETD.

The article is presented in its original form, formatted for this dissertation. Author was lead author and lead investigator on study. Coauthor Zhiming Gao performed the Autonomie simulations and coauthor Robert Wagner's guidance and revisions were instrumental in its publication. Additional data related to the RCCI map is presented in the appendix for engine performance and emissions (Appendix 2.2).

Abstract

In-cylinder blending of gasoline and diesel to achieve reactivity controlled compression ignition (RCCI) has been shown to reduce NOX and PM emissions while maintaining or improving brake thermal efficiency as compared to conventional diesel combustion (CDC). The RCCI concept has an advantage over many advanced combustion strategies in that the fuel reactivity can be tailored to the engine speed and load allowing stable low-temperature combustion to be extended over more of the light-duty drive cycle load range. However, the current range of the experimental RCCI engine map investigated here does not allow for RCCI operation over entirety of some drive cycles. A multi-mode RCCI strategy is employed where the engine switches from RCCI to CDC when speed and load fall outside of the experimentally determined RCCI range. The potential for RCCI to reduce drive cycle fuel economy and emissions is not clearly understood and is explored here by simulating the fuel economy and emissions for a multi-mode RCCI-enabled vehicle operating over a variety of U.S. drive cycles using experimental engine maps for multi-mode RCCI, CDC and a 2009 port-fuel injected (PFI) gasoline engine. Simulations are completed assuming a conventional mid-size passenger vehicle with an automatic transmission. RCCI fuel economy simulation results are compared to the same vehicle powered by a representative 2009 PFI gasoline engine over multiple drive cycles Engine-out drive cycle emissions are compared to CDC and observations regarding relative gasoline and diesel tank sizes needed for the various drive cycles are also summarized.

1 Introduction

The United States Department of Energy (DOE) Vehicle Technologies Office's (VTO) mission is to develop more energy-efficient and environmentally friendly highway transportation technologies that will enable the United States to use significantly less petroleum and reduce greenhouse gas emissions and criteria air pollutants [1]. Fuel efficiency improvements and petroleum displacement are the overarching goals of the DOE VTO, and within these research activities, resolving the interdependent emissions challenges from high efficiency engines is important not only because of a regulatory and market barrier standpoint but also in terms of total engine system efficiency. Engine system efficiency includes not only the fuel energy required for the production of motive or shaft power but also the fuel penalties associated with exhaust aftertreatments. For diesel engines, these fuel penalties include fuel regeneration of diesel particulate filters as well as fuel regeneration of lean NO_x traps, or reductant addition for selective catalytic reduction systems. The DOE VTP Advanced Combustion Engine research and development program's strategic goals are to reduce petroleum dependence by removing critical technical barriers to mass commercialization of high-efficiency, emissions-compliant internal combustion engine powertrains in passenger and commercial vehicles [2]. Improvements in engine efficiency and engine systems efficiency through advanced combustion strategies is an important pathway to this goal. For advanced combustion strategies to be able to meet these goals, their effectiveness over different driving cycles [3] will have to be determined.

In-cylinder blending of gasoline and diesel to achieve reactivity controlled compression ignition (RCCI) has been shown to reduce NO_x and particulate matter (PM) emissions while maintaining or improving brake thermal efficiency as compared to conventional diesel combustion (CDC). The ability to control the percent premixed low reactivity fuel along with the timing and number of injections of the direct injected high reactivity fuel reactivity allows for not only reactivity stratification but also temperature and equivalence ratio stratification in the cylinder, providing further control of combustion phasing and cylinder pressure rise rate. The RCCI concept, as shown in Figure 21, has an advantage over many advanced combustion strategies [4-11] in that the fuel reactivity can be tailored to the engine speed and load, allowing stable LTC operation to be extended over more of the light-duty drive cycle load range [12].

Previous computational fluid dynamics (CFD) modeling and single-cylinder engine results have demonstrated high gross thermal efficiencies with ultra-low NO_x and soot emissions. Through reviews of RCCI single-cylinder engine experiments and CFD modeling advances can be found in papers by Kokjohn, Splitter, Hanson, and Reitz [12-16].

Previous experiments have investigated the translational effects of taking CFD modeling and single-cylinder engine experiments to multi-cylinder engines (MCE) on efficiency, emissions, and controls [17-23]. These effects include the behavior of real turbomachinery, effects of real exhaust gas recirculation (EGR), cylinder-to-cylinder imbalances, and swirl. Despite the translational effects, MCE RCCI has been shown to be capable of diesel-like efficiency at lower engine loads and greater than diesel efficiency at higher engine loads with an order of magnitude reduction in engine out NO_x as compared to CDC. Previous experiments have shown the benefits of increased control over the combustion process allowed by RCCI operation on extending the operating range of low temperature combustion (LTC) compared to diesel premixed charge compression ignition (PCCI) on a multi-cylinder light-duty compression ignition engine [19, 20].

To date the potential vehicle fuel economy improvements that RCCI could allow are not well understood. Kokjohn and Reitz examined the potential for meeting light-duty NO_x and fuel economy targets from single cylinder results [24]. Previous multi-cylinder studies by Curran et al. [19, 20] looked at using the Fuels Working group's ad-hoc modal points [7] to estimate drive cycle emissions with RCCI as compared to CDC. These modal points are representative of key areas of the federal drive testing protocol and have weighting factors attached to them linked to the amount of drive cycle spent at similar conditions. That work showed that the ability to obtain noise-constrained RCCI operation over all of the ad-hoc modal points was dependent on the fuels used. The light-duty MCE experiments showed that the hard acceleration modal point of 2600 RPM, 8.8 bar brake mean effective pressure (BMEP) was not obtainable with a 46 Cetane ultra-low sulfur diesel (ULSD) and certification gasoline with an research octane number (RON) of 96 (UTG-96) [20] while adhering to a cylinder pressure rise rate limit of 10 bar/deg. A follow-up study showed that the 2600 RPM, 8.8 bar BMEP point was achievable with RCCI using E85 and ULSD [19]. The results of the RCCI modal point studies showed that significant weighted composite NO_x reductions (~66%) were made possible with RCCI operation as compared to CDC. The results also showed significant increases in engine out HC and CO emissions from RCCI operation. The RCCI modal point studies only examined estimated drive cycle emissions and did not attempt to apply the weighting factors to fuel economy improvements.

In the United States, the US Environmental Protection Agency (EPA) regulates emissions based on federal drive cycle compliance [3]. There are a number of EPA dynamometer driving cycles that attempt to take into account the real-world driving conditions seen with light-duty passenger vehicles. If an engine cannot be operated in an advanced combustion over the entire speed and load range demanded by the drive-cycle in question, then the engine would have to operate in a multi-mode strategy in which the engine would switch to

conventional combustion when engine power demands cause the engine to operate outside of the advanced combustion speed and load operating range. There have been a number of studies examining the potential for LTC/multi-mode operation with diesel engine baselines [25, 26]. For LTC/CDC multi-mode operation, the engine switches to CDC for areas of the engine map that fell outside the LTC region. The need for multi-mode operation has implications for the needs of the aftertreatment system to be able to meet stringent federal emissions standards over the prescribed drive cycles, namely for NO_x control if the engine has to switch to CDC mode for higher loads in regions of the map that produce high amounts of NO_x.

It is difficult to draw conclusions on drive cycle fuel economy and emissions performance for combustion strategies in the development stage that have demonstrated only a limited number of steady-state operating points. Vehicle systems simulation tools such as Autonomie developed by Argonne National Laboratory for DOE can be used to simulate vehicle operation using model-based simulations [27]. The simulations use performance-based measurements including fuel consumption and exhaust properties such as emissions and temperature, which are tabulated allowing for the generation interpolated response surfaces over the entire operating range of the engine maps. Previous work by Gao et al. has demonstrated the use of steady-state engine maps in transient drive cycle simulations [28, 29]. Previous work by Gao has examined this type of simulation with multi-mode advanced combustion steady-state engine data for engine performance and emissions modeling [29].

This work investigates the potential fuel economy of multi-mode RCCI operation using vehicle systems simulations with experimental steady-state engine maps compared to a representative 2009 gasoline port-fuel injected (PFI) engine as baseline for comparison. Experimental steady-state RCCI operating points on a modified multi-cylinder GM 1.9-L engine using an in-house methodology, described in [20], for RCCI combustion were used to develop an RCCI speed/load map consistent with a light-duty drive-cycle with sufficient detail to support vehicle simulations. A certification grade gasoline was used for the low-reactivity fuel and a splash blended B20 was used for the high reactivity fuel. B20 had been previously shown to allow for improvements in both low-load and high-load RCCI performance as compared to the ULSD fuel with a CN of 42.5 [22]. The RCCI map developed here represents an increase in RCCI operation over previous low-temperature combustion operation maps [30] but was still not able to cover the engine speed and load required to meet all power demands over the light-duty drive cycles with the self-imposed constraints on the engine experiments leading to the RCCI engine map. The simulations used a multi-mode RCCI/diesel operating strategy where the engine would operate in RCCI mode whenever possible, but at the highest and lowest engine operating points, the engine would switch to diesel mode. All simulations were carried out in

Autonomie using a 1580 kg passenger vehicle (mid-size sedan, i.e., Chevrolet Malibu) over numerous US federal light-duty drive cycles. A representative 2009 gasoline PFI engine map was obtained from an automotive original equipment manufacturer (OEM) for use in the vehicle simulations. A 2009 gasoline PFI baseline is standard in DOE programmatic goals [1]. Multi-mode RCCI fuel economy simulation results are compared to the same vehicle powered by a representative 2009 PFI gasoline engine over multiple drive cycles. Engine-out drive cycle emissions are compared to CDC, and observations regarding relative gasoline and diesel tank sizes needed for the various drive cycles are also summarized.

2 Methodology

For this study three engine maps are used for the vehicle systems simulations. A multi-mode experimental RCCI map, which is described in the next section, is used along with a CDC map for multi-mode operation. An experimental CDC map is employed using the stock pistons with the same base engine used for the RCCI experiments. CDC mapping was conducted on the base engine with the OEM pistons using the Euro IV calibrations maps in DRIVEN. An experimental 4.0 L 2009 PFI gasoline engine map was provided from an OEM partner. The PFI map was for fuel consumption only, so no comparisons with modeled emissions can be made. The fuel economy modeling is performed using vehicle systems simulations with experimental engine data.

2.1 Experimental Setup

The engine used for this study is a modified 2007 General Motors 4 cylinder 1.9 L turbocharged diesel engine. The base engine has a rated power of 110 kW and a rated torque of 315 Nm. The OEM pistons were replaced with pistons modified for RCCI. The RCCI-modified piston bowl geometry was designed for RCCI using CFD modeling by the University of Wisconsin. The piston design is based on a heavy duty piston and minimizes the surface area of the piston to minimize heat transfer losses and also results in a lowered compression from 17.1 in the OEM configuration to 15.1 to allow for higher load operation while maintaining reasonable pressure rise rate limits. More information about the piston design can be found in the paper by Hanson et al. [23]. The direct injection (DI) diesel injection system and variable geometry turbocharger were left in production form. The intake manifold was modified to incorporate extended tip narrow spray-angle PFI injectors for the gasoline supply. For a more in-depth discussion, the intake manifold modifications can be found in Curran et al. [20]. Figure 22 shows the overall fuel system layout for RCCI operation. Table 7 shows engine specifications for the base engine. Table 8 and Table 9 show the injector specifications for the DI and PFI injectors respectively.

The OEM engine control unit was replaced with a full-pass DRIVEN control system that allowed simultaneous control of the PFI and DI fuel systems and all other engine parameters. Engine torque was measured using an absorbing eddy-current dynamometer. The DI fuel flow rate was measured with a Micro Motion Coriolis fuel meter, while the PFI fuel flow rate was measured using a Max Machinery 710-213 positive displacement volumetric flow measurement system. The intake air flow rate was measured using a laminar flow element.

Engine-out emissions were measured using standard analysis techniques. A heated flame ionization detector was used to measure total unburned hydrocarbons. A heated chemiluminescence instrument was used to measure NO_x . CO and CO_2 were measured using non-dispersive infrared (NDIR) instruments. Intake and exhaust O_2 was measured using a paramagnetic detector (PMD). Both intake and exhaust CO_2 were measured to provide the EGR rate. Sampled emissions were chilled before measurement by PMD and NDIR instruments. Both intake and exhaust sample streams were conveyed from heated filters to the instruments through heated lines maintained at 190°C . Conditioned air was supplied to the engine at a constant temperature of 25°C and a relative humidity of 58%. An AVL 415S smoke meter was used to measure filter smoke number (FSN). Engine emissions, as well as important temperatures, pressures, flow rates, and engine speed and torque were sampled for 180 seconds after 120 seconds of stable operation had been attained.

High-speed in-cylinder pressure data were acquired using Kistler model 6058A pressure sensors installed in the glow plug ports of all 4 cylinders. Individual Kistler type 5010 dual-mode amplifiers were used to process the pressure signals, and the built-in combustion package from DRIVEN was used to process the data. Combustion metrics were monitored and recorded using the DRIVEN combustion analysis toolkit. All brake thermal efficiencies presented here are calculated using the lower heating value of the fuels used and brake power as measured from the dynamometer.

The base DI fuel used in this study was a 2007 certification grade ULSD fuel with a cetane number (CN) of 42.5; the gasoline was UTG 96 with an anti-knock index of 92.1 and containing no ethanol. The B20 biodiesel blend (20% biodiesel, 80% ULSD) used in this study was splash blended on-site by volume using the base ULSD described earlier with a soy-based methyl ester B100 with a pre-blended level of bio-extend oxidative stability additive. Key fuel specifications for both fuels are shown in Table 10.

2.2 RCCI Engine Mapping

Multi-cylinder mapping experiments made use of a systematic approach based on previous MCE experimental results and modeling. The robustness of

dual-fuel RCCI allows for rapid map exploration and development; however, the parameter space is nontrivial. Self-imposed experimental constraints of pressure rise rate and CO emissions were used to define the upper and lower limits of the engine operating windows. Cylinder maximum pressure rise rate (MPRR) of < 10bar/deg and CO emissions of < 5000 ppm were adhered to. High-pressure EGR was used at low engine loads to control equivalence ratio and intake temperature.

RCCI operation was achieved through an early single pulse of diesel fuel (between 30 and 70°BTDC) and port fueling of gasoline onto a closed intake valve. RCCI operation was achieved using a systematic approach described in the paper by Curran et al. without the direct use of modeling [20]. Fuel rail pressure was decreased as diesel fuel start of injection (SOI) timing was advanced to avoid spray impingement on the cylinder walls. Cylinder-to-cylinder balancing of cylinder pressure rise rate and indicated mean effective pressure was performed for successful RCCI operation and had to be adjusted based on operating condition and EGR level. Once cylinder-to-cylinder balancing was performed, no other real-time controls were needed to maintain stable operation.

PFI fuel injection pressure was set to the manufacturer's recommended injector specification of 3.8 bar for all points. DI rail pressure was fixed at 500 bar for all engine loads. For the RCCI map exploration, the MPRR and CO constraints were observed and using the RCCI operating point procedure; engine operating points at every 500 RPM and every 1.0 bar BMEP were explored, resulting in a 41-point operating map.

The experimental RCCI map with brake thermal efficiency (BTE) contours is shown in Figure 23, with the 1 Hz Urban Dynamometer Driving Cycle (UDDS) discrete engine speed and load points overlain. For comparison, the CDC operating map is shown in Figure 24, also with the UDDS points overlain with BTE contours.

The difference in BTE between RCCI and CDC is shown in Figure 25 for % BTE. For example, at 2700 rpm, 6.0bar BMEP the BTE for the CDC point was 35% and RCCI had a BTE of 42%, the difference is 7% BTE. Figure 25 also illustrates the areas in low load and high load in which multi-mode switching to CDC will be necessary to meet the drive cycle requirements.

The RCCI mapping results for NO_x are shown in Figure 26 and show very low NO_x across the majority of the map except for the areas of lowest load and highest speed in which additional diesel fuel was required to maintain stable combustion.

The CDC map used for comparison in this study was a Euro IV calibration, which used high amounts of EGR to keep NO_x emissions low in the lower speed and load range of the map. Figure 27 shows NO_x emissions as a function of BTE for RCCI and CDC.

As shown in previous studies, RCCI operation results in a significant increase in HC and CO emissions as compared to CDC operation. Figure 28 shows that the RCCI hydrocarbon emissions are above 9 g/kwh for the entire map. One of potential challenges with RCCI is the elevated CO and HC emissions combined with the lower exhaust temperatures as shown in Figure 29. Those temperatures were measured in the exhaust at a location similar to placement of the close-coupled diesel oxidation catalyst in the stock vehicle configuration of the base diesel engine. The elevated HC and CO emissions along with lower exhaust temperatures are important to note at the lowest engine loads when making decisions with regards to CDC or RCCI operation in a multi-mode strategy if the NO_x and BTE are similar. The variation in premixed ratio is shown in Figure 30.

The PM emissions from RCCI are not reported here as it is not clear that any correlation to PM concentration can be made to a FSN reading. A limitation to using a smoke meter based on the blackening of filter paper (reflectivity) is that it may not accurately account for condensable organic hydrocarbons in the PM, which have been shown to be the primary PM mode with RCCI. Previous studies have compared the results of FSN and PM filter mass measurements from RCCI operation and have shown that the RCCI PM is mostly organic carbon with almost no elemental carbon [30, 31].

3 Vehicle Systems Simulations

Vehicle system drive cycle simulations were performed using steady-state experimental/industry engine maps on the same base vehicle in Autonomie. In addition to standard Autonomie features, a previously published methodology was used to account for fuel consumption, emissions, and temperature transients in the engine exhaust [28]. This approach assumes that fuel consumption and exhaust properties can be estimated by applying dynamic correction factors to steady-state engine maps. The Autonomie model does address fuel consumption and exhaust properties during highly transient vehicle operation.

The base vehicle used for all drive cycle simulations is a conventional 1,580 kg mid-size passenger vehicle with an automatic transmission available in Autonomie. The engine maps were changed to conduct the comparative simulations for the vehicle operating in CDC, multi-mode RCCI, and PFI modes. The engine mapping experiments revealed that for the majority of the driving schedules examined here, it will be possible to use RCCI. However, when those

engine conditions are out of the RCCI operating range, the engine must shift back to CDC. To simulate such multi-mode operation, two sets of steady-state engine maps and transient correction parameters were combined for the relevant speed and load operating regions. The engine controller model is not calibrated for transient operation however. Mode-switching behavior is not accounted for in this study (perfect step change). A limitation of this simulation is that the multi-mode map uses an RCCI map with modified pistons, while the CDC map was created using the stock pistons.

The fuel economy and emissions from the simulated conventional vehicle over multiple urban and highway driving cycles, including the UDDS, the Highway Fuel Economy Driving Schedule (HWFET), US06, and New York City driving cycles, were completed. Hot cycle simulations were performed in which standard transmission controls are applied and the engine switches from CDC into RCCI when speed and load fall in the allowed RCCI range depicted in the RCCI enabled zone. No warm-up portion or cold start emissions were considered. The multi-mode RCCI and CDC fuel economy simulation results are compared to the same vehicle powered by a representative 2009 port-fuel injected gasoline engine over these multiple-standard EPA driving cycles.

Four drive cycles are used for vehicle systems simulations in this study. The UDDS is also known as the LA4 or city test and is used to represent city driving conditions. HWFET represents highway driving under 60 miles per hour. The US06 is an aggressive driving cycle that is also called the “supplemental FTP.” The New York City Schedule (NYC) represents stop-and-go driving and heavy traffic. Figure 31 shows RCCI coverage of speed and load over the different drive cycles and illustrates the need for multi-mode operation with the current RCCI map for both low- and high-load operation.

4 RESULTS

Vehicle systems simulations were performed for the RCCI multi-mode, 2009 gasoline PFI and CDC engines over all four of the drive cycles examined here.

4.1 Drive Cycle Coverage

The various drive cycles examined here have distinctly different power demands over the length of the cycle, as shown for each drive cycle in Figure 31. The amount of the drive cycle that the vehicle could run in RCCI mode varied significantly, as shown in Table 11. The UDDS, which represents city driving, had 72% of the cycle by distance run in RCCI mode but only 55% by time since significant portions of the DC were very low load with interspersed periods of idle. The HWFET, which is representative of highway driving, had very little idling, and

RCCI mode was achievable over 88% of the DC by distance and 86% by time. Table 11 also summarizes the total diesel fuel used over the drive cycle including multi-mode operation as well as for RCCI mode. For all of the drive cycles except HWFET, multi-mode operation had more diesel fuel than gasoline. The percentage of diesel fuel (B20) used during RCCI-only mode ranged from a low of 31% in the high load US06, which would have a high amount of time run in high load RCCI, which would be predominately gasoline, to a low of 43% in the stop-and-go NYC.

4.2 Modeled Fuel Economy

The fuel economy results for multi-mode RCCI were compared with cases run with a 2009 PFI gasoline engine and CDC with the same base engine as the RCCI engine. Results over the four drive cycles are shown in Figure 32 and are summarized in Table 12. Multi-mode RCCI operation fuel economy improvements ranged from 39% for US06 to as high as 67% for NYCC. The improvements seen for the UDDS and HWFET were 59% and 53% respectively. The fuel economy improvements compared to CDC operation ranged from 8% to a high of 15%.

4.3 Modeled Emissions

The engine out emissions were modeled using the steady-state emissions data for CDC and RCCI multi-mode operation over the drive cycles and are presented in Table 13.

The reductions in city and highway NO_x were only between 17 and 21% compared to CDC operation mainly because of the high NO_x emissions as seen during the excursions in CDC mode during high load operation. The HC and CO emissions were significantly increased compared to CDC operation, both of which were low across the entire drive cycle.

Though not a focus of this study, the exhaust temperatures during the drive cycles were also simulated in Autonomie. It was found that the exhaust temperatures during RCCI multi-mode were significantly lower than CDC only operation, as shown in Figure 33. This is to be expected from the previous experimental results but puts the future aftertreatment integration challenges into perspective.

4.2 Comparison to PFI Fuel Economy

The vehicle systems simulations were performed for only one 4.0 L PFI gasoline engine. The engine was matched in terms of torque but not for power or vehicle acceleration. To put the results of the fuel economy modeling into

perspective, the EPA database was mined for 2009 PFI vehicle data and are shown in Figure 34. For the HWFET results, the raw HWFET values are shown in Figure 35.

The results are summarized in Table 14 and show that for both the UDDS and HWFET, multi-mode RCCI operation offers a greater than 15% fuel economy improvement for all vehicles examined.

5 SUMMARY/CONCLUSIONS

Multi-mode operation was shown through vehicle system simulations using experimental engine data to have the potential to offer greater than 15% fuel economy improvement over a 2009 gasoline PFI baseline over many light-duty driving cycles. RCCI fuel economy improvements were observed despite lack of complete drive cycle coverage. The results showed how much of an effect multi-mode operation can have on engine out NO_x emissions depending on the amount of the drive cycle coverage that RCCI operation can allow. Modeled drive cycle emissions results showed between 17 and 21% reduction in NO_x with multi-mode RCCI compared with diesel-only operation. If an engine has to switch to CDC operation during high engine loads, the engine out NO_x will be very high and quickly can degrade the NO_x reduction potential of a multi-mode RCCI strategy.

Fuel usage over the drive cycles showed that nearly equal amounts of gasoline and diesel fuel would most likely be needed to be carried on board for RCCI multi-mode operation. During RCCI only operation, fuel usage was found to be between 57 and 69% gasoline.

Limitations of the study include the use of a multi-mode operating map that switched between piston types; a follow-up study is planned to create a multi-mode RCCI operating map using only the RCCI modified pistons. Further development into pistons that are suited for multi-mode operation is also of interest. Other limitations included the lack of transient engine performance for same mode and mode switching to calibrate the model that would account for transient performance.

Disclaimer

This manuscript has been authored by a contractor for the US Government under contract number DE-AC05-00OR22725. Accordingly, the US Government retains a nonexclusive, royalty-free license to publish or reproduce the published form of this contribution, or allow others to do so, for the US Government.

Acknowledgments

This work was supported by the US Department of Energy (DOE) Office of Vehicle Technologies. The authors gratefully acknowledge the support and guidance of Gurprett Singh, Ken Howden, Kevin Stork, and Steve Przesmitzki at DOE. The authors would like to acknowledge the input from their colleagues at the University of Wisconsin, Professor Rolf Ritz and Sage Kokjohn, and support from General Motors and Delphi.

References

1. US Department of Energy, Office of Vehicle Technologies Multi-Year Program Plan 2011-2015, 2010, www1.eere.energy.gov/vehiclesandfuels/pdfs/program/vt_mypp_2011-2015.pdf.
2. Vehicle Technologies Office. Advanced Combustion Engines, www1.eere.energy.gov/vehiclesandfuels/technologies/engines/index.html.
3. US Environmental Protection Agency, Testing and Measuring Emissions, www.epa.gov/nvfe/testing/dynamometer.htm.
4. Sluder C, Wagner R, Storey J, et al. Implications of Particulate and Precursor Compounds Formed During High-Efficiency Clean Combustion in a Diesel Engine. SAE 2005-01-3844, 2005.
5. Wagner R, Green J, Dam T, et al. Simultaneous Low Engine-Out NOX and Particulate Matter with Highly Diluted Diesel Combustion. SAE 2003-01-0262, 2003.
6. Sluder C, Wagner R, Lewis S, et al. Fuel Property Effects on Emissions from High Efficiency Clean Combustion in a Diesel Engine. SAE Technical Paper 2006-01-0080, 2006.
7. Sluder C and Wagner R. An Estimate of Diesel High-Efficiency Clean Combustion Impacts on FTP-75 Aftertreatment Requirements. SAE 2006-01-3311, 2006.
8. Cho K, Han M, Wagner R, et al. Mixed-Source EGR for Enabling High-Efficiency Clean Combustion Modes in a Light-Duty Diesel Engine. SAE 2008-01-0645, 2008.
9. Inagaki K, Fuyuto T, Nishikawa et al. Dual-Fuel PCCI Combustion Controlled by In-Cylinder Stratification of Ignitability. SAE paper 2006-01-0028, 2006.
10. Chadwell C, Alger T, Roberts C, et al. Boosting Simulation of High Efficiency Alternative Combustion Mode Engines. SAE 04-12-2011, 2011.
11. Manente V, Johansson B, and Tunestal P. Partially Premixed Combustion at High Load using Gasoline and Ethanol, a Comparison with Diesel. SAE 04-20-2009, 2009.
12. Kokjohn S, Hanson R, Splitter D, et al. Experiments and Modeling of Dual-Fuel HCCI and PCCI Combustion Using In-Cylinder Fuel Blending. SAE 2009-01-2647, 2009.
13. Splitter D, Hanson R, Kokjohn S, et al. Reactivity Controlled Compression Ignition (RCCI) Heavy-Duty Engine Operation at Mid-and High-Loads with Conventional and Alternative Fuels. SAE 2011-01-0363, 2011.
14. Hanson R, Kokjohn S, Splitter D, et al. An Experimental Investigation of Fuel Reactivity Controlled PCCI Combustion in a Heavy-Duty Engine. SAE 2010-01-0864, 2010.
15. Kokjohn S, Reitz R, Splitter D, et al. Investigation of Fuel Reactivity Stratification for Controlling PCI Heat-Release Rates Using High-Speed

Chemiluminescence Imaging and Fuel Tracer Fluorescence. SAE 2012-01-0375, 2012.

16. Kokjohn S, Hanson R, Splitter D, et al. Fuel Reactivity Controlled Compression Ignition (RCCI) Combustion in Light- and Heavy-Duty Engines. SAE 2011-01-0357, 2011.

17. Curran S, Prikhodko V, Cho K, et al. In-Cylinder Fuel Blending of Gasoline/Diesel for Improved Efficiency and Lowest Possible Emissions on a Multi-Cylinder Light-Duty Diesel Engine. SAE 2010-01-2206, 2010.

18. Curran S, Cho K, Briggs T, et al. Drive Cycle Efficiency and Emissions Estimates for Reactivity Controlled Compression Ignition in a Multi-Cylinder Light-Duty Diesel Engine. In: Proceedings of the 2011 Internal Combustion Engine Division Fall Technical Conference, ICEF2011, Morgantown WV, 2011.

19. Curran S, Hanson R, and Wagner R. Effect of E85 on RCCI Performance and Emissions on a Multi-Cylinder Light-Duty Diesel Engine. SAE 2012-01-0376, 2012.

20. Curran S, Hanson R, and Wagner R. Reactivity controlled compression ignition (RCCI) combustion on a multi-cylinder light-duty diesel engine, *International Journal of Engine Research* 2012; 13(3): 216–225.

21. Hanson R, Curran S, Reitz R, et al. Piston optimization for RCCI in Light-Duty Multi-Cylinder Engine. SAE Paper 2012-01-0380, 2012.

22. Curran S, Szybist J, and Wagner R. Reactivity Controlled Compression Ignition Performance with Renewable Fuels.” ICEF2012-92192, In: Proceedings of the ASME 2012 Internal Combustion Engine Division Fall Technical Conference, ICEF2012, September 23-26, 2012, Vancouver, BC, Canada, 2012.

23. Hanson R, Curran S, Reitz R, et al. Effects of Biofuel Blends on RCCI combustion in a Light-Duty, Multi-Cylinder Diesel Engine. SAE 2013-01-1653, 2013.

24. Kokjohn S, and Reitz R. Reactivity controlled compression ignition and conventional diesel combustion: A comparison of methods to meet light-duty NOx and fuel economy targets. *International Journal of Engine Research* 2013; 14(5): 452-468.

24. Prikhodko V and Parks J. Implications of Low Particulate Matter Emissions on System Fuel Efficiency for High Efficiency Clean Combustion. SAE 2009-01-2709, 2009.

25. Sluder C, Wagner R, Storey J, et al. Implications of Particulate and Precursor Compounds Formed During High-Efficiency Clean Combustion in a Diesel Engine. SAE technical paper 2005-01-3844, 2005.

26. Gopal R and Rousseau A. System Analysis Using Multiple Expert Tools. SAE technical paper, 2011-01-0754, 2011.

27. Gao Z, Conklin J, Daw C, et al. A proposed methodology for estimating transient engine-out temperature and emissions from steady state maps. *International Journal of Engine Research* 2009; 11: 137.

28. Gao Z, Daw C, Wagner R, et al. Simulating the impact of premixed charge compression ignition on lightduty diesel fuel economy and emissions of particulates and NOx. *Journal of Automobile Engineering* 2012; 0(0): 1-21.
29. Curran S, Hanson R, Reitz R, et al. Efficiency and Emissions Mapping of RCCI in a Light-Duty Diesel Engine. SAE 2013-01-0289, 2013.
30. Prikhodko V, Curran S, Barone T, et al. Emission Characteristics of a Diesel Engine Operating With In-Cylinder Gasoline and Diesel Fuel Blending. SAE 2010-01-2266, 2010.
31. Barone T, Storey J, Prikhodko V, et al. Particle Emissions Reduction by In-Cylinder Blending of Gasoline and Diesel Fuel, 21st CRC Real World Emissions Workshop, San Diego CA, 2011.

Appendix 2.1

Table 7. Experimental engine specifications

Specification	Value
Displacement, liters	1.9
Number of cylinders	4
Bore, mm	82.0
Stroke, mm	90.4
Compression ratio	15.1
Rated power, kW	110
Rated torque, Nm	315

Table 8. Experimental diesel injector specifications

Specification	Value
Number of nozzle holes	7
Included spray angle, °	148

Table 9. Experimental PFI injector specifications

Specification	Value
Number of nozzle holes	4
Cone angle, °	15
Separation angle, °	22

Table 10. Experimental fuel properties

Specification	UTG-96	B20
Lower heating value (kJ/kg)	43124	41653
Specific gravity	0.7389	0.862
H (weight %)	13.9	12.9
C (weight %)	86.1	85.0
Oxygen (weight %)	0.0	2.1
Aromatics (weight %)	32.7	-
Initial boiling point (°C)	34	-
Final boiling point (°C)	185	-
Research octane number (RON)	96.1	NA
Motor octane number (MON)	88.2	NA
(RON + MON)/2	92.1	NA
Cetane number	NA	43.8

Table 11. Multi-mode RCCI drive cycle performance

RCCI results	% DC by distance	% DC by time	Total diesel Fuel	% Diesel during RCCI
UDDS	72%	55%	56%	41%
HWFET	88%	86%	44%	37%
US06	66%	56%	66%	31%
NYCC	69%	36%	65%	43%

Table 12. Drive cycle fuel improvements with multi-mode RCCI operation compared with PFI and CDC

% Fuel economy improvement with RCCI	Vs PFI (%)	Vs CDC (%)
UDDS (city)	59	14
HWFET (highway)	53	15
US06 (high speed)	39	8
NY City (stop and go)	67	13

Table 13. Modeled emissions reductions compared with CDC operation (number with a plus sign in red indicates increases)

Reductions	NO_x (%)	HC (%)	CO (%)
With RCCI			
UDDS	17	+240	+150
HWFET	21	+300	+140
US06	8	+310	+140
NY City	+4	+220	+150

Table 14. Multi-mode RCCI fuel economy compared with downsized PFI engines

	4.0L PFI Baseline Comparison	2.4L PFI	2.0L PFI	1.8L PFI
UDDS RCCI Improvement	59%	33%	22%	15%
PFI UDDS_mpg	23.6	27.5	29.6	32.6
HWFET RCCI Improvement	53%	34%	30%	19%
PFI HWFET_mpg	37.5	42.6	43.9	48.1

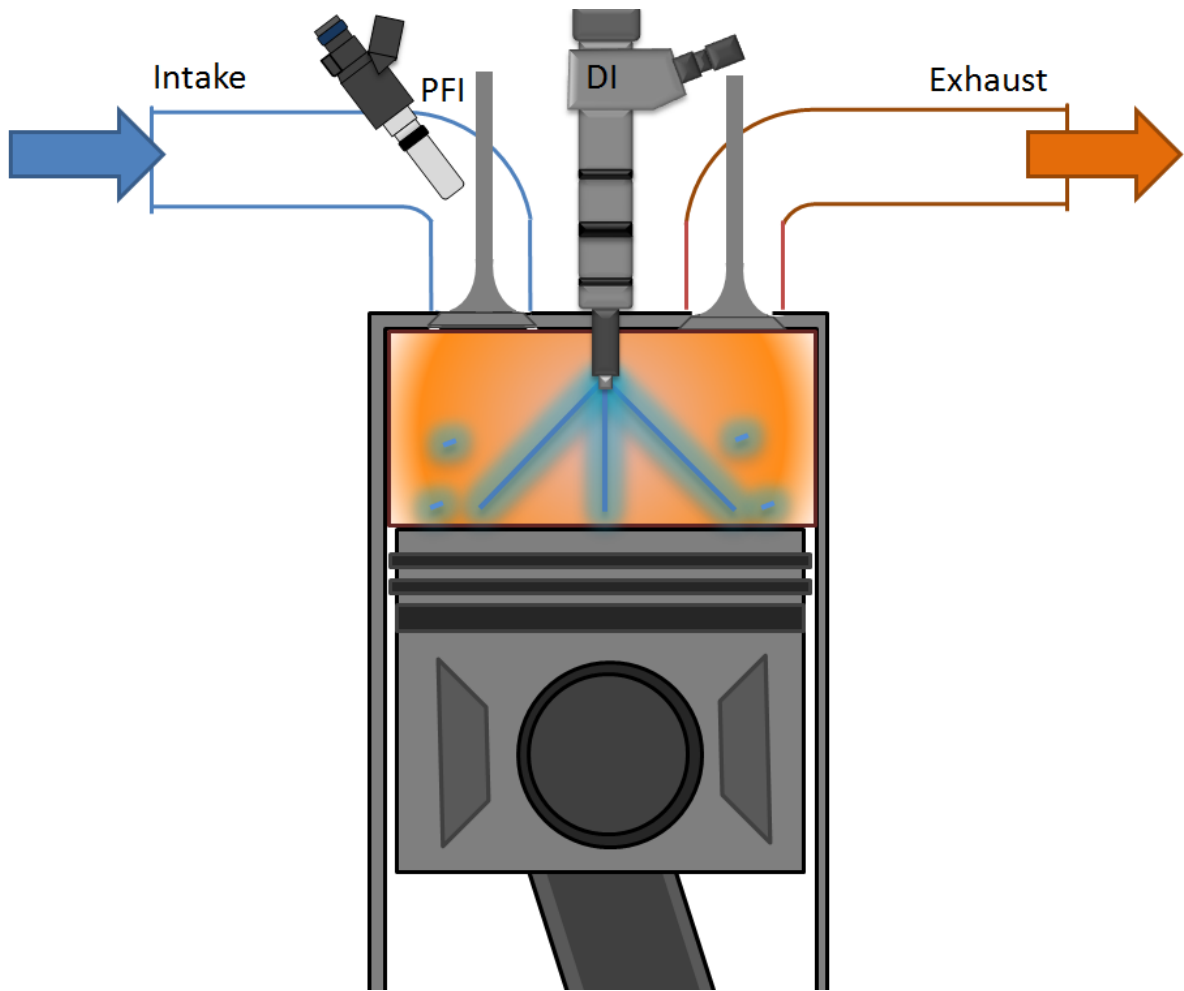


Figure 21. Dual-fuel RCCI injection strategy for experiments.

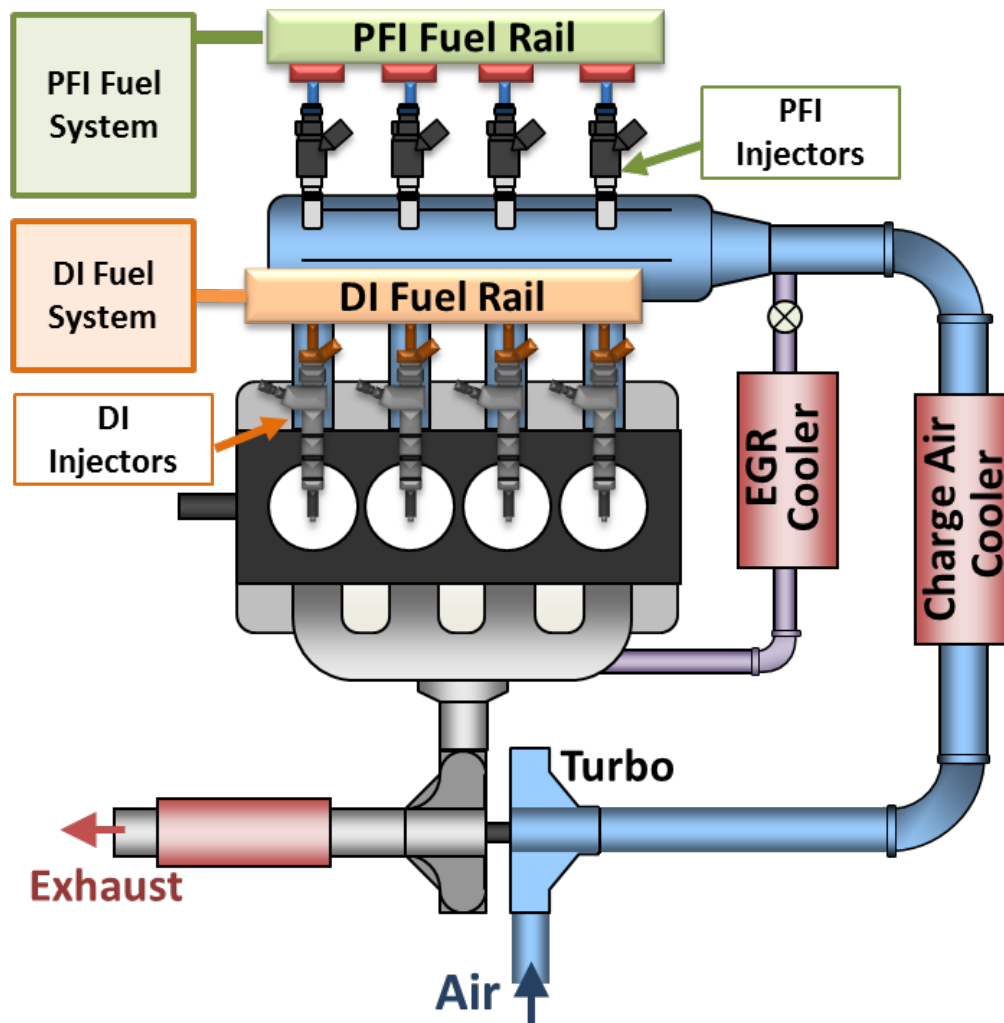


Figure 22. Experimental ORNL multi-cylinder RCCI engine.

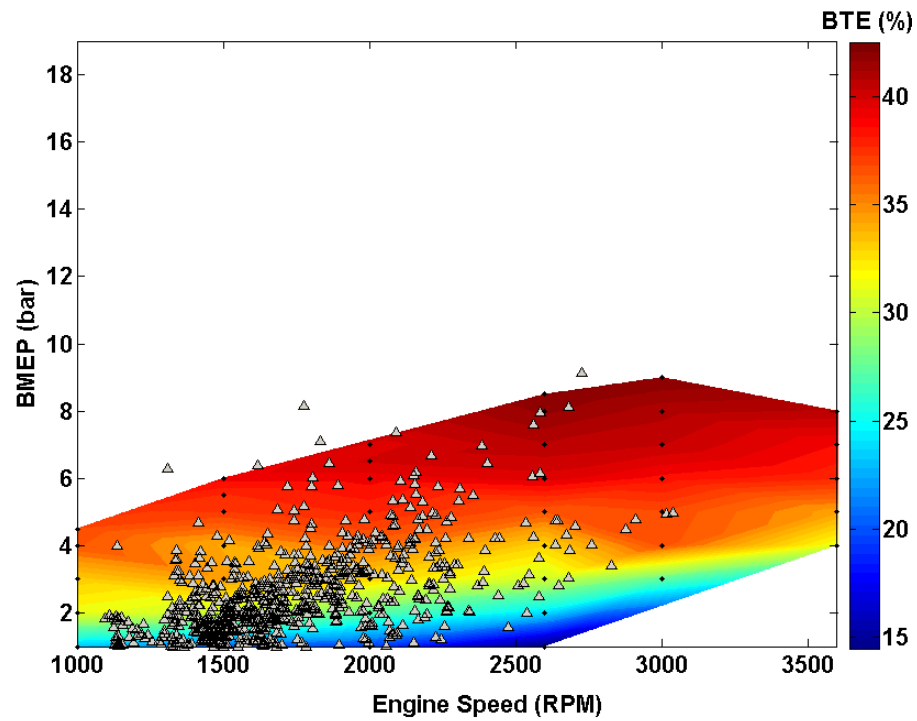


Figure 23. Experimental RCCI map with UDDS drive cycle point overlain.

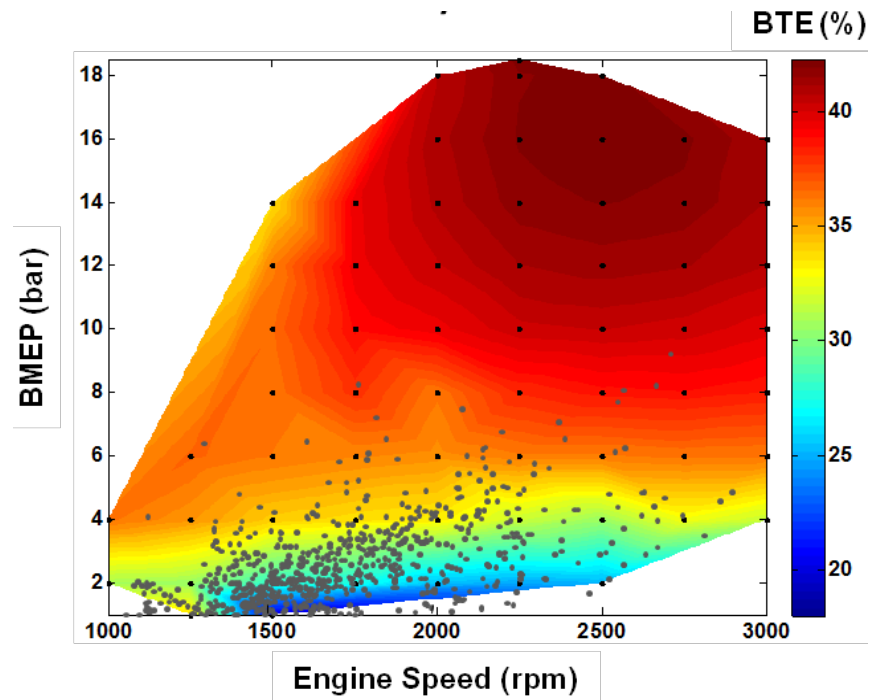


Figure 24. Experimental CDC map with stock pistons with UDDS drive cycle point overlain.

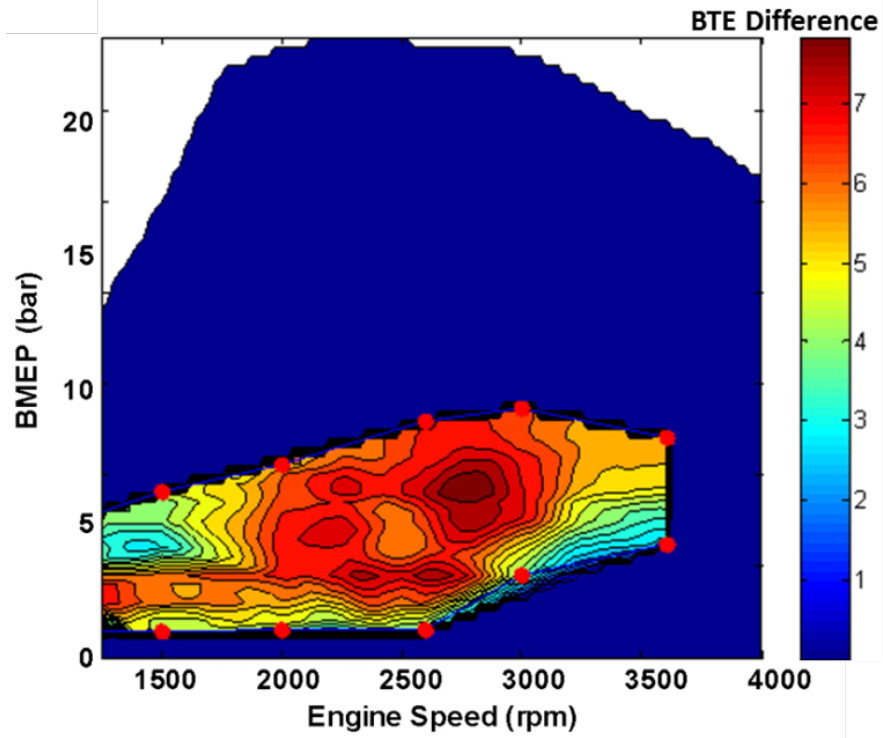


Figure 25. Difference in RCCI and CDC BTE.

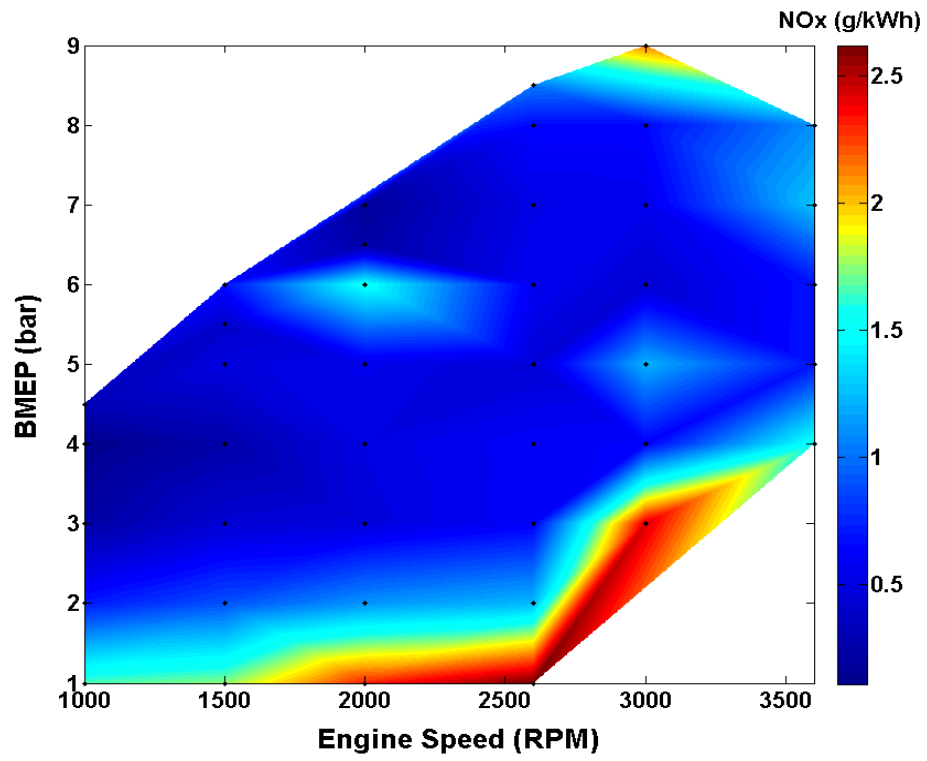


Figure 26. Experimental RCCI NO_x.

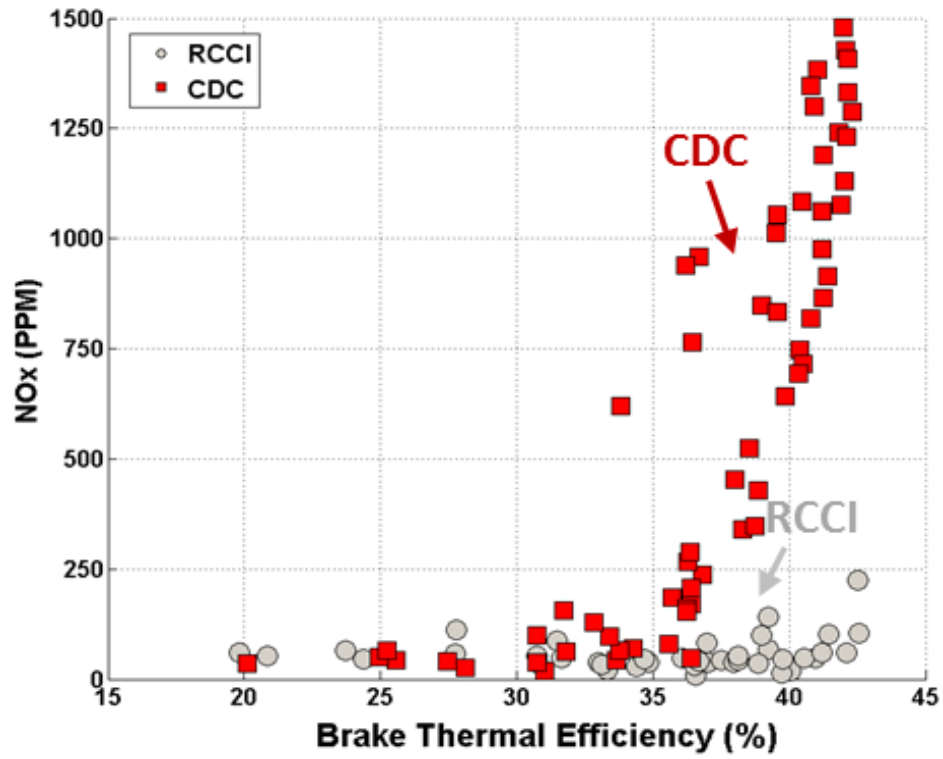


Figure 27. RCCI engine out NOx compared with CDC (grey circles).

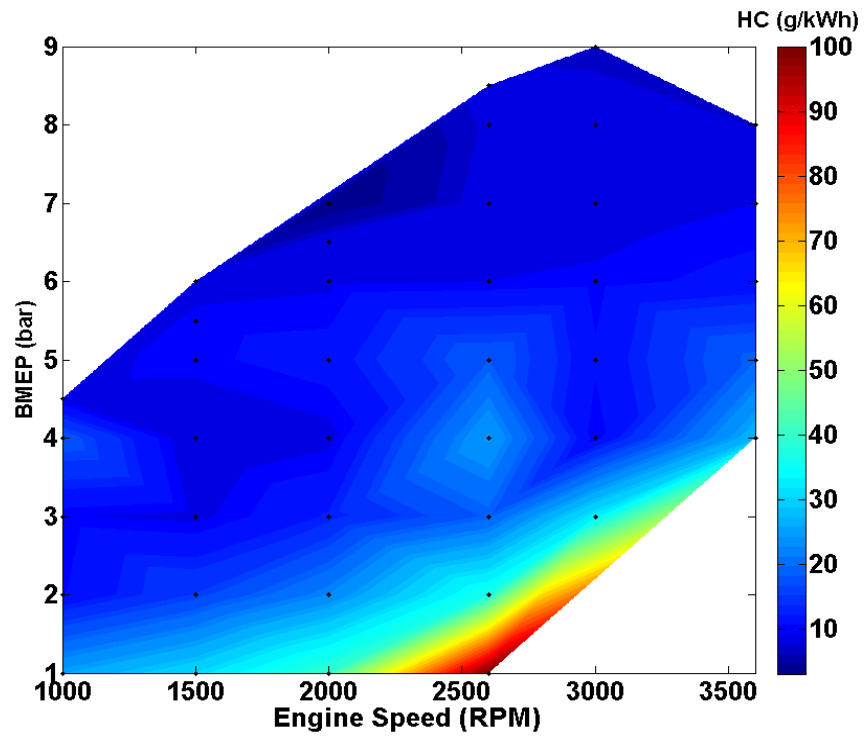


Figure 28. Experimental RCCI HC emissions.

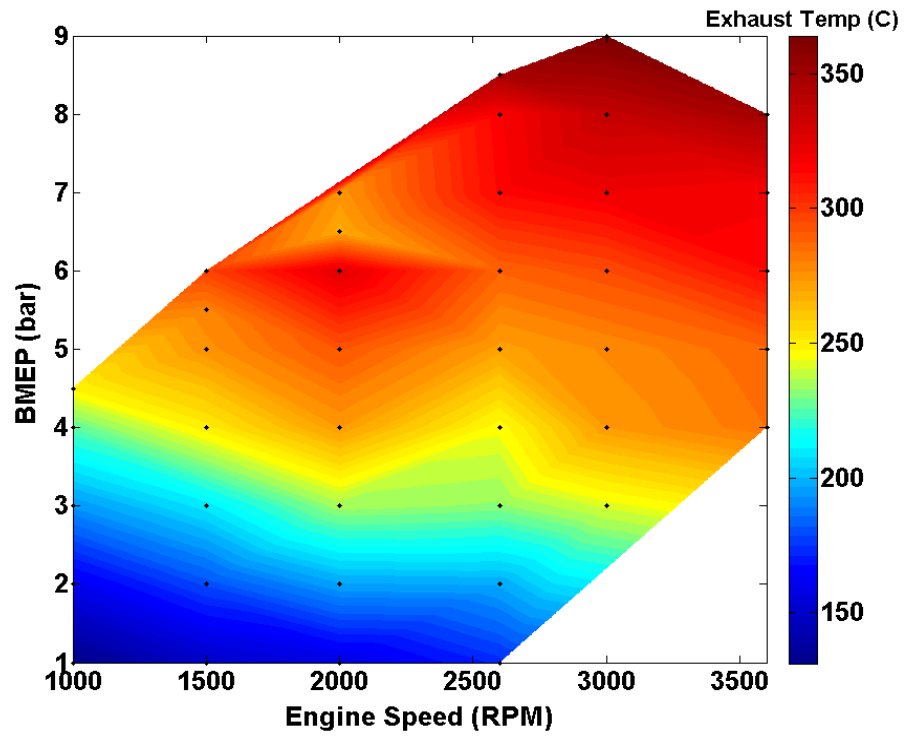


Figure 29. Experimental RCCI exhaust temperature.

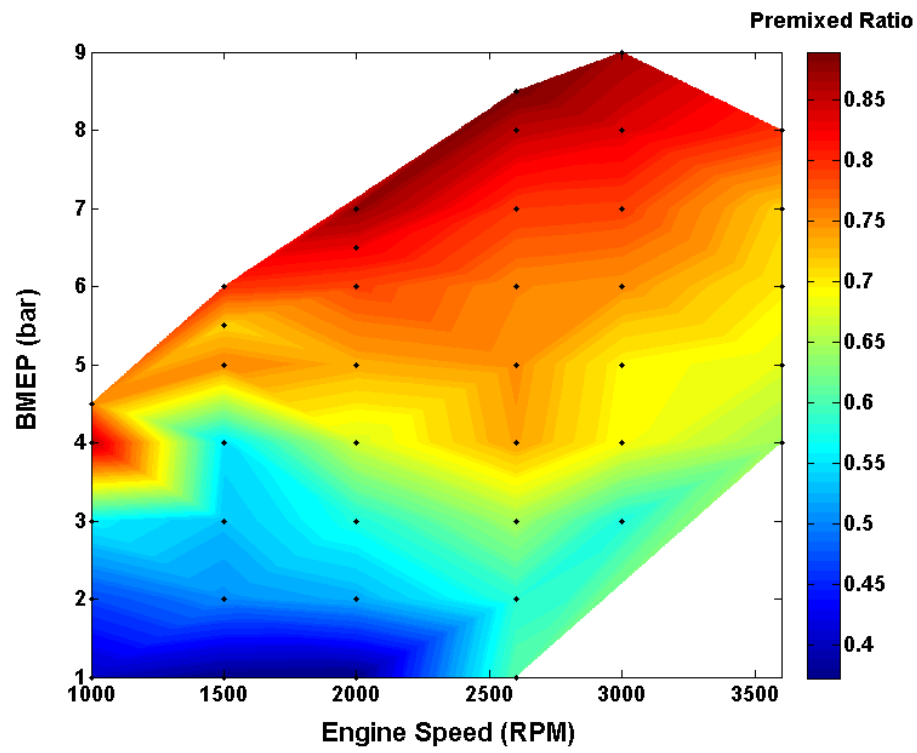


Figure 30. Experimental RCCI premixed ratio.

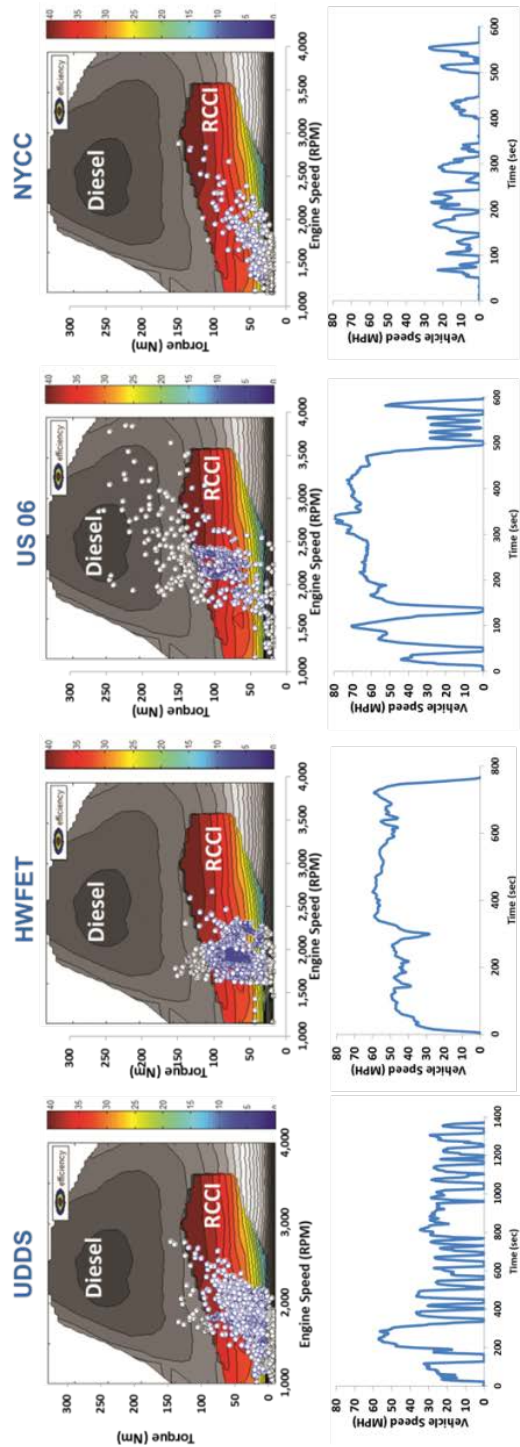


Figure 31. RCCI coverage of various drive cycles investigated with 1 HZ engine speed and load points overlain.

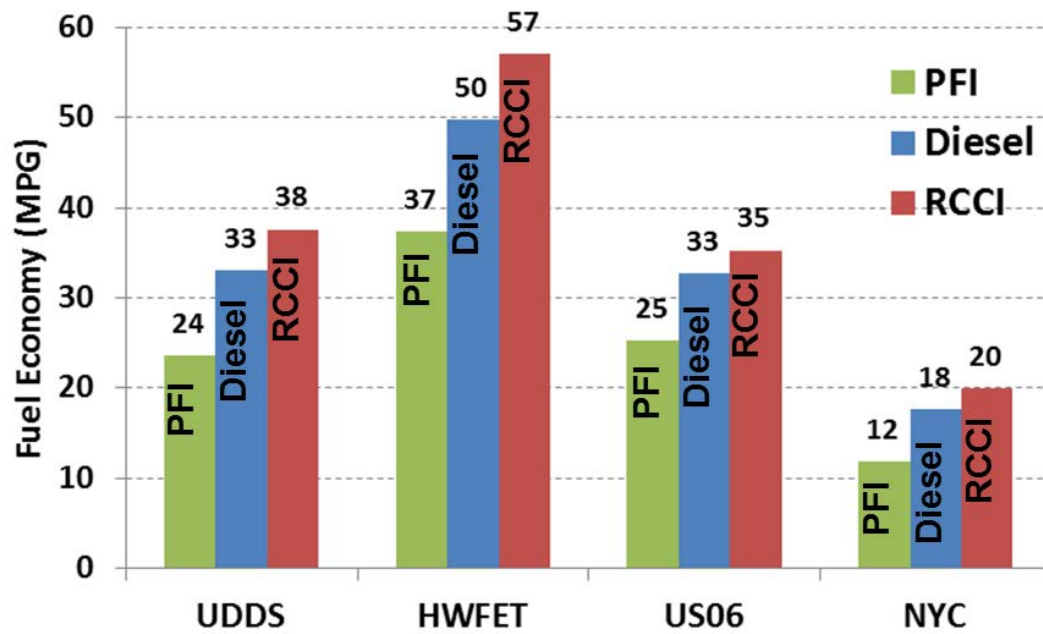


Figure 32. Drive cycle fuel economy for PFI, CDC, and multi-mode RCCI operation.

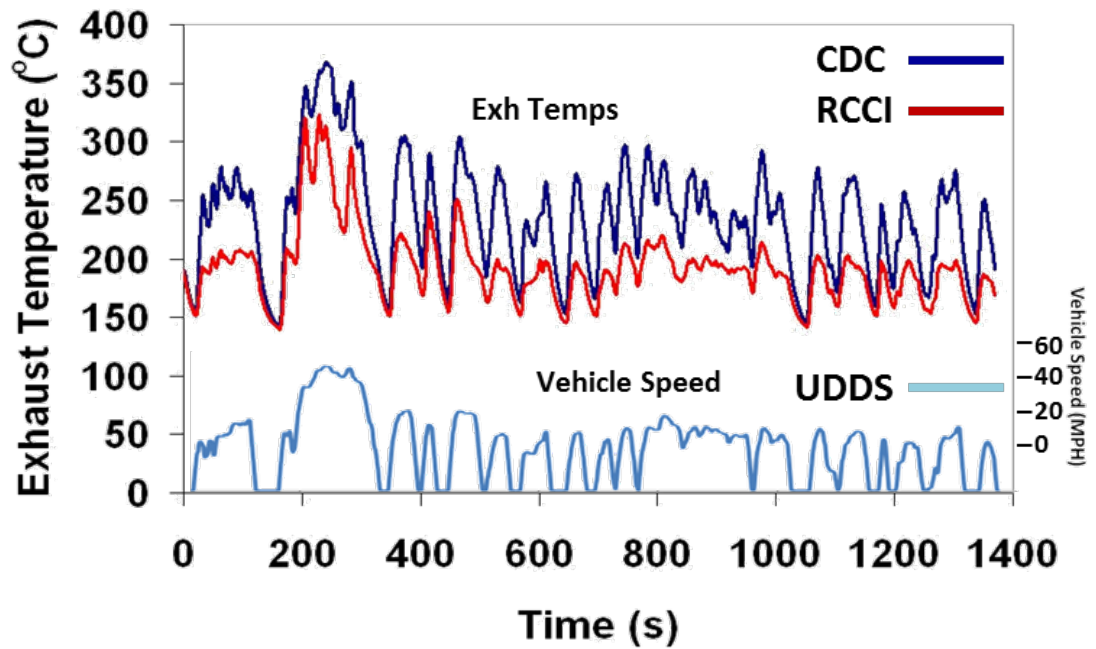


Figure 33. Modeled exhaust temperatures for CDC and RCCI over the UDDS.

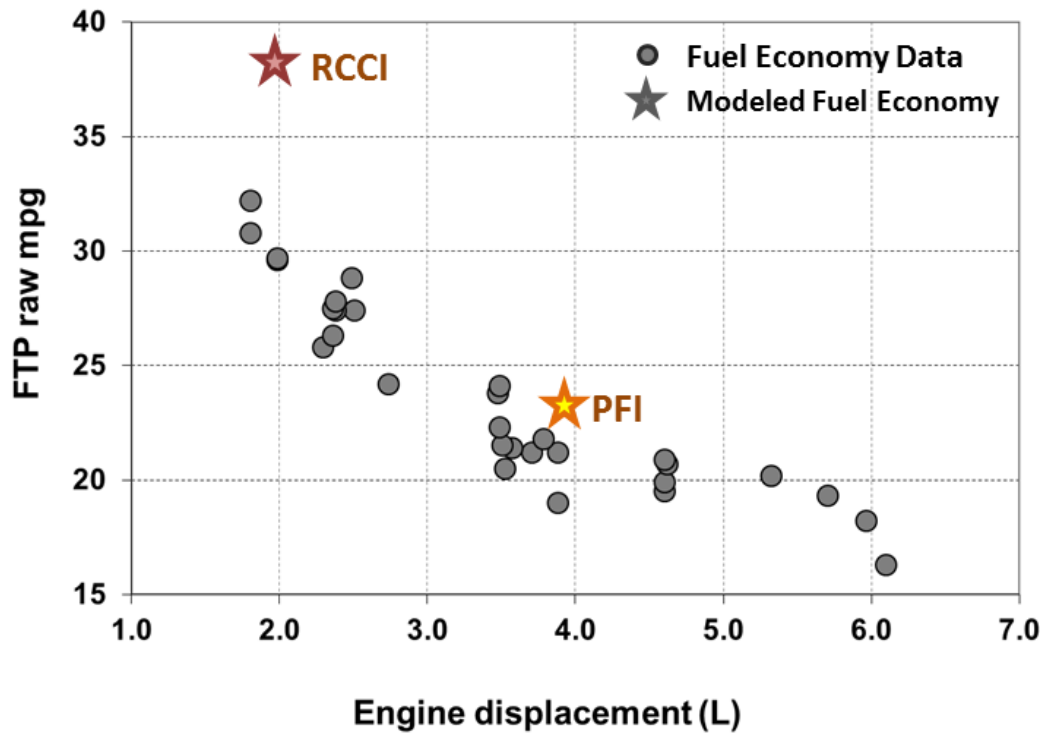


Figure 34. FTP (UDDS) fuel economy for PFI engines of various displacement with the modeled RCCI (red star) and modeled PFI data (yellow star).

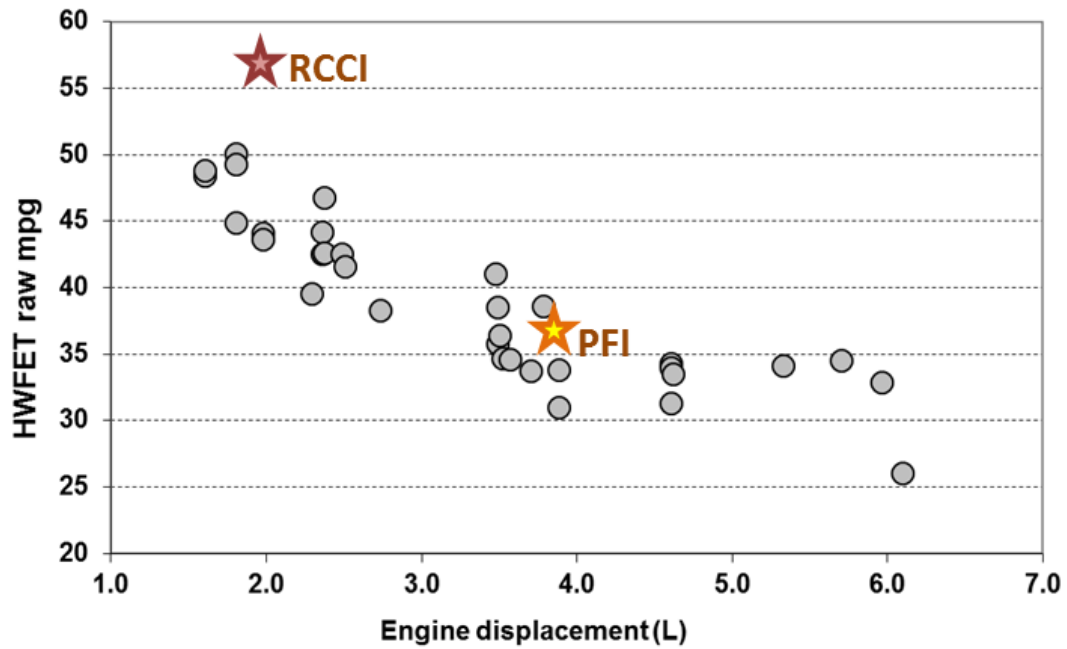


Figure 35. HWFET fuel economy for PFI engines of various displacement with the modeled RCCI (red star) and modeled PFI data (yellow star).

Appendix 2.2

Table 15. B20 Map Performance

BMEP (bar)	Torque (ft-lb)	Diesel Rate (g/s)	Gasoline rate (g/s)	rp	BTE (%)	D_eq BSFC (g/kwhr)
7.0	78.68	0.387	1.036	0.712	38.75	228.0
1.0	11.11	0.095	0.063	0.403	23.74	355.2
2.0	22.83	0.130	0.113	0.470	31.64	266.7
3.0	33.80	0.152	0.190	0.561	33.32	253.6
4.0	45.13	0.058	0.355	0.861	36.58	232.0
4.5	50.56	0.115	0.344	0.753	37.00	229.1
1.0	10.89	0.167	0.098	0.376	20.85	404.2
2.0	22.66	0.186	0.187	0.505	30.75	274.6
3.0	33.40	0.228	0.257	0.534	34.84	242.4
4.0	45.18	0.301	0.363	0.552	34.40	245.6
5.0	56.33	0.188	0.568	0.755	37.52	225.9
5.5	62.57	0.236	0.595	0.720	37.97	223.1
6.0	66.99	0.173	0.686	0.802	39.24	216.1
1.0	11.70	0.253	0.147	0.372	19.83	424.9
2.0	22.81	0.266	0.288	0.525	27.75	304.4
3.0	33.77	0.295	0.395	0.578	33.00	256.1
4.0	45.32	0.280	0.565	0.673	36.09	234.5
5.0	56.91	0.269	0.735	0.736	38.12	222.3
6.0	67.14	0.247	0.901	0.789	39.25	216.0
6.5	73.10	0.209	1.015	0.832	40.07	211.7
7.0	78.46	0.162	1.161	0.879	39.73	213.7
1.0	11.05	0.264	0.405	0.610	14.48	584.1
2.0	22.52	0.340	0.469	0.585	24.38	346.7
3.0	33.57	0.339	0.615	0.649	30.77	275.0
4.0	44.93	0.311	0.875	0.742	33.10	256.0
5.0	56.93	0.347	1.013	0.749	36.54	231.9
6.0	67.22	0.365	1.110	0.756	39.78	213.0
7.0	79.00	0.350	1.334	0.795	40.94	207.1
8.0	90.06	0.272	1.591	0.856	42.13	201.5
8.5	95.44	0.216	1.736	0.891	42.56	199.5

Table 15. Continued

BMEP (bar)	Torque (ft-lb)	Diesel Rate (g/s)	Gasoline rate (g/s)	rp	BTE (%)	D_eq BSFC (g/kwhr)
3.0	33.62	0.522	0.702	0.578	27.77	304.4
4.0	55.77	0.479	1.055	0.692	36.69	230.8
5.0	56.07	0.469	1.061	0.698	36.96	229.1
6.0	66.69	0.440	1.289	0.749	38.85	218.1
7.0	78.95	0.416	1.545	0.791	40.53	209.2
8.0	89.56	0.355	1.831	0.840	41.21	205.9
9.0	100.97	0.314	2.074	0.871	42.51	199.7
4.0	45.62	0.627	1.129	0.648	31.48	268.8
5.0	55.79	0.632	1.315	0.680	34.69	244.1
6.0	67.02	0.639	1.489	0.704	38.11	222.2
7.0	70.93	0.627	1.574	0.719	38.99	217.2
8.0	89.03	0.523	2.070	0.802	41.47	204.5

Table 16. B20 Map Emissions

Speed (RPM)	BMEP (bar)	EGR Rate (%)	AFR mass	HC (ppm)	NOx	CO_High	CO2 In	CO2 Ex	O2 In	O2 Ex
2000	7.0	0.00	34.2	2818	15.9	1338	0.0	5.7	21.1	12.9
1000	1.0	49.74	43.8	3329	64.4	4856	2.3	4.6	17.6	13.9
1000	2.0	40.38	34.4	2368	46.8	3651	2.5	6.1	17.4	12.1
1000	3.0	35.48	26.7	2990	20.4	2327	2.7	7.7	17.1	10.0
1000	4.0	0.78	37.6	4318	7.6	1888	0.0	5.1	21.0	13.6
1000	4.5	27.55	22.7	3593	37.4	1399	2.5	9.0	17.5	8.4
1500	1.0	40.65	50.6	3058	51.6	4381	1.3	3.3	19.0	15.8
1500	2.0	36.23	37.2	3171	53.5	4237	1.7	4.7	18.5	13.9
1500	3.0	33.03	29.6	2638	37.4	2768	2.1	6.3	18.1	11.8
1500	4.0	30.28	21.6	2984	28.9	1692	2.5	8.3	17.5	9.3
1500	5.0	1.29	31.4	3024	42.7	1043	0.1	5.9	21.0	12.5
1500	5.5	1.03	29.7	3180	37.2	1207	0.1	6.1	21.0	12.3
1500	6.0	0.95	28.8	2968	66.9	1003	0.1	6.6	21.0	11.6
2000	1.0	38.57	54.1	3491	60.8	4355	1.2	3.2	19.1	16.0
2000	2.0	36.75	39.1	3897	57.0	4272	1.7	4.6	18.5	14.0
2000	3.0	36.72	31.4	3292	37.0	3006	2.3	6.1	17.8	12.0
2000	4.0	29.44	28.0	2864	47.2	1786	2.1	7.2	18.1	10.8
2000	5.0	1.23	34.5	3137	43.5	1429	0.1	5.7	21.0	12.8
2000	6.0	0.89	30.3	2972	141.7	903	0.1	6.7	21.0	11.4
2000	6.5	1.52	38.2	2409	18.0	1312	0.1	5.4	21.0	13.2
2000	7.0	1.41	37.2	775	14.6	60	0.1	6.0	21.0	12.6
2600	1.0	29.72	53.0	6588	52.0	4731	0.8	2.7	19.7	16.5
2600	2.0	26.68	47.2	4573	46.0	4904	0.9	3.5	19.6	15.4
2600	3.0	28.50	37.5	3782	36.1	4193	1.4	4.9	18.9	13.7
2600	4.0	1.65	43.3	4653	33.6	3426	0.1	4.0	21.0	14.9
2600	5.0	1.29	38.7	4282	31.5	3070	0.1	4.6	21.0	14.1
2600	6.0	0.85	36.9	2582	45.4	1740	0.0	5.3	21.0	13.3
2600	7.0	0.76	33.3	2662	47.1	1520	0.0	5.9	21.0	12.5
2600	8.0	0.73	32.6	2578	60.6	1078	0.0	6.1	21.0	12.3
2600	8.5	0.64	30.2	2977	104.7	1136	0.0	6.6	21.0	11.6
3000	3.0	1.93	44.2	4941	110.5	4909	0.1	3.8	20.9	15.2
3000	4.0	1.65	39.8	2297	41.7	2758	0.1	4.8	20.9	14.1
3000	5.0	1.49	39.4	2525	82.0	2677	0.1	4.8	20.9	13.9

Table 16. Continued

Speed (RPM)	BMEP (bar)	EGR Rate (%)	AFR mass	HC (ppm)	NOx	CO_High	CO2 In	CO2 Ex	O2 In	O2 Ex
3000	6.0	1.26	36.5	2638	34.4	2585	0.1	5.2	20.9	13.4
3000	7.0	1.07	33.6	2573	48.2	1936	0.1	5.9	20.9	12.6
3000	8.0	0.98	32.1	2986	59.9	2142	0.1	6.1	21.0	12.2
3000	9.0	0.82	29.3	2466	224.2	814	0.1	7.0	21.0	11.1
3600	4.0	1.28	39.7	5243	87.6	4498	0.1	4.4	21.0	14.2
3600	5.0	1.17	39.0	4208	44.6	4707	0.1	4.6	21.1	14.0
3600	6.0	0.96	36.4	2925	51.9	3268	0.1	5.3	21.1	13.2
3600	7.0	0.90	36.0	2581	99.0	2214	0.1	5.6	21.1	12.8
3600	8.0	0.76	32.7	2391	100.8	1499	0.0	6.3	21.0	12.1

CHAPTER III
REACTIVITY CONTROLLED COMPRESSION IGNITION DRIVE
CYCLE EMISSIONS AND FUEL ECONOMY ESTIMATIONS USING
VEHICLE SYSTEMS SIMULATIONS WITH E30 AND ULSD

A version of this chapter was originally published by Scott Curran, Zhiming Gao and Robert Wagner:

S. J. Curran, Z. Gao, and R. M. Wagner, "Reactivity Controlled Compression Ignition Drive Cycle Emissions and Fuel Economy Estimations Using Vehicle Systems Simulations with E30 and ULSD", *SAE Int. J. Engines* Number: V123-3EJ; Published: 2014-07-20

The article is presented in its original form, formatted for this dissertation including renumbering tables and figures. Author was lead author and lead investigator on study. Coauthor Zhiming Gao performed the Autonomie simulations, and coauthor Robert Wagner's guidance and revisions were instrumental in its publication. Additional data for the E30 RCCI maps is presented in Appendix 3.2 for engine performance and emissions.

Abstract

In-cylinder blending of gasoline and diesel to achieve reactivity controlled compression ignition (RCCI) has been shown to reduce NO_x and PM emissions while maintaining or improving brake thermal efficiency as compared to conventional diesel combustion (CDC). The RCCI concept has an advantage over many advanced combustion strategies in that the fuel reactivity can be tailored to the engine speed and load allowing stable low-temperature combustion to be extended over more of the light-duty drive cycle load range. However, the current range of the experimental RCCI engine map investigated here does not allow for RCCI operation over the entirety of some drive cycles and may require a multi-mode strategy where the engine switches from RCCI to CDC when speed and load fall outside of the RCCI range. The potential for RCCI to reduce drive cycle fuel economy and emissions is explored here by simulating the fuel economy and emissions for a multi-mode RCCI-enabled vehicle operating over a variety of U.S. drive cycles using experimental engine maps for multi-mode RCCI with E30 and ULSD, CDC and a variety of 2009 port-fuel injected (PFI) gasoline engines ranging from 1.8L to 4.0L. Simulations are completed assuming a conventional mid-size passenger vehicle with an automatic transmission that is optimized for each engine. RCCI fuel economy simulation results are compared to the same vehicle powered by a representative 2009 PFI gasoline engine over multiple drive cycles and showing at least a 20% improvement in fuel economy over a PFI baseline. Engine-out drive cycle emissions are compared to CDC and observations regarding relative gasoline and diesel tank sizes needed for the various drive cycles are also summarized.

Introduction

The United States Department of Energy (DOE), Vehicle Technologies Office's (VTO) mission is to develop more energy-efficient and environmentally friendly highway transportation technologies that will enable the United States to use significantly less petroleum and reduce greenhouse gas emissions and criteria air pollutants [1]. Fuel efficiency improvements and petroleum displacement are the overarching goals of the DOE VTO and within these research activities, resolving the interdependent emissions challenges from high efficiency engines is important. Emissions challenges are relevant not only in terms of market barrier and regulatory standpoints, but also in terms of total engine system fuel efficiency. Engine system efficiency includes not only the fuel energy required for the production of motive or shaft power, but also the fuel penalties associated with exhaust aftertreatments and sub-optimal combustion (i.e. stoichiometric spark ignition allowing a three-way catalyst or retarded injection timing for NO_x control in compression ignition engines). For diesel engines operating lean, these fuel penalties include fuel regeneration of diesel particulate filters (DPF) and either fuel regeneration of lean NO_x traps (LNT), or reductant addition for selective catalytic reduction (SCR) systems. Within the DOE VTO, the Advanced Combustion Engine research and development subprogram's strategic goals are to reduce petroleum dependence by removing critical technical barriers to mass commercialization of high-efficiency, emissions-compliant internal combustion engine powertrains in passenger and commercial vehicles [2]. Improvements in engine efficiency and engine systems efficiency through advanced combustion strategies is an important pathway to this goal. For advanced combustion strategies to be able to meet these goals, their effectiveness over driving cycles [3] will have to be determined.

In the United States, the U.S. Environmental Protection Agency (EPA) regulates emissions based on federal drive cycle compliance [3]. There are a number of EPA dynamometer driving cycles which attempt to take into account the real world driving conditions seen with light-duty passenger vehicles. If a the engine cannot be operated in an advanced combustion mode over the entire speed and load range demanded by all the regulatory drive-cycles, then the engine would have to operate in a multi-mode strategy in which the engine would switch to a conventional combustion mode when engine power demands cause the engine to operate outside of the advanced combustion speed and load operating range. The need for multi-mode operation has implications for the design of the fuel system and combustion geometry to allow this as well as the aftertreatment system which will need to allow for emissions compliance over both modes.

In-cylinder blending of gasoline and diesel to achieve reactivity controlled compression ignition (RCCI) has been shown to reduce NO_x and PM emissions while maintaining or improving brake thermal efficiency as compared to conventional diesel combustion (CDC). The ability to control the percent

premixed low reactivity fuel along with the timing and number of injections of the direct injected high reactivity fuel reactivity allows for not only reactivity stratification but also temperature and equivalence ratio stratification in the cylinder providing further control of combustion phasing and cylinder pressure rise rate. The RCCI concept as shown in Figure 36, has an advantage over many advanced combustion strategies [4 – 11] in that the fuel reactivity can be tailored to the engine speed and load allowing stable low-temperature combustion to be extended over more of the light-duty drive cycle load range [12] and allow for increased controllability over the combustion process.

Previous computational fluid dynamics (CFD) modeling and single cylinder engine (SCE) results have demonstrated high gross thermal efficiencies (GTE) with ultra-low NO_x and soot emissions with RCCI. Thorough reviews of RCCI SCE experiments and CFD modeling advances can be found in papers by Kokjohn, Splitter, Hanson and Reitz [12-16].

Previous experiments have investigated the translational effects of taking CFD modeling and single cylinder engine experiments to multi-cylinder engines (MCE) on efficiency, emissions, and controls [17-23]. These effects include the behavior of real turbomachinery, effects of real EGR, cylinder to cylinder imbalances and swirl with production viable engine components. Despite the translational effects, MCE RCCI has been shown to be capable of diesel-like efficiency at lower engine loads and greater than diesel efficiency at higher engine loads with an order of magnitude reduction in engine out NO_x as compared to CDC. Previous experiments have shown the benefits of increased control over the combustion process allowed by RCCI operation on extending the operating range of low temperature combustion (LTC) compared to diesel premixed charge compression ignition (PCCI) on a multi-cylinder light-duty compression ignition engine [19, 20].

There have been a number of studies examining the potential for multi-mode LTC/CDC operation with diesel engine baselines for PCCI and more recently RCCI [24, 25]. For LTC/CDC multi-mode operation, the engine switches to CDC for areas of the engine map that fell outside LTC region. The need for multi-mode operation has implications for the needs of the aftertreatment system to be able to meet stringent federal emissions standards over the prescribed drive cycles, namely for NO_x control if the engine has to switch to CDC mode for higher loads in regions of the map that produce high amounts of NO_x . It is difficult to draw conclusions on light-duty drive cycle fuel economy and emissions performance for combustion strategies in the development stage which only have demonstrated a limited number of steady state operating points. To date there have been few published studies that investigate the potential vehicle fuel economy improvements that RCCI could allow. Previous studies by Curran et al. [19, 20] looked at using the Fuels Working group's ad-hoc modal points [7] to estimate drive cycle emissions with RCCI as compared to

conventional diesel combustion. These modal points are representative of key areas of the federal drive testing protocol and have weighting factors attached to them linked to the amount of drive cycle spent at similar conditions. That work showed that the ability to obtain noise constrained RCCI operation over all of the ad-hoc modal points was dependent on the fuels used. The light-duty MCE experiments showed that the hard acceleration modal point of 2600 RPM, 8.8 bar BMEP was not obtainable with a 46 Cetane ULSD and certification gasoline with an RON of 96 (UTG-96) [20] while adhering to a cylinder pressure rise rate limit of 10bar/deg. A follow-up study showed that the 2600 RPM, 8.8 bar BMEP point was achievable with RCCI using E85 and ULSD [19]. The results of the RCCI modal point studies showed significant weighted composite NO_x reductions (~66%) were made possible with RCCI operation as compared to CDC. The results also showed significant increases in engine out HC and CO emissions resulted from RCCI operation. The RCCI modal point studies only examined estimated drive cycle emissions and did not attempt to apply the weighting factors to fuel economy improvements.

Vehicle systems simulation tools such as Autonomie developed by Argonne National Laboratory for the Department of Energy can be used to simulate vehicle operation using model based simulations [26]. The simulations use performance based measurements including fuel consumption and exhaust properties such as emissions and temperature which are tabulated allowing for the generation interpolated response surfaces over the entire operating range of the engine maps. Previous work by Gao et al. has demonstrated the use of steady state engine maps in transient drive cycle simulations [27, 28]. Previous work by Gao has examined this type of simulation with multi-mode advanced combustion steady state engine data for engine performance and emissions modeling [28].

Initial drive cycle performance modeling using vehicle systems simulations using engine maps [29] derived from experimental data in Curran and Gao [showed multi-mode operation RCCI/CDC had the potential to offer greater than 15% fuel economy improvement over representative 2009 gasoline PFI baselines over many light-duty driving cycles [30]. RCCI fuel economy improvements were observed despite lack of complete drive cycle coverage. These simulations were performed on the same engine being investigated in this study using certification grade gasoline and B20 (20% biodiesel, 80% diesel) for the DI fuel. The results showed how much of an effect multi-mode operation can have on engine out NO_x emissions depending on the amount of the drive cycle coverage that RCCI operation can allow. Modeled drive cycle emissions results showed between a 17% and 21% reduction in NO_x with multi-mode RCCI as compared to diesel only operation. If an engine has to switch to CDC operation during high engine loads, the engine out NO_x will be very high and quickly can degrade the NO_x reduction potential of RCCI. Fuel usage over the drive cycles showed that nearly

equal amounts of gasoline and diesel fuel would most likely needed to be carried on board for RCCI multi-mode operation. During RCCI only operation fuel usage was found to be between 57% and 69% gasoline.

The ability of ethanol fuels to increase the high load operating range of RCCI with potential compromise to the lower load operability and the effect on drive cycle coverage is not well understood. This work investigates the potential fuel economy of multi-mode RCCI operation using vehicle systems simulations with experimental steady-state engine maps compared to a representative 2009 gasoline PFI engine as baseline for comparison using diesel fuel and E30 (30% ethanol, 70% gasoline). Experimental steady-state RCCI operating points on modified multi-cylinder GM 1.9-L engine using an in-house methodology for RCCI combustion were used to develop an RCCI speed/load map consistent with a light-duty drive-cycle with sufficient detail to support vehicle simulations. The RCCI map developed as part of this study represents an increase in RCCI operation over previous low temperature combustion operation maps [30], but was still not able to cover the engine speed and load required to meet all power demands over the light-duty drive cycles with the self-imposed constraints imposed on the engine experiments leading to the RCCI engine map. The simulations used a multi-mode RCCI/diesel operating strategy where the engine would operate in RCCI mode whenever possible but at the highest and lowest engine operating points, the engine would switch to diesel mode. All simulations were carried out in Autonomie using a 1580 kg passenger vehicle (mid-size sedan i.e. Chevrolet Malibu) over numerous U.S. federal light-duty drive cycles. A representative 2009 gasoline PFI engine map was obtained from an automotive original equipment manufacturer (OEM) for use in the vehicle simulations. A 2009 gasoline PFI baseline is standard in DOE VTO programmatic goals [1,2]. RCCI fuel economy simulation results are compared to the same vehicle powered by a representative 2009 PFI gasoline engine over multiple drive cycles. Engine-out drive cycle emissions are compared to CDC and observations regarding relative gasoline and diesel tank sizes needed for the various drive cycles are also summarized.

Methodology

For this study 6 engine maps were used for the vehicle systems simulations. A multi-mode experimental RCCI map, which is described in the next section, was used along with a CDC map for multi-mode operation. An experimental CDC map was used using the stock pistons with the same base engine used for the RCCI experiments. CDC mapping was conducted on the base engine with the OEM pistons using Euro IV calibrations maps providing fuel consumption and emissions data for the simulations. Experimental naturally aspirated 2009 PFI gasoline engine maps ranging 1.8L to 4.0L were provided by an OEM partner. The PFI maps were for fuel consumption only so no comparisons with modeled emissions can be made. The fuel economy modeling

was performed with using vehicle systems simulations with experimental engine data.

Experimental setup

The engine used for this study is a modified 2007 General Motors 4 cylinder 1.9L turbocharged diesel engine. The base engine has a rated power of 110 kW and a rated torque of 315 Nm. The original equipment manufacturer (OEM) pistons were replaced with pistons modified for RCCI. The RCCI modified piston bowl geometry was designed for RCCI using CFD modeling by UW. The piston design is based on a heavy duty piston and minimizes the surface area of the piston to minimize heat transfer losses and also results in a lowered compression from 17.1 in the OEM configuration to 15.1 to allow for higher load operation while maintaining reasonable pressure rise rate limits. More information about the piston design can be found in the paper by Hanson et al [23]. The diesel injection system and variable geometry turbo charger (VGT) were left in production form. The intake manifold was modified to incorporate extended tip narrow spray angle PFI injectors for the gasoline supply. A more in-depth discussion the intake manifold modifications can be found in Curran et al [20]. Figure 37 shows the overall fuel system layout for RCCI operation.

Table 17 shows engine specifications for the base engine. Table 18 and Table 19 show the injector specifications for the DI and PFI injectors respectively. The stock ECU was replaced with a full-pass DRIVEN control system which allowed simultaneous control of the PFI and DI fuel systems and all other engine parameters. Engine torque was measured using an absorbing eddy-current dynamometer. The DI fuel flowrate was measured with a Micro Motion Coriolis fuel meter, while the PFI fuel flowrate was measured using a Max Machinery 710-213 positive displacement volumetric flow measurement system. The intake air flowrate was measured using a laminar flow element and the stock intake mass-airflow sensor.

Engine-out emissions were measured using standard analysis techniques. A heated flame ionization detector (FID) was used to measure total unburned hydrocarbons. A heated chemiluminescence (CLD) instrument was used to measure NO_x . CO and CO_2 were measured using non-dispersive infrared (NDIR) instruments. Intake and exhaust O_2 was measured using a paramagnetic detector (PMD). Both intake and exhaust CO_2 were measured to provide the EGR rate. Sampled gas streams were chilled to remove water prior to measurement by PMD and NDIR instruments. Both intake and exhaust sample streams were conveyed from heated filters to the instruments through heated lines maintained at 190°C. Conditioned air was supplied to the engine at a constant temperature of 25°C and a relative humidity of 58%. An AVL 415S smoke meter was used to measure filter smoke number (FSN). A limitation to using a smoke meter based on the blackening of filter paper (reflectivity) is that it

may not accurately account for condensable organic hydrocarbons in the PM, which have been shown to be the primary PM mode with RCCI. Previous studies have compared the results of FSN and PM filter mass measurements from RCCI operation and have shown that the RCCI PM is mostly organic carbon with almost no elemental carbon [29, 30]. Engine emissions as well as important temperatures, pressures, flowrates as well as engine speed and torque were sampled for 180 seconds after 120 seconds of stable operation had been attained.

High speed combustion data was acquired using Kistler model 6058A pressure sensors installed in the glow plug ports of all 4 cylinders. Individual Kistler type 5010 Dual-Mode Amplifiers were used to process the pressure signals and the built in combustion package from Drivven was used to process the data. Combustion metrics were monitored and recorded using the DRIVVEN combustion analysis toolkit (DCAT). All brake thermal efficiencies presented here are calculated using the lower heating value (LHV) of the fuels used and brake power as measured from the dynamometer.

The DI fuel used in this study was a 2007 certification grade Ultra Low Sulfur Diesel (ULSD) fuel with a cetane number of 42.5, the PFI fuel was an E30 gasoline/ethanol blend with an anti-knock index (AKI) of 92.1. The E30 was splash blended with 30% anhydrous ethanol and 70% 87 AKI gasoline containing no ethanol. Ethanol blends had been previously shown to allow for improvements in the high load RCCI performance as compared to certification grade gasoline an AKI of 93 [22]. Key fuel specifications both fuels are shown in Table 20.

RCCI Engine Mapping Results

Multi-cylinder mapping experiments made use of a systematic approach based on previous MCE experimental results and modeling described in the paper by Curran et al. without the direct use of modeling [20]. The robustness of dual-fuel RCCI allows for rapid map exploration and development however, the parameter space is non-trivial. Self-imposed experimental constraints of pressure rise rate and CO emissions. Cylinder pressure rise < 10bar/deg and CO emissions < 5000 ppm were adhered to. Additionally, a self-imposed constraint on the coefficient of variance (COV) of indicated mean effective pressure (IMEP) of 3%. IMEP is defined as the indicated cycle work calculated from the cylinder pressure using the compression & expansion strokes only (-180° ATDC to 180° ATDC) calculated divided by the engine displacement volume.

RCCI operation was achieved through an early single pulse of diesel fuel (between 30 and 70 °BTDC) and port fueling of gasoline onto a closed intake valve. Fuel rail pressure was decreased as diesel fuel start of injection (SOI) timing was advanced to avoid spray impingement on the cylinder walls. Cylinder to cylinder balancing of cylinder pressure rise rate and IMEP was performed for

successful RCCI operation and had to be adjusted based on operating condition and EGR level. Once cylinder-to-cylinder balancing was performed, no other real-time controls were needed to maintain stable operation. The 32 point RCCI map shown in Figure 38 was specifically to be used with vehicle simulations to estimate the potential drive cycle fuel economy and emissions potential of RCCI combustion as compared to a representative 2009 PFI gasoline vehicle. The premixed ratio (rp) varied with engine speed and load as shown in Figure 39.

The initial drive cycle simulations for RCCI using experimental data with 96 RON gasoline and B20 demonstrated a need for increasing the upper load range to have the greatest improvements on BTE and NO_x over the various drive cycles with a multi-mode strategy [30]. In order to increase the maximum load under the self-imposed pressure rise rate constraint, a splash blended E30 blend with 87 AKI pump gasoline was used for the port-fuel-injected low-reactivity fuel and certification grade ULSD was used for the direct injected high-reactivity fuel. NO_x emissions across the entire engine operating map averaged 0.62g/kW-hr and where at or below 1.0 g/kW-hr under all but the highest speed high load points with a maximum NO_x rate of 1.57 g/kW-hr. HC and CO emissions were similar to previous multi-cylinder RCCI results with portions of the map under 10 g/kW-hr. Combustion noise results showed the MPRR limited map were below 100.6 dB across the entire map with most of the map under 96 dB. The power density of RCCI does not match that of the conventional diesel combustion baseline as shown in Figure 40 and Figure 41 respectively which show the BTE contours as a function of speed and load. The figures are shown with 1-hz speed and load points from the UDDS drive cycle overlain which shows that almost all of the upper load UDDS points covered in RCCI map. The high BTE operation compressed to drive-cycle region with RCCI as compared to CDC and as such less focus on power performing low load conditions (<27 % BTE regions). The difference in BTE between the two maps is up to a 7 BTE point difference in a given operating condition with RCCI.

The focus for RCCI operation is as much on the low NO_x as high BTE. Figure 42 and Figure 43 show the NO_x emissions over the RCCI map and CDC map respectively. Key findings are low NO_x across high BTE operation as compared to Euro-IV diesel map. NO_x emissions reductions are generally on the order of 50% to 92% except at lowest loads. At the lowest loads, 1500 RPM, 2.0bar, CDC can have slightly lower NO_x than RCCI (very high EGR and retarded injection timing with a pilot injection allowing PCCI-like NO_x emissions). Small BTE/ NO_x advantage at lowest loads may not be worth additional HC and HC emissions with current catalyst technologies – effect will be more apparent with drive cycle modeling

Vehicle Systems Simulations

Vehicle drive cycle simulations were performed using steady-state experimental engine maps on the same base vehicle available in Autonomie. In

addition to standard Autonomie features, a previously published methodology was also utilized to account for fuel consumption, emissions and temperature transients under drive cycle conditions [27, 28]. This approach assumes that transient fuel consumption and exhaust properties can be estimated by applying dynamic correction factors to steady-state engine maps. The previous studies have shown that the transient exhaust properties predicted by the updated Autonomie agree well with experimental chassis dynamometer measurements.

The base vehicle used for all drive cycle simulations is a conventional 1,580kg mid-size passenger vehicle with an automatic transmission available in Autonomie. The engine maps were changed to conduct the comparative simulations for the vehicle operating in CDC, multi-mode RCCI, and PFI modes. The engine mapping experiments revealed that for the majority of the driving schedules examined here, it will be possible to utilize RCCI. However, when those engine conditions are out of the RCCI operating range, the engine must shift back to CDC. To simulate such multi-mode operation, two sets of steady-state engine maps and transient correction parameters were combined for the relevant speed and load operating regions, as is similar to the literature [27]. The engine controller model is not calibrated for transient operation however. Mode switching was assumed to occur as a perfect step change between the two maps. A limitation of this simulation is that the multi-mode map uses an RCCI map with modified pistons while the CDC map was created using the stock pistons.

The fuel economy and emissions from the simulated conventional vehicle over multiple urban and highway driving cycles were evaluated. Hot-start cycle simulations were performed in which standard transmission controls are applied and the engine switches from CDC into RCCI when speed and load fall in the allowed RCCI range depicted in the RCCI enabled zone as shown in Figure 44. No warm-up portion or cold start emissions were considered. The multi-mode RCCI and CDC fuel economy simulation results are compared to the same vehicle powered by a representative 2009 port-fuel injected gasoline engine over these multiple standard EPA driving cycles. For all simulations the transmission shifting strategies used were matched to the engine based on maximum fuel economy.

Drive cycles

The EPA Federal Test Procedure (FTP) cycles that are used for vehicle systems simulations in this study are the Urban Dynamometer Driving Schedule (UDDS), which is also known as the LA4 or city test and is used to represent city driving conditions. The Highway Fuel Economy Test (HWFET) cycle represents highway driving under 60 miles per hour. Two of the so-called the “supplemental FTP” tests were also examined. The US06 is an aggressive driving with high acceleration and the SCO3 which is the FTP with air conditioner driving

schedule. Figure 45 shows speed and load traces and the RCCI coverage of engine speed and load over the different drive cycles and illustrates need for multi-mode operation with the current RCCI map for both low load operation and high load operation.

Results

To determine the most representative PFI baseline for comparison, all PFI engine maps were used to determine 0-60 mph acceleration to match performance. The fuel economy of each engine was then modeled and compared.

0-60 mph Performance

In the initial drive cycle simulation study performed by Curran and Gao [30], the only direct modeling comparison for 2009 PFI engines was a 4.0 L engine obtained from an OEM partner. Since additional 2009 maps were acquired for this study, it was possible to perform 0-60 mph acceleration tests to match the 2009 baseline in terms of performance. As seen in Figure 45 the 2.7 L PFI engine was the best match for performance and 1.8 L PFI is clearly underpowered for vehicles in the size class used for simulations. Figure 46 and Table 21 show the results of the 0-60 acceleration simulations.

Modeled PFI Fuel Economy for Mid-Size Passenger Sedans

Modeled fuel economy results for the range of 2009 PFI Engines maps that were obtained from OEM was completed. The 2.4L engine with optimized transmission achieved the best fuel economy engine in simulations over range of US Federal Test Procedure drive cycles with midsize sedan as shown in Figure 47. It should be noted that for similar vehicle size class in the U.S. market, vehicles such as the Chevrolet Malibu and other use a 2.4 L liter PFI gasoline engine.

Drive Cycle Fuel Use for RCCI/CDC

Multi-mode operation modeled fuel economy results were also used to predict the amount of the drive cycle that could be covered using the RCCI mode as shown in Table 22 for % RCCI by time and distance as well as the total amount of diesel fuel used over the cycle and total fraction of diesel used in RCCI only operation. The total diesel fuel amount varied from 54.7% in the HWFET simulation to as high as 71.7% during the aggressive US06 simulation. The amount of diesel fuel used during RCCI operation varied by speed and load but was between 33.3% and 42.4%.

Figure 48 and Figure 49 show representative fuel consumption simulation results for RCCI/CDC operation as compared to CDC only operation.

Fuel Economy Comparisons

The modeled fuel economy results for all of the engines in the mid-size passenger car with the fuel economy optimized transmissions are shown in Figure 50. The improvements are shown in Table 23. Noting that the 2.7L engine matched the engine performance of the RCCI/CDC engine, it was found that the 2.4L PFI engine performed the best in terms of fuel economy for the PFI engines. It was found that the 1.8L PFI was under powered for the vehicle used in the simulation and operated in the enrichment portion of the map to a greater extent reducing fuel economy performance.

Modeled fuel economy results showed a 10% improvement over the CDC baseline with the city and highway cycles and 6 to 8% on the supplemental drive cycles with the RCCI/CDC maps. The RCCI/CDC engine was found to have greater than 40% fuel economy improvement for all drive cycles as compared to the 2.7 PFI baseline which was the most representative and at least a 30% fuel economy improvement over the 2.4L PFI baseline which had the best fuel economy performance of the PFI engines examined.

To put the results of the fuel economy modeling into perspective and provide a more complete comparison against best-in-class PFI engines, the EPA and ORNL chassis laboratory databases were mined for 2009 PFI vehicle data. Figure 51 shows how city (UDDS/FTP) fuel economy trends with displacement. The results are for all vehicle size classes offered in the US, not just midsize passenger vehicles.

Modeled Drive Cycle Engine-Out Emissions Trends

Drive cycle engine out emissions were modeled using the same transient correction factors as for fuel economy. Though these results are not intended to predict actual emissions results over hot-start drive cycles, the trends can be valuable as an indication of aftertreatment needs. Table 24 shows the modeled drive cycle emissions for RCC/CDC operation as compared to CDC. Engine out NO_x emissions were between 16 and 18.6% better with considerable high CO and HC emissions. The concern with the elevated exhaust temperatures is more apparent when the exhaust temperatures as shown Figure 52 are found [31] to be significantly reduced from CDC mode with a line at 200C where a conventional DOC has been shown to have little effectiveness on reducing HC/CO.

Summary

ORNL made use of a reactivity controlled compression ignition (RCCI) engine map in vehicle systems simulations to model the potential fuel economy improvements with RCCI compared to a 2009 port fuel injection gasoline engine on the same vehicle platform. This made use of an in-house methodology and experimental steady-state RCCI operating points on a modified multi-cylinder GM

1.9-L engine using an in-house methodology for RCCI combustion to develop an RCCI speed/load map consistent with a light-duty drive-cycle with sufficient detail to support vehicle simulations. All simulations were carried out in Autonomie using a 1580 kg passenger vehicle (mid-size sedan i.e. Chevrolet Malibu) over numerous U.S. federal light-duty drive cycles. Representative 2009 PFI engine maps ranging from 1.8L to 4.0L were obtained from an OEM partner for use in the vehicle simulations. The RCCI map used E30 for the port fuel injection and diesel for the direct-injection fuel. This enabled improved upper load expansion as compared to previous RCCI engine maps, but was still not able to cover the engine speed and loads required to meet all power demands over the light-duty drive cycles. Note that speed and load constraints were self-imposed on the engine experiments based on pressure rise rate and HC/CO emissions. The simulations used a multi-mode RCCI/diesel operating strategy where the engine would operate in RCCI mode whenever possible, and would switch to diesel mode for conditions outside of the RCCI operating window. For the lowest loads, high-EGR diesel combustion was able to achieve similar NO_x emissions as RCCI with similar BTE. Vehicle systems simulation results showed that greater than a 20 % increase in fuel economy was made possible with the multi-mode RCCI operating strategy as compared to all of the 2009 PFI baselines over all of the federal drive cycles examined. Fuel usage over the drive cycles showed that nearly equal amounts of gasoline and diesel fuel would most likely be needed on board for RCCI multi-mode operation. During RCCI only operation fuel usage was found to be between 57% and 69% gasoline. City and highway drive cycle coverage was found to be 51% and 74.3% respectively by distance for RCCI operation. The results of the simulations were also able to provide insights into the relative proportions of E30 and diesel fuel usage with multi-mode RCCI operation over the various drive cycles.

Conclusions

RCCI fuel economy improvements were demonstrated despite lack of complete drive cycle coverage. The use of E30 for the low-reactivity fuel shifted the drive cycle coverage to a higher load. Increasing the RCCI drive cycle coverage is possible and being investigated through changes in engine hardware and fuel choices. The high HC and CO shown in the simulations along with the decreased exhaust temperature will pose a challenge for meeting Federal emissions regulations and may require a modification the low load operating strategy or advancements in catalysts. Limitations of the study include the use of a multi-mode operating map that switched between piston types a follow up study is planned to create a multi-mode RCCI operating map using only the RCCI modified pistons. Other limitations included the lack of transient engine performance for same mode and mode switching to calibrate the model which would account for transient performance.

References

1. U.S. Department of Energy, Office of Vehicle Technologies Multi-Year Program Plan 2011-2015, 2010, http://www1.eere.energy.gov/vehiclesandfuels/pdfs/program/vt_mypp_2011-2015.pdf.
2. Vehicle Technologies Program. Advanced Combustion Engines. <http://www1.eere.energy.gov/vehiclesandfuels/technologies/engines/index.html>.
3. U.S. Environmental Protection Agency, Testing and Measuring Emissions, <http://www.epa.gov/nvfe/testing/dynamometer.htm>.
4. C Sluder, R Wagner, J Storey, S Lewis (2005) "Implications of Particulate and Precursor Compounds Formed During High-Efficiency Clean Combustion in a Diesel Engine," SAE Paper 2005-01-3844, 2005.
5. R Wagner, J Green, T Dam, K Edwards, J Storey (2003) "Simultaneous Low Engine-Out NO_x and Particulate Matter with Highly Diluted Diesel Combustion," SAE Paper 2003-01-0262, 2003.
6. C Sluder, R Wagner, S Lewis, J Storey (2006) "Fuel Property Effects on Emissions From High Efficiency Clean Combustion in a Diesel Engine," SAE Paper 2006-01-0080, 2006.
7. C Sluder, R Wagner (2006) "An Estimate of Diesel High-Efficiency Clean Combustion Impacts on FTP-75 Aftertreatment Requirements". SAE Paper 2006-01-3311, 2006.
8. K Cho, M Han, R Wagner, C Sluder (2008), "Mixed-Source EGR for Enabling High-Efficiency Clean Combustion Modes in a Light-Duty Diesel Engine," SAE 2008-01-0645, 2008.
9. K Inagaki, T Fuyuto, K Nishikawa, K Nakakita (2006) "Dual-Fuel PCCI Combustion Controlled by In-Cylinder Stratification of Ignitability," SAE paper 2006-01-0028, 2006.
10. C Chadwell, T Alger, C Roberts, S Arnold (2011) "Boosting Simulation of High Efficiency Alternative Combustion Mode Engines," SAE 04-12-2011, 2011.
11. V Manente, B Johansson, P Tunestal (2009) "Partially Premixed Combustion at High Load using Gasoline and Ethanol, a Comparison with Diesel," SAE Paper 2009-01-0944, 2009.
12. S Kokjohn, R Hanson, D Splitter, R Reitz (2009) "Experiments and Modeling of Dual-Fuel HCCI and PCCI Combustion Using In-Cylinder Fuel Blending," SAE Paper 2009-01-2647, 2009.
13. D Splitter, R Hanson, S Kokjohn, R. Reitz (2011) "Reactivity Controlled Compression Ignition (RCCI) Heavy-Duty Engine Operation at Mid-and High-Loads with Conventional and Alternative Fuels," SAE Paper 2011-01-0363, 2011.
14. R Hanson, S Kokjohn, D Splitter, R Reitz (2010) "An Experimental Investigation of Fuel Reactivity Controlled PCCI Combustion in a Heavy-Duty Engine," SAE Paper 2010-01-0864, 2010.

15. S Kokjohn, R Reitz, D Splitter, M Musculus (2012) "Investigation of Fuel Reactivity Stratification for Controlling PCI Heat-Release Rates Using High-Speed Chemiluminescence Imaging and Fuel Tracer Fluorescence," SAE Paper 2012-01-0375, 2012.
16. S Kokjohn, R Hanson, D Splitter, J Kaddatz, R Reitz (2011) "Fuel Reactivity Controlled Compression Ignition (RCCI) Combustion in Light- and Heavy-Duty Engines," SAE Paper 2011-01-0357, 2011.
17. S Curran, V Prikhodko, K Cho, C Sluder, J Parks, R Wagner, S Kokjohn (2010) "In-Cylinder Fuel Blending of Gasoline/Diesel for Improved Efficiency and Lowest Possible Emissions on a Multi-Cylinder Light-Duty Diesel Engine," SAE Paper 2010-01-2206, 2010.
18. S Curran, K Cho, T Briggs, R Wagner (2011) "Drive Cycle Efficiency and Emissions Estimates for Reactivity Controlled Compression Ignition in a Multi-Cylinder Light-Duty Diesel Engine". Proceedings of the 2011 Internal Combustion Engine Division Fall Technical Conference, ICEF2011, Morgantown Wv.
19. S Curran, R Hanson, R. Wagner (2012) "Effect of E85 on RCCI Performance and Emissions on a Multi-Cylinder Light-Duty Diesel Engine," SAE Paper 2012-01-0376, 2012.
20. S. Curran, R. Hanson, R. Wagner (2012) "Reactivity controlled compression ignition (RCCI) combustion on a multi-cylinder light-duty diesel engine", International Journal of Engine Research, 13(3), 216-225, 2012.
21. R Hanson, S Curran, R Reitz, and R Wagner (2012) "Piston optimization for RCCI in Light-Duty Multi-Cylinder Engine," SAE Paper 2012-01-0380, 2012.
22. S Curran, J Szybist, R Wagner (2012) "Reactivity Controlled Compression Ignition Performance with Renewable Fuels," ICEF2012-92192, Proceedings of the ASME 2012 Internal Combustion Engine Division Fall Technical Conference, ICEF2012, September 23-26, 2012, Vancouver, BC, Canada, 2012.
23. R Hanson, S Curran, R. Wagner, R Reitz (2013) "Effects of Biofuel Blends on RCCI combustion in a Light-Duty, Multi-Cylinder Diesel Engine," SAE Int. J. Engines 6(1):488-503, 2013, doi:10.4271/2013-01-1653.
24. V Prikhodko, J Parks (2009) "Implications of Low Particulate Matter Emissions on System Fuel Efficiency for High Efficiency Clean Combustion," SAE Paper 2009-01-2709, 2009.
25. C Sluder, R Wagner, J Storey, S Lewis (2005) "Implications of Particulate and Precursor Compounds Formed During High-Efficiency Clean Combustion in a Diesel Engine," SAE Paper 2005-01-3844, 2005.
26. R Gopal, A Rousseau (2011) "System Analysis Using Multiple Expert Tools," SAE Paper 2011-01-0754, 2011.
27. Z Gao, J Conklin, C Daw, and V Chakravarthy (2010) "A proposed methodology for estimating transient engine-out temperature and emissions from steady-state maps," International Journal of Engine Research, 11(2), 137-151, 2010.

28. Z Gao, C Daw, R Wagner, K Edwards, D Smith (2013) "Simulating the impact of premixed charge compression ignition on light-duty diesel fuel economy and emissions of particulates and NO_x," Proceedings of the Institution of Mechanical Engineers, Part D: Journal of Automobile Engineering 227(1), 31-51, 2013.
29. S Curran, R Hanson, R Reitz, R Wagner (2013) "Efficiency and Emissions Mapping of RCCI in a Light-Duty Diesel Engine", SAE Paper 2013-01-0289.
30. S Curran, Z Gao, R Wagner, "Reactivity controlled compression ignition drive cycle emissions and fuel economy estimations using vehicle systems simulations" IJER, Submitted, 2013.
31. V Prikhodko, S Curran, T Barone, S Lewis, J Storey, C Cho, R Wagner, J Parks (2010) "Emission Characteristics of a Diesel Engine Operating With In-Cylinder Gasoline and Diesel Fuel Blending," SAE Paper 2010-01-2266, 2010.
32. T Barone, J Storey, V Prikhodko, S Curran, J Parks, R Wagner (2011) "Particle Emissions Reduction by In-Cylinder Blending of Gasoline and Diesel Fuel", 21st CRC Real World Emissions Workshop, San Diego Ca, 2011.

Disclaimer

This manuscript has been authored by a contractor for the U.S. Government under contract number DE-AC05-000R22725. Accordingly, the U.S. Government retains a nonexclusive, royalty-free license to publish or reproduce the published form of this contribution, or allow others to do so, for the U.S. Government.

Acknowledgments

The authors wish to thank their colleagues at the University of Wisconsin, Prof. Rolf Reitz, Reed Hanson, Prof. Sage Kokjohn and Derek Splitter (now at ORNL) for their modeling guidance, piston design and input on RCCI operation. This work was supported by the U.S. Department of Energy (DOE), Vehicle Technologies Office. The authors gratefully acknowledge the support and guidance of Gurpreet Singh, Ken Howden, Leo Breton, Kevin Stork and Steve Przesmitzki at DOE

Appendix 3.1

Table 17. GM 1.9 L CIDI Base Configuration for E30 RCCI Experiments

Number of Cylinders	4
Bore (mm)	82.0
Stroke (mm)	90.4
Compression Ratio	15.1

Table 18. Diesel injector specifications for E30 RCCI Experiments

Number of Nozzle Holes	7
Included Spray Angle (°)	148

Table 19. Port-fuel injector specifications for E30 RCCI Experiments

Number of Nozzle Holes	4
Cone Angle (°)	15
Separation Angle (°)	22

Table 20. Fuel specification for E30 and ULSD

Specification	E30	ULSD
Lower Heating Value (kJ/kg)	37742	42880
Specific Gravity	0.7445	0.848
H (weight %)	13.73	13.2
C (weight %)	74.4	86.8
Oxygen (weight %)	11.34	0
Aromatics (weight %)	16.4	29.9
Ethanol (vol %)	32.59	0
Initial Boiling Point (°C)	86	184
Final Boiling Point (°C)	379	332
Research Octane Number	101.3	NA
Motor Octane Number (MON)	88.5	NA
(RON + MON)/2	94.9	NA
Cetane Number	NA	42.5

Table 21. 0-60 MPH Acceleration Modeling

Engine	Distance(M)	Time(S)
CDC	154.0	9.50
CDC/RCCI	154.1	9.50
PFI4.0	124.5	7.90
PFI2.7	155.0	9.80
PFI2.4	169.0	10.90
PFI1.8	234.7	15.20

Table 22. RCCI drive cycle coverage and amount of diesel fuel consumption over the drive cycle simulations

FE/Emissions	%RCCI Distance	%RCCI Time	%Total Diesel	%Diesel for RCCI
UDDS	51.8%	39.0%	64.2%	42.4%
HWFET	74.3%	39.9%	54.7%	38.9%
US06	56.5%	20.4%	71.7%	33.3%
SC03	44.9%	15.3%	69.1%	40.2%

Table 23. Fuel economy improvements for RCCI/CDC operation as compared to CDC and PFI baselines

Engine Size	1.9 CIDI	1.8L PFI	2.4L PFI	2.7L PFI	4.0L PFI
UNIT	MPG	MPG	MPG	MPG	MPG
UDDS	10.1	33.1%	31.1%	45.8%	59.2%
HWFET	10.1%	41.6%	36.8%	45.7%	55.4%
US06	6.3%	50.5%	38.4%	47.4%	38.2%
SC03	8.3%	33.1%	27.7%	41.9%	52.0%

Table 24. RCCI/CDC missions results compared to CDC baseline (positive numbers indicate improvement over CDC baseline)

Emissions	CO%	HC%	NO %
UDDS	-82.5%	-	16.0%
HWFET	-	-	18.6%
US06	-89.1%	-	9.5%
SC03	-78.6%	-	10.7%

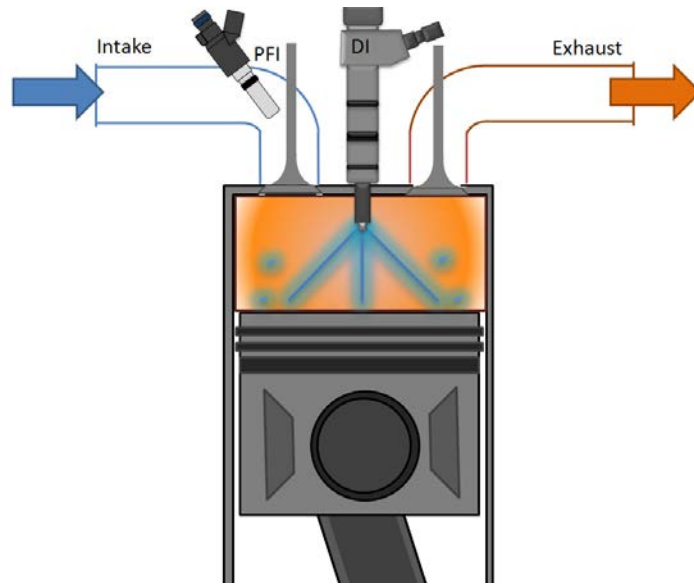


Figure 36. Dual-Fuel RCCI Injection Strategy for E30 RCCI Experiments

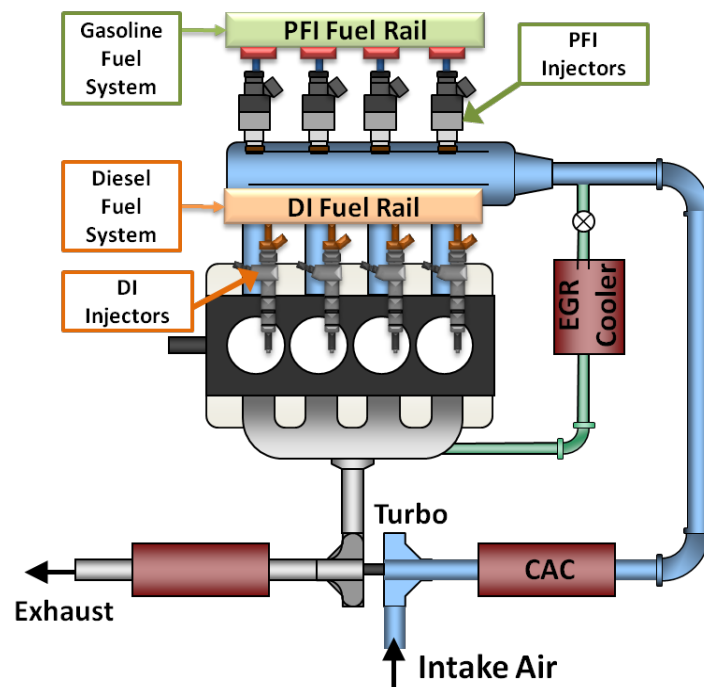


Figure 37. ORNL Multi-Cylinder RCCI Engine for E30 RCCI Experiments

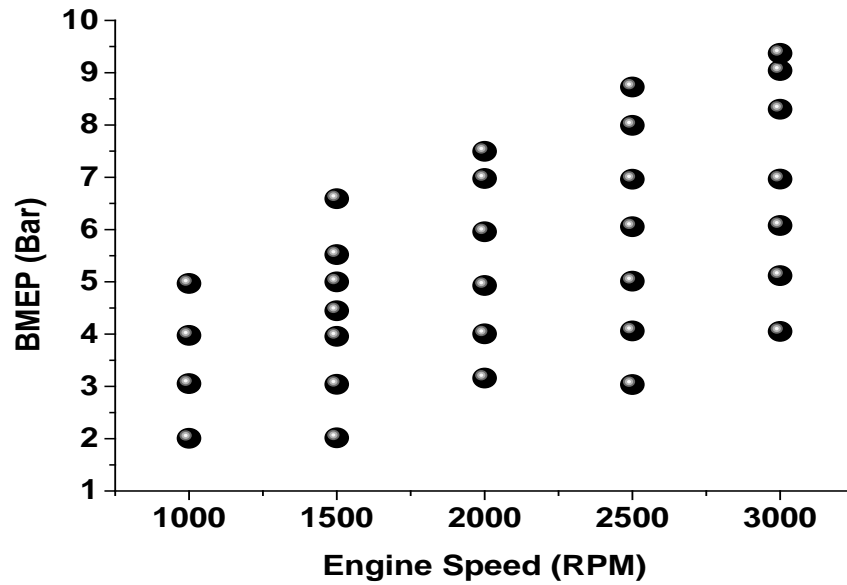


Figure 38. RCCI Map with E30 and ULSD with 32 data points

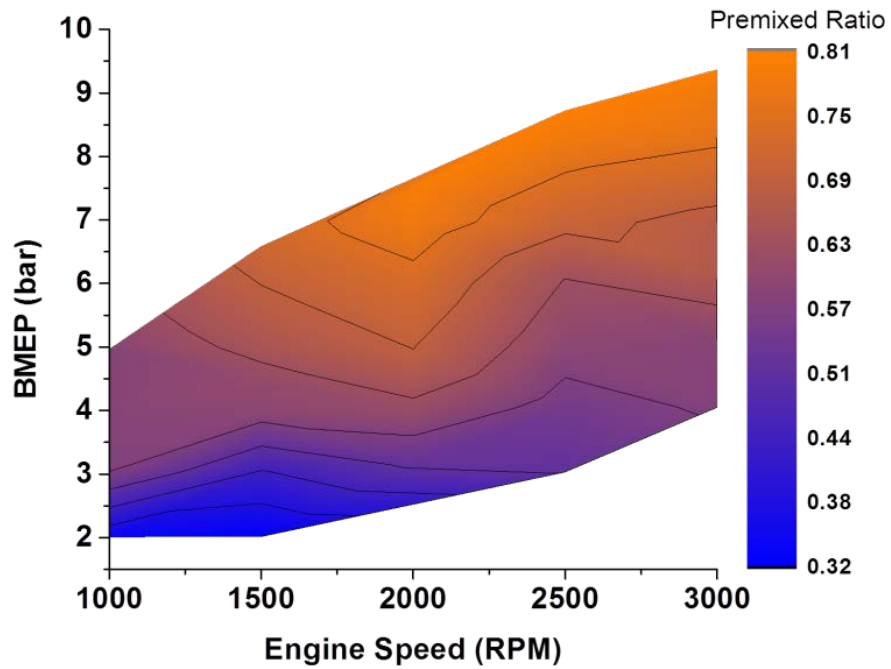


Figure 39. RCCI premixed ratio as a function of engine speed and load for E30 RCCI Experiments

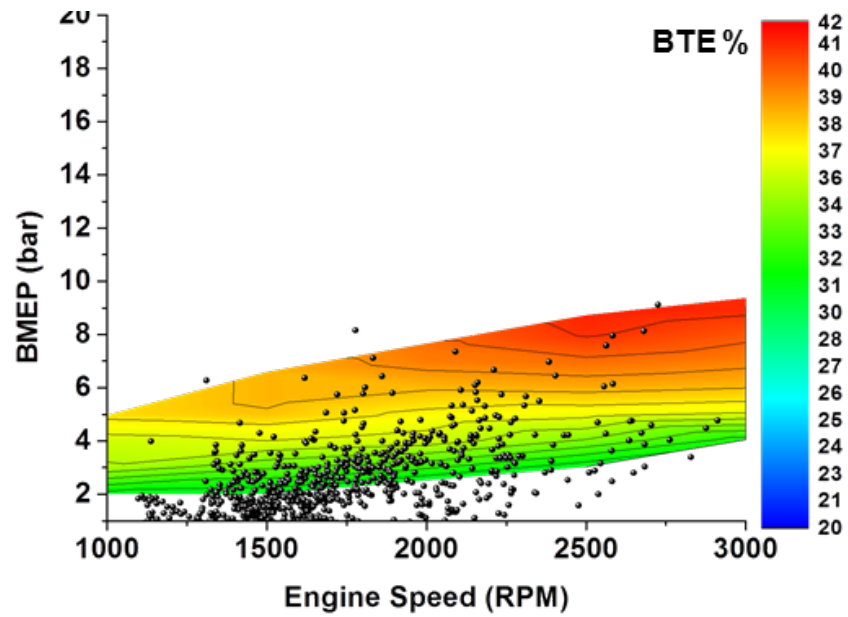


Figure 40. RCCI BTE as a function of engine speed and load for E30 RCCI Experiments

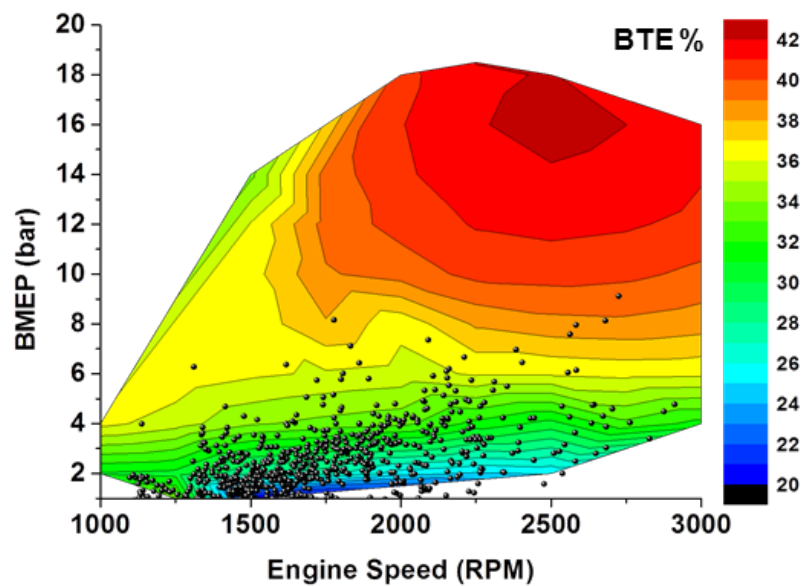


Figure 41. CDC BTE as a function of engine speed and load for E30 RCCI Experiments

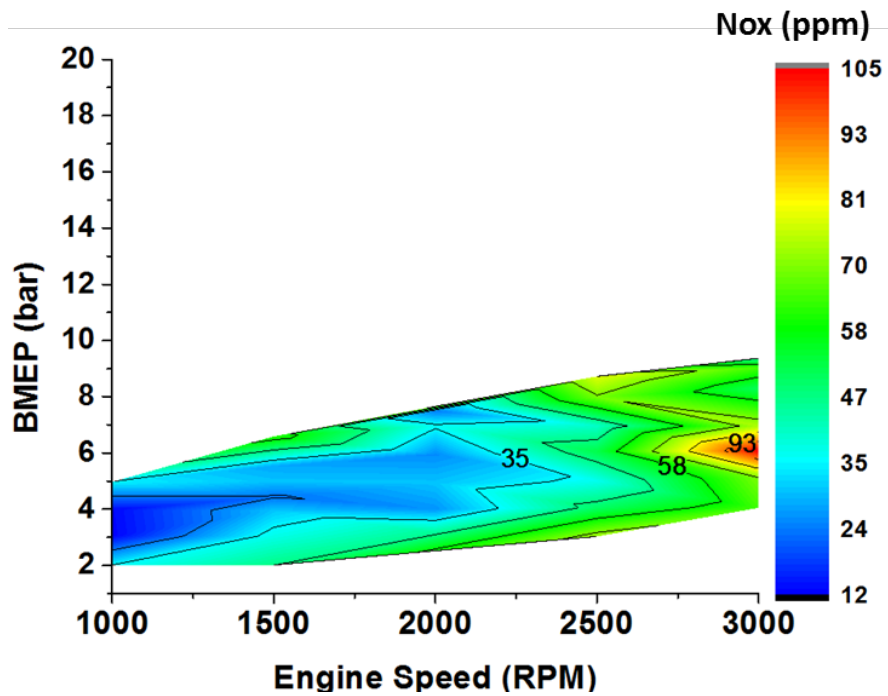


Figure 42. RCCI NOX with ppm labeled contours

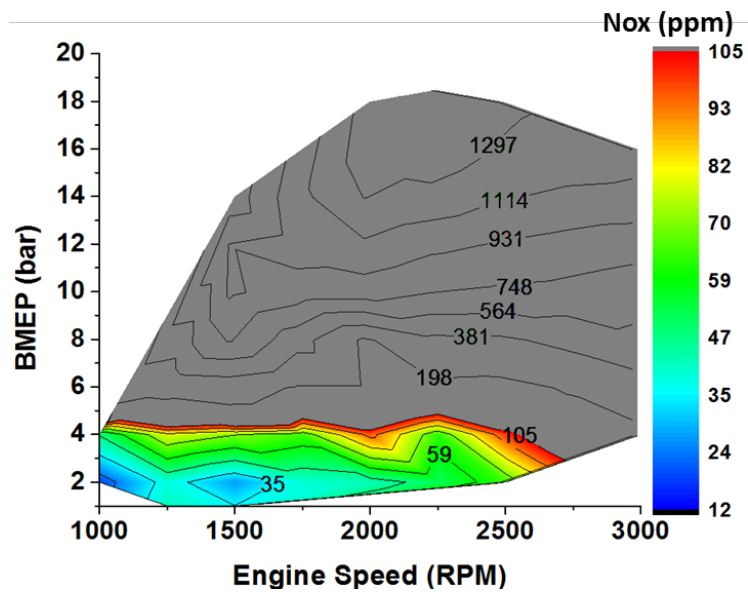


Figure 43. CDC NOX with areas over 105 ppm not colored with ppm labeled contours

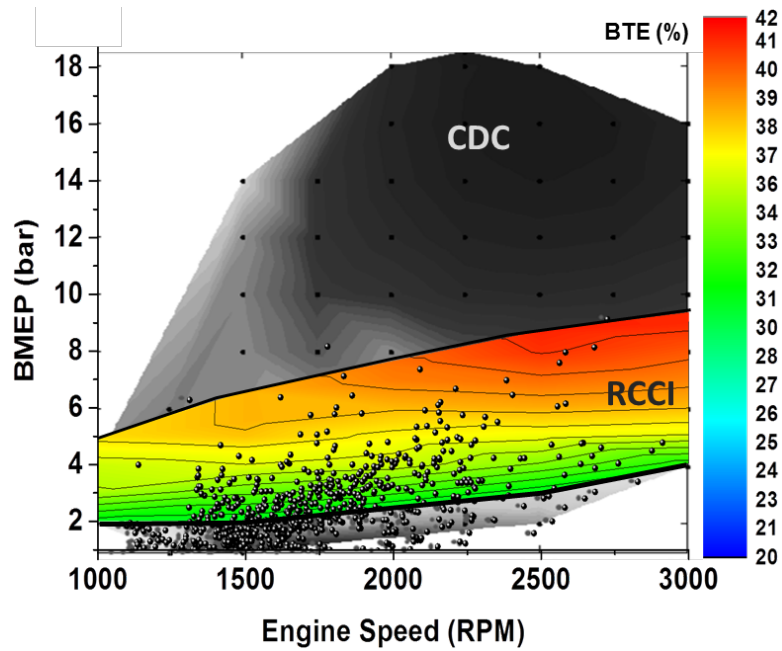


Figure 44. E30 Multi-mode RCCI/CDC map

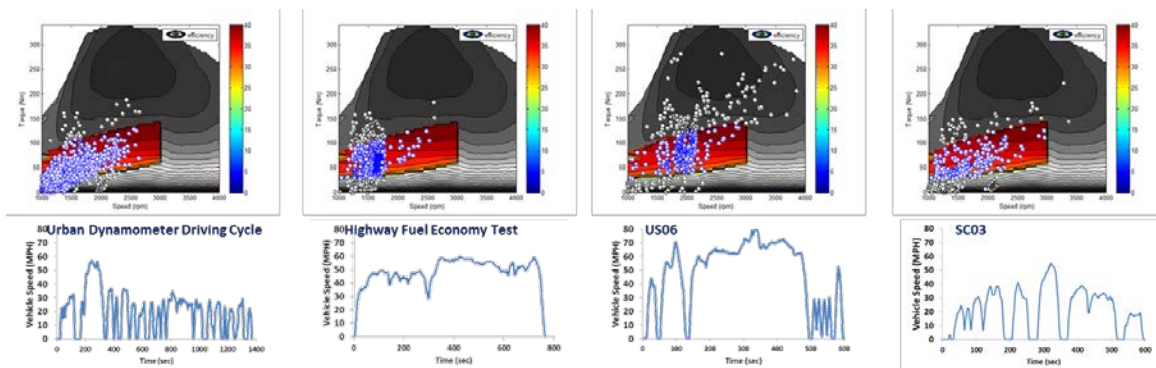


Figure 45. Multi-mode E30 RCCI/CDC map coverage regulatory drive cycles used for the drive cycle simulations

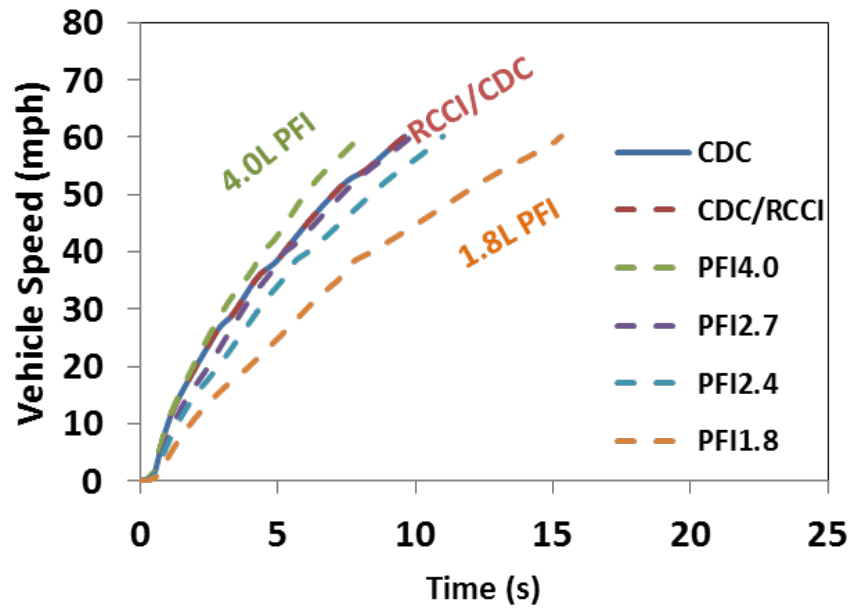


Figure 46. Simulated time for 0-60 mph acceleration

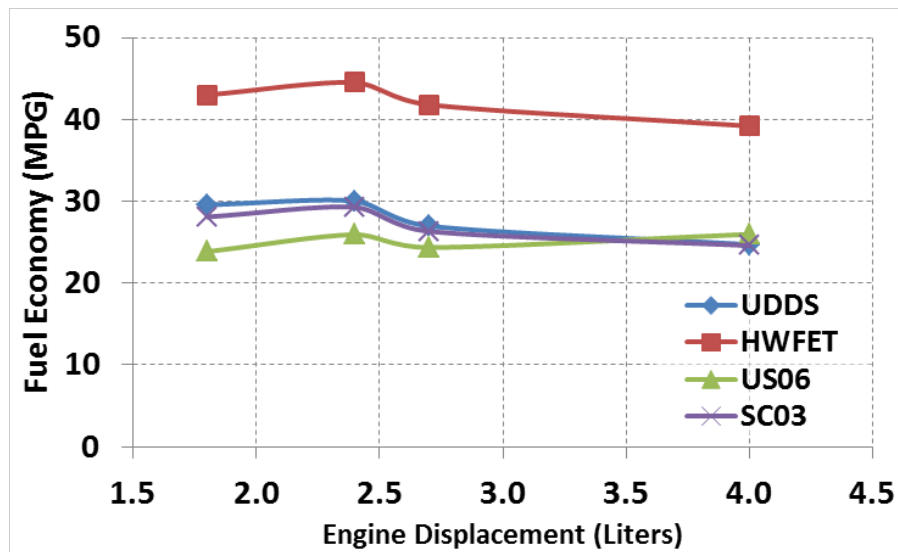


Figure 47. Modeled fuel economy results for 2009 PFI engines with transmissions optimized for fuel economy as a function of displacement

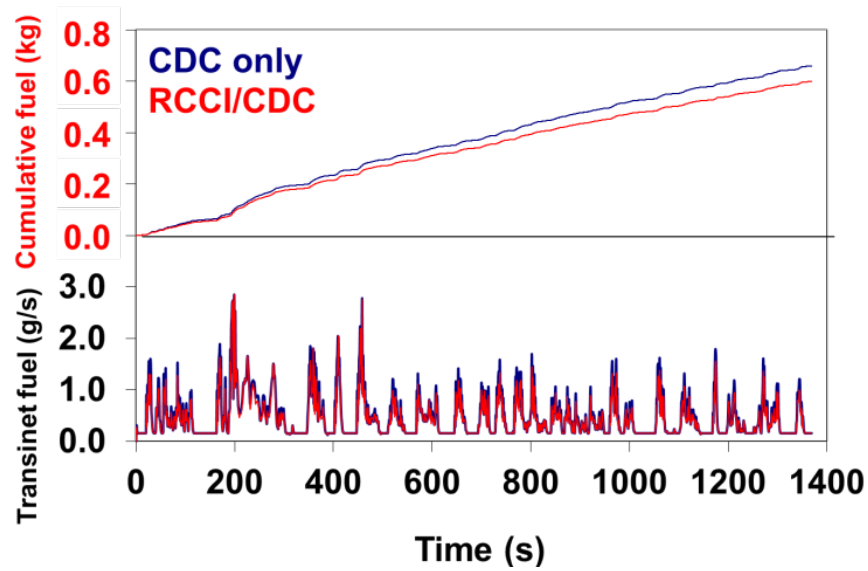


Figure 48. Fuel consumption modeling over the UDDS

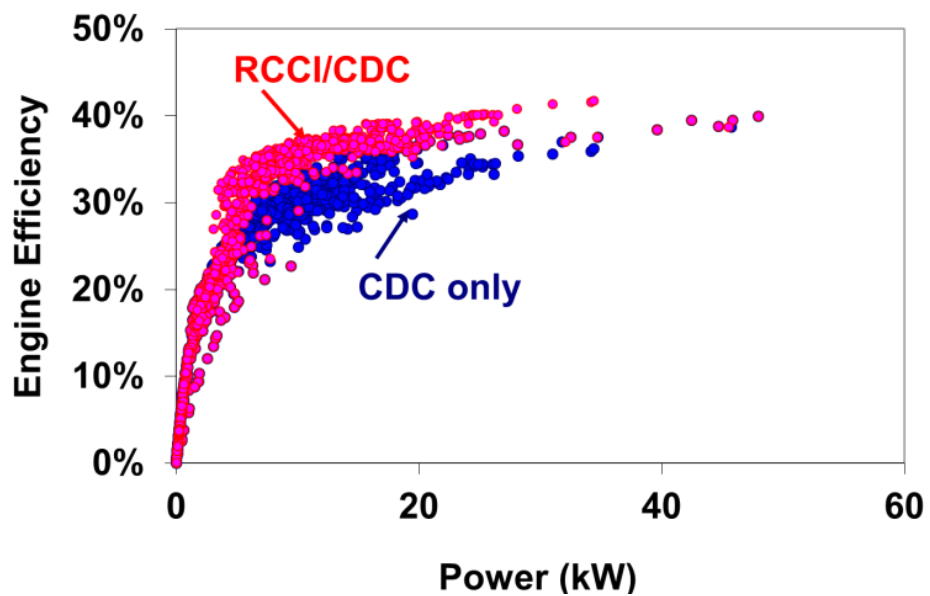


Figure 49. Engine efficiency as a function of power demand over the UDDS

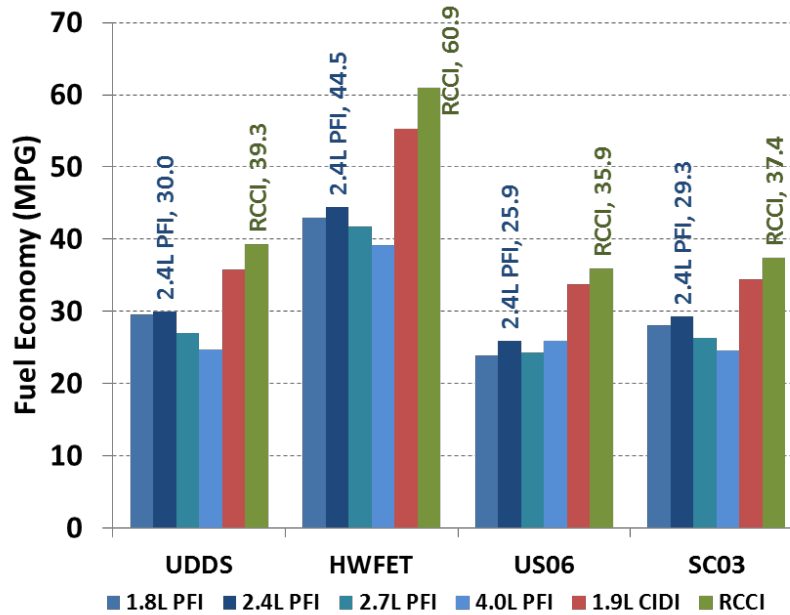


Figure 50. Fuel economy results for all PFI engines, CDC only operation with the base CIDI engine and RCCI/CDC multi-mode operation

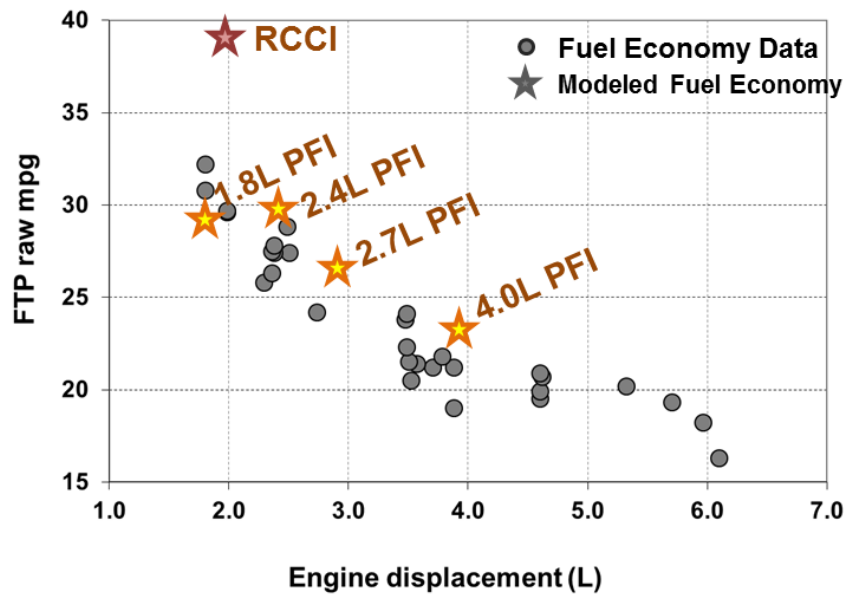


Figure 51. Modeled fuel economy results compared to actual vehicle dynamometer data using EPA and ORNL data.

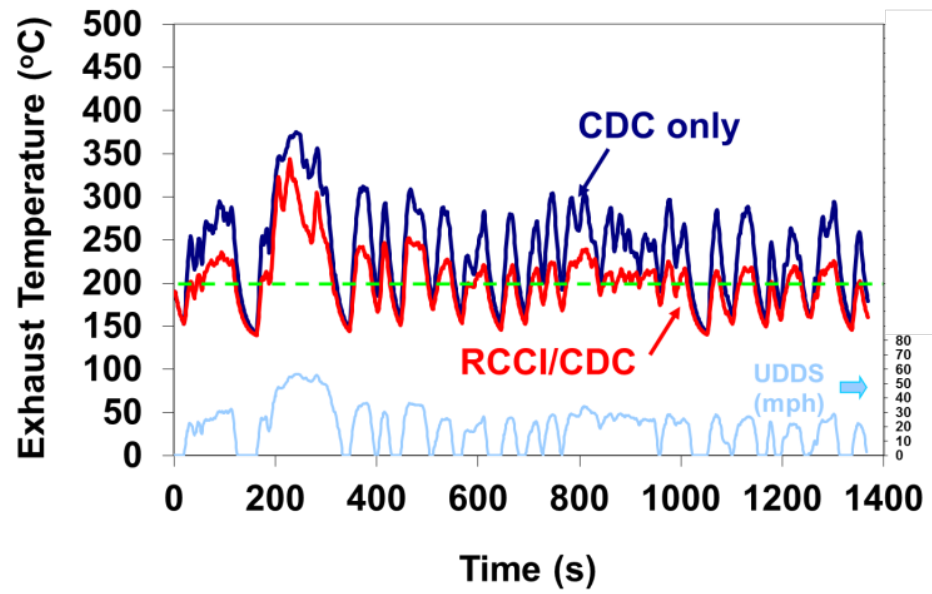


Figure 52. Modeled RCCI/CDC exhaust temperatures compared to CDC operation under the hot-start UDDS cycle.

Appendix 3.2

Table 25. E30 Map - Performance

Speed (RPM)	BMEP (bar)	Torque (ft-lb)	Diesel Rate (g/s)	Gasoline rate (g/s)	rp	BTE (%)
1000	2.0	22.5	0.159	0.094	0.345	30.73
1000	3.1	34.2	0.140	0.206	0.568	35.10
1000	4.0	44.6	0.173	0.271	0.582	35.72
1000	5.0	55.9	0.151	0.410	0.708	35.95
1500	5.0	55.7	0.311	0.482	0.581	37.47
1500	2.0	22.6	0.250	0.134	0.323	30.47
1500	3.0	34.1	0.284	0.251	0.441	33.47
1500	4.0	44.4	0.252	0.404	0.588	36.12
1500	4.4	49.9	0.267	0.457	0.604	36.80
1500	5.0	56.0	0.261	0.531	0.645	38.05
1500	5.5	61.5	0.323	0.564	0.609	37.11
1500	5.5	61.9	0.265	0.604	0.670	38.40
1500	6.0	67.6	0.296	0.635	0.656	39.05
1500	6.1	68.3	0.296	0.707	0.680	36.73
1500	6.6	73.9	0.276	0.766	0.712	38.39
2000	3.2	35.4	0.346	0.413	0.515	32.94
2000	4.0	44.9	0.324	0.573	0.612	35.74
2000	4.9	55.3	0.313	0.768	0.686	36.82
2000	6.0	66.8	0.315	0.947	0.728	38.27
2000	7.0	78.2	0.286	1.150	0.781	39.62
2000	7.5	84.0	0.285	1.253	0.797	39.82
2500	3.0	34.0	0.454	0.528	0.509	30.54
2500	4.1	45.5	0.504	0.674	0.544	34.19
2500	5.0	56.2	0.524	0.845	0.590	36.53
2500	6.1	67.9	0.546	1.023	0.626	38.66
2500	7.0	78.0	0.481	1.279	0.703	39.95
2500	8.0	89.6	0.426	1.543	0.763	41.29
2500	8.0	90.0	0.429	1.541	0.762	41.46
2500	8.7	97.8	0.379	1.764	0.806	41.64

Table 25. Continued

Speed (RPM)	BMEP (bar)	Torque (ft-lb)	Diesel Rate (g/s)	Gasoline rate (g/s)	rp	BTE (%)
3000	3.9	44.2	0.610	0.922	0.574	30.78
3000	4.1	45.4	0.608	0.918	0.574	31.74
3000	5.1	57.4	0.652	1.029	0.585	36.44
3000	6.1	68.1	0.602	1.310	0.660	38.37
3000	7.0	78.1	0.648	1.482	0.671	39.50
3000	8.3	93.0	0.548	1.936	0.759	40.77
3000	9.0	101.4	0.528	2.135	0.783	41.53
3000	9.1	101.9	0.528	2.143	0.783	41.63
3000	9.4	105.1	0.480	2.290	0.810	41.52

Table 26. E30 Map Emissions

Speed (RPM)	BMEP (bar)	HC (ppm)	NOx	CO_High	CO2 In	CO2 Ex	O2 In	O2 Ex
1000	2.0	2247.712	35.3	4900	2.2	5.6	17.7	12.5
1000	3.1	3046.039	12.4	3292	1.3	5.4	19.1	12.8
1000	4.0	3165.967	12.9	1289	0.8	5.7	19.8	12.7
1000	5.0	3712.434	28.0	1099	0.3	6.0	20.7	12.2
1500	5.0	3956.758	34.6	1547	0.1	5.6	21.0	12.8
1500	2.0	2694.131	46.6	4722	1.2	4.6	19.1	13.9
1500	3.0	2588.166	37.7	3635	0.8	5.1	19.9	13.3
1500	4.0	3425.134	30.4	2846	0.1	4.7	21.0	13.9
1500	4.4	3356.627	23.0	2307	0.1	5.0	21.0	13.4
1500	5.0	3196.241	30.3	1621	0.1	5.4	21.0	13.0
1500	5.5	3282.853	34.6	1229	0.1	5.8	20.9	12.5
1500	5.5	3158.415	27.8	1394	0.1	5.8	21.0	12.5
1500	6.0	3021	50.9	1042	0.0	6.5	20.9	11.9
1500	6.1	3128.837	54.2	1081	0.1	6.2	20.9	11.9
1500	6.6	2978.028	62.1	962	0.1	6.5	20.9	11.5
2000	3.2	4025.201	45.3	4237	0.9	5.0	19.6	13.3
2000	4.0	3214.128	26.0	3329	1.0	5.2	19.6	13.1
2000	4.9	3190.722	30.4	2318	0.1	4.6	20.9	14.1
2000	6.0	2699.895	25.3	1690	0.1	5.1	20.9	13.4
2000	7.0	3138.485	36.2	1334	0.1	5.8	20.9	12.4
2000	7.5	3044.812	23.8	1269	0.1	5.9	20.9	12.3
2500	3.0	3656.271	73.0	4491	0.3	3.6	20.6	15.3
2500	4.1	2935.94	49.4	4204	0.1	4.0	20.9	14.8
2500	5.0	3103.107	37.0	3925	0.1	4.6	20.9	13.9
2500	6.1	2538.213	52.1	2240	0.1	5.4	20.9	12.9
2500	7.0	2713.471	40.5	1688	0.1	5.8	20.9	12.5
2500	8.0	2508.79	69.1	1213	0.1	6.1	20.9	12.0
2500	8.0	2487.587	85.1	1077	0.1	6.2	20.9	12.0
2500	8.7	2687.263	78.4	1205	0.1	6.5	21.0	11.5
3000	3.9	6892.556	31.8	5486	0.4	3.9	20.4	14.6
3000	4.1	5198.3	64.6	4647	0.3	4.2	20.7	14.4
3000	5.1	2487.319	69.6	2979	0.1	4.9	20.9	13.7

Table 26. Continued

Speed (RPM)	BMEP (bar)	HC (ppm)	NOx	CO_High	CO2 In	CO2 Ex	O2 In	O2 Ex
3000	6.1	3054.712	104.0	2203	0.1	5.4	21.0	12.9
3000	7.0	2612.212	73.8	2084	0.1	5.5	21.0	12.9
3000	8.3	2469.405	50.9	1892	0.1	5.3	20.9	13.1
3000	9.0	2347.529	64.5	1400	0.1	5.8	20.9	12.5
3000	9.1	2286.598	79.2	1339	0.1	5.8	20.9	12.4
3000	9.4	2325.709	45.4	1439	0.1	5.7	20.9	12.6

CHAPTER IV
WELL-TO-WHEEL COMPARISON OF MULTI-MODE ADVANCED
COMBUSTION STRATEGIES AND OTHER ADVANCED
LIGHT-DUTY VEHICLE TECHNOLOGIES

A version of this chapter will be submitted to *Energy* by Scott Curran, Robert Wagner, Joshua Fu and David Irick:

S. J. Curran, R. M. Wagner, J. Fu, and D. K. Irick, "Well-to-wheel comparison of multi-mode advanced combustion strategies and other advanced light-duty vehicle technologies". This article has not been published anywhere, nor will it be before I turn in the final version of my ETD.

The article is presented in its original form, formatted for this dissertation including renumbering tables and figures. Author was lead author and lead investigator on study. Coauthor's Joshua Fu, Robert Wagner and David Irick's guidance and revisions were instrumental. Additional data related to the Autonomie modeling of the Nissan Leaf is presented in the appendix (Appendix 4.2).

Abstract

Vehicle fuel efficiency and emissions regulations are driving a radical shift in the need for high efficiency powertrains along with control of criteria air pollutants and greenhouse gases. High efficiency powertrains including vehicle electrification, engine downsizing, and advanced combustion concepts all seek to accomplish these goals. Homogeneous charge compression ignition (HCCI) concepts have been proposed but have not been able to demonstrate the controllability to operate over a sufficient engine speed and load range to make it practical for implementation in production vehicles. In-cylinder blending of gasoline and diesel to achieve reactivity controlled compression ignition (RCCI) has been shown to reduce NO_x and PM emissions while maintaining or improving brake thermal efficiency as compared to conventional diesel combustion (CDC). The RCCI concept has an advantage over many advanced combustion strategies in that the fuel reactivity can be tailored to the engine speed and load allowing stable low-temperature combustion to be extended over more of the light-duty drive cycle load range. The potential for advanced combustion concepts such as RCCI to reduce drive cycle fuel economy has been explored by simulating the fuel economy and emissions for a multi-mode RCCI-enabled vehicle operating over a variety of U.S. drive cycles using experimental engine maps for multi-mode RCCI, CDC and a 2009 port-fuel injected (PFI) gasoline engine. The well-to-wheel energy of this concept has not been investigated as compared to conventional combustion or electric vehicles. The RCCI fuel economy simulation results are compared to the same vehicle powered by PFI gasoline engines, a conventional diesel engine and an electric powertrain over the city and highway driving cycles. The well-to-wheel energy and greenhouse gas emissions from these drive cycle simulations running various amounts of biofuels are examined and compared to the state-of-the art in conventional, electric and hybrid powertrains. Electric powertrain analysis also

takes into account proposed EPA regulations on reducing CO₂ emissions from power plants.

1. Introduction

The technological landscape of vehicle technologies is rapidly changing in the light of technology and regulation driven improvements in vehicle efficiency. Advancements in vehicle system efficiency with vehicle electrification, greater than 6-speed transmissions, advanced engine technologies, advanced combustion engine strategies and other are being driven by ever increasing regulations on fuel economy and control of criteria air pollutants and greenhouse gas emissions. A concise and up-to-date summary of emissions regulations around the globe can be found in [1]. The recent changes in US fuel economy standards and emissions controls have placed an unprecedented challenge to the vehicle system to deliver extraordinary fuel economy, low emissions and still meet consumer expectations of performance and safety.

Looming U.S. light-duty fuel economy and emissions regulations will continue to tighten. The 2025 Corporate Average Fuel Economy (CAFE) standard enacted by the U.S. National Highway Transportation Safety Administration (NHTSA) will require a corporate average fuel economy target of 54.4 miles per gallon [2]. The EPA proposed a new LEV III/Tier 3 standard (starting from 2017) which puts further restrictions on criteria air pollutants and gives a combined NO_x and NMOG standard. These regulations for fuel economy and emissions require a suite of transient drive cycles under the CFR [3].

The continued increase in consumers choosing alternative fuel and advanced vehicle powertrains also raises the question of energy and emissions system boundaries, especially with lifecycle greenhouse gas emissions. It is well recognized that improving the efficiency of internal combustion engines is one of the most promising and cost-effective near- to mid-term approaches to increasing highway vehicles' fuel economy [4-6]. The US DOE Vehicle Technologies Office's research and development activities address critical barriers to commercializing higher efficiency, very low emissions advanced internal combustion engines for passenger and commercial vehicles. This technology has great potential to reduce U.S. petroleum consumption, resulting in greater economic, environmental, and energy security [7] where it is implied that these engines need to meet regulations for criteria air pollutants. The development in vehicle efficiency may at first glance appear to have been stagnant over the last decade but in fact we have seen remarkable advancements in the understanding of engine efficiency, powertrain efficiency and the role of vehicle electrification. Light duty vehicles (cars and light trucks under 6500 lb gross vehicle weight)

have continued to become larger and meet new crash safety standards while meeting stringent emissions standards while maintaining a flat fuel economy average. The scientific understanding of the combustion process through the aid of high fidelity computational fluid dynamics coupled to chemical kinetics solvers has allowed for the acceleration of engine development. During the same time period, developments in microprocessor enabled engine control units; fuel injection equipment and advanced air handling have allowed for remarkable flexibility in the design and development of internal combustion engines.

Light duty vehicle fuel economy and criteria air pollutant emissions in the US are regulated by the US DOT NHTSA and US Environmental Protection Agency (EPA) respectively [8]. The nature of how light-duty vehicles are used primarily for personal transporting in both urban and rural driving conditions is taken into consideration in the regulation by defining the fuel economy and emissions regulations over prescribed drive cycles. In the United States, the EPA regulates emissions based on federal drive cycle compliance [9]. There are a number of EPA dynamometer driving cycles that attempt to take into account the real-world driving conditions seen with light-duty passenger vehicles as shown in Figure 53. Vehicles follow these drive cycles on a chassis dynamometer where repeatable results can be used to make comparisons between vehicles. The federal test procedure (FTP) is made up of three urban dynamometer driving schedule (UDDS) representing city driving conditions, the highway fuel economy test (HWFET), representing highway driving conditions under 60 mph. There are two supplemental test procedures, the SC03 and US06 which represent additional load with air conditioners and aggressive highway driving respectively. The last test in the EPA 5-cycle method is a cold start FTP [4]. The emissions standards are set by EPA for criteria air pollutants are oxides of nitrogen (NO_x – $\text{NO} + \text{NO}_2$), non-methane organic gases (NMOG) which are unburned hydrocarbons except CH_4 , carbon monoxide (CO) and particulate matter (PM).

With the increasing market penetration of hybrid electric powertrains, internal combustion engines will be co-evolving to have synergies with the various types of hybrid powertrains and will need to continue to operate safely, reliably and cleanly in the more complex propulsion systems. These interactions are further complicated when examining the regulatory drive cycles to which vehicles are certified for emissions compliance in the US. These transient drive cycles strive to mimic real-world conditions and present a range of operation. This transient nature also makes evaluating future engines and future powertrains difficult when only limited steady state engine data is available. The efficiency of a vehicle over these drive cycles depends not only on the vehicle powertrain architecture and body design including coefficient of drag, frontal area and rolling resistance of tires but also the drive cycle itself.

The wide range of vehicle electrification ranges from conventional hybrid electric vehicles which have no ability to plug in to the grid to battery electric vehicles which have no prime mover on-board the vehicle. This requires total energy and greenhouse analysis on well-to-wheels basis since electric vehicles generate zero emissions at the “tailpipe” but most often have upstream emissions associated with electricity generation. The amount of upstream emissions associated with electricity generation depends entirely on the electrical generating mix and the fuels used.

For a conventional ICE powertrain that has a conventional transmission, the fuel energy conversion efficiency is determined by engine efficiency, drivetrain losses and speed dependent losses. The peak efficiency of a conventional diesel light-duty engine is ~ 42.3% measured at the driveshaft with peak efficiencies as high as 45% demonstrated with the use of waste heat recovery [10]. Conventional vehicles do not operate near the peak efficiency often over the drive cycles which is a strong motivation for the development of advanced combustion modes and hybrid vehicle powertrains.

Low temperature combustion (LTC) techniques, also known as advanced combustion or high efficiency clean combustion (HECC) have been shown to significantly reduce engine-out emissions of NOX and soot while achieving high thermal efficiencies[7-20]. LTC techniques on compression ignition engine platforms include single fuel techniques such as homogenous charge compression ignition (HCCI), premixed charge compression ignition (PCCI) and partially premixed combustion (PPC). These techniques are limited in range by the reactivity of the fuel and by the engine architecture including compression ratio. More recently, there have been advances in dual-fuel LTC strategies, namely reactivity controlled compression ignition (RCCI). RCCI most often uses direct injection of a high-reactivity fuel such as ultra-low sulfur diesel (ULSD) fuel, and port injection of a low-reactivity fuel such as gasoline. RCCI has been shown to achieve diesel-like thermal efficiencies at lower loads and greater than diesel efficiency at high loads [20].

The advantage of using a dual-fuel rather than a single fuel LTC approach is that the reactivity of the fuel mixture can be controlled and thereby tailored to controlling combustion. RCCI allows control over start of combustion with the global fuel reactivity and further control over heat release rate with the reactivity stratification. The motivation for dual-fuel LTC techniques such as RCCI came from early studies showing that the optimal fuel for HCCI would have properties in between that of highly reactive diesel fuel and gasoline which has low reactivity [12] . An important note needs to be made that if an engine cannot be operated in an advanced combustion over the entire speed and load range demanded by the drive-cycle in question, then the engine would have to operate in a multi-mode strategy in which the engine would switch to conventional

combustion when engine power demands cause the engine to operate outside of the advanced combustion speed and load operating range. There have been a number of studies examining the potential for LTC/multi-mode operation with diesel engine baselines [26]. For LTC/CDC multi-mode operation, the engine switches to CDC for areas of the engine map that fell outside the LTC region.

Meeting these previously discussed future fuel economy and emissions regulations will be a non-trivial task which will in all likelihood require more expensive technologies and rapid development in vehicle systems efficiency. The advent of vehicle electrification and the continuing adoption of alternative fuels from a wide variety of feedstocks make comparing vehicles total energy use on both a miles/gallon and a well-to-wheels energy use necessary.

With pending national and international policies concerning the regulation of GHGs from power generation, transportation, and industrial processes including proposed rules on GHG limits on vehicles, more attention is being paid to carbon dioxide (CO_2) and other GHG emissions than ever before [25-27]. There are three widely accepted GHGs that result from stationary power generation from combustion, CO_2 , CH_4 and nitrous oxide (N_2O) [28]. The greatest bulk contributor to GHG emissions is CO_2 , which results from the combustion of any hydrocarbon fuel. Carbon dioxide emissions make up between 87% and 99% of the total GHG emissions from stationary power, assuming proper emissions controls are in place. The global warming potentials (GWPs) of CH_4 and N_2O are greater than that of CO_2 over a given time scale (often 100 years). Commonly agreed upon GWP values for CH_4 and N_2O for use in regulations come from the Intergovernmental Panel on Climate Change (IPCC) [24]. For example CH_4 , which has a strong role in atmospheric chemistry, has a GWP that is 21 times greater than that of CO_2 . Nitrous oxide, which is only produced in very small amounts from combustion, has a GWP that is 310 times greater than that of CO_2 , meaning that even small amounts of N_2O can have a very strong effect on GHG emissions. GHG emissions values are presented in terms of CO_2 equivalent ($\text{CO}_{2\text{eq}}$), taking into account all of the generated GHGs and their global warming potentials, which are shown in Table 27. To report GHG emissions on a CO_2 equivalent basis, the resultant emissions for each of the GHGs are multiplied by their individual GWP and added.

A WTW energy and emissions analysis is used to make a direct comparison between the total energy costs and emissions of the different vehicle technologies taking into account fuel cycle aspects as illustrated in Figure 54. This study takes advantage of the WTW analysis tool known as the Greenhouse Gas, Regulated Emissions and Energy Use in Transportation (GREET) model developed for the U.S. Department of Energy by Argonne National Laboratory (ANL). The total energy for each scenario by type as well as GHG emissions and criteria air pollutants are estimated to make a complete comparison.

The upstream or well-to-pump (WTP) part captures the fuel production energy costs and emissions, including transmission and distribution (T&D) pathways, from the point of fuel feedstock extraction to the point where the fuel is transferred to a vehicle in units of kilojoules or grams per megajoule of fuel at the pump for energy use and emissions respectively. The tank-to-wheels (TTW) part of the analysis only considers the vehicle use energy and emissions in units of kilojoules or gallons per kilometer respectively.

Though previous studies have compared the WTW energy use and GHG emissions of both conventional and advanced powertrains including various HEV architectures [29-31], they have not specifically addressed the use of an advanced combustion enabled vehicle in an apples-to-apples comparison of currently available technologies. The paper by Wang et al. examined the various natural gas to transportation fuel pathways, including modeling results for many long-term vehicle technologies [32], but did not evaluate low temperature combustion strategies.

The potential for advanced combustion concepts to reduce well-to-wheel energy use and GHG emissions compared to other state-of-the-art powertrains is still unknown. This study uses a combination of vehicle system simulations to model drive cycle fuel use and emissions and well-to-wheel analysis to estimate the potential for WTW energy use and GHG reductions for two multi-mode RCC/CDC vehicles with fuel economy results from vehicle systems simulations compared to other powertrains. Vehicle systems simulations are performed in Autonomie. Calculations are performed using the GREET model (GREET1_2013) [33].

2. Methodology

The analysis presented here uses fuel economy estimates from vehicle systems simulations that were published in the 2013 and 2014 papers by Curran et al [34-35]. The following sections on RCCI experiments and vehicle systems simulations provide the background context for this study with additional details on the experiments and simulations found in [30-31].

3.1 RCCI experiments leading to map

The engine used for this study is a modified 2007 General Motors 4 cylinder 1.9L turbocharged diesel engine. The base engine has a rated power of 110 kW and a rated torque of 315 Nm. The original equipment manufacturer (OEM) pistons were replaced with pistons modified for RCCI. The RCCI modified piston bowl geometry was designed for RCCI using CFD modeling by UW. The piston design is based on a heavy duty piston and minimizes the surface area of the piston to minimize heat transfer losses and also results in a lowered compression from 17.1 in the OEM configuration to 15.1 to allow for higher load

operation while maintaining reasonable pressure rise rate limits. More information about the piston design can be found in the paper by Hanson et al [23]. The diesel injection system and variable geometry turbo charger (VGT) were left in production form. The intake manifold was modified to incorporate extended tip narrow spray angle PFI injectors for the gasoline supply. A more in-depth discussion the intake manifold modifications can be found in Curran et al [20].

Multi-cylinder engine (MCE) mapping experiments made use of a systematic approach based on previous MCE experimental results and modeling described in the paper by Curran et al. without the direct use of modeling [36]. The robustness of dual-fuel RCCI allows for rapid map exploration and development however, the parameter space is non-trivial. Self-imposed experimental constraints of pressure rise rate and CO emissions. Cylinder pressure rise $< 10\text{bar/deg}$ and CO emissions $< 5000\text{ ppm}$ were adhered to. Additionally, a self-imposed constraint on the coefficient of variance (COV) of indicated mean effective pressure (IMEP) of 3%. IMEP is defined as the indicated cycle work calculated from the cylinder pressure using the compression & expansion strokes only (-180° ATDC to 180° ATDC) calculated divided by the engine displacement volume.

RCCI operation was achieved through an early single pulse of diesel fuel (between 30 and 70° BTDC) and port fueling of gasoline onto a closed intake valve. Fuel rail pressure was decreased as diesel fuel start of injection (SOI) timing was advanced to avoid spray impingement on the cylinder walls. Cylinder to cylinder balancing of cylinder pressure rise rate and IMEP was performed for successful RCCI operation and had to be adjusted based on operating condition and EGR level. Once cylinder-to-cylinder balancing was performed, no other real-time controls were needed to maintain stable operation.

3.2 Vehicle Systems simulations leading to RCCI fuel economy estimates

The RCCI multi-mode maps used for the vehicle system simulations in Autonomie[37] were generated using experimental engine data. The two maps explored here are an E30/ULSD engine map and an UTG-96/ B20 map. In both cases the CDC portion of the map is assumed to use the base fuel.

Simulated fuel economy of multi-mode RCCI operation using vehicle systems simulations with experimental steady-state engine maps compared to a representative 2009 gasoline PFI engine as baseline for comparison using diesel fuel and E30 (30% ethanol, 70% gasoline). Experimental steady-state RCCI operating points on modified multi-cylinder GM 1.9-L engine using an in-house methodology for RCCI combustion were used to develop an RCCI speed/load map consistent with a light-duty drive-cycle with sufficient detail to support

vehicle simulations. The RCCI map developed as part of this study represents an increase in RCCI operation over previous low temperature combustion operation maps [30] [30], but was still not able to cover the engine speed and load required to meet all power demands over the light-duty drive cycles with the self-imposed constraints imposed on the engine experiments leading to the RCCI engine map shown in Table 27.

Tables 28 and 29 show the results for E30/ULSD and gasoline/B20 RCCI maps respectively. The simulations used a multi-mode RCCI/diesel operating strategy where the engine would operate in RCCI mode whenever possible but at the highest and lowest engine operating points, the engine would switch to diesel mode as shown in Figure 55. All simulations were carried out in Autonomie using a 1580 kg passenger vehicle (mid-size sedan i.e. Chevrolet Malibu) over numerous U.S. federal light-duty drive cycles. A representative 2009 gasoline PFI engine map was obtained from an automotive original equipment manufacturer (OEM) for use in the vehicle simulations. It should be noted that a 2009 gasoline PFI baseline is standard in DOE VTO programmatic goals [38]. The 2014 paper by Curran et al determined that a 2.7 PFI baseline was the best match to the multi-mode RCCI engine in terms of 0-60 acceleration [30].

In addition to those vehicles in previous vehicle systems simulations, a battery electric vehicle (BEV) based on a 2012 Nissan Leaf was also simulated in Autonomie for comparison here. The next section validates these vehicles system simulations of the PFI, CDC and BEV baselines to dynamometer data.

3.3 Benchmarking simulations to actual data

Validation of the vehicle systems simulations was conducted through comparing published dynamometer drive cycle results for vehicles with the correct size and model year as those used in study. Since the 1.8 L engine class is not present in any mid-size passenger sedan, the lowest fuel economy was used, for the 4.0L the highest fuel economy was used. For the 2.4 and 2.7, the average of midsize vehicles was used. A factor of 1.038 was used to convert FTP to UDDS fuel economy. Argonne National Laboratory chassis dynamometer data was used to compare an Opel Astra with the same engine as used in this study with a test weight of 1360.78 KG and a 6-speed manual transmission.

It is often assumed that weight can result in 1-2% decrease in fuel economy per 100 lb (44kg) [39]. To see how what this effect had keeping all other elements of the vehicle constant, UDDS and HWFET simulations with a conventional gasoline baseline in Autonomie were run. As shown in Figure 57, there is a 0.01025 MPG/KG weight penalty for the vehicle systems simulations.

Table 30 shows the corrected UDDS and HWFET MPG for the various engine classes based on chassis dynamometer testing assuming a 0.01025%/kg

reduction in fuel economy determined by the Autonomie modeling. It is worth noting that these values are within 3% of the corrected values assuming a 1.5%/100lb weight penalty. The largest differences for the 1.8 L PFI class could be accounted for with noting that the smaller vehicles will most likely have a lower aerodynamic drag coefficient (frontal area and coefficient of drag) and possible lower rolling resistant tires, neither of which are accounted for in the simple mass correction. But in general, the vehicle systems simulations used here have been validated to actual chassis dynamometer data to within 7.5% of the combined cycle average and within 4.1% for all vehicles except the 1.8 L PFI baseline. For the BEV case, no weight correction was needed. The vehicle systems simulation combined MPGGE was 171 mpgge while the ANL chassis dynamometer testing [40] gave a 161.9 MPGGE for a difference of 6% and within the range of differences from the other baselines.

It should be noted that these combined cycle fuel economy averages are higher than the EPA sticker fuel economies for the test vehicles as these are uncorrected fuel economy values over the UDDS and HWFET only and do not have EPA corrections applied accounting for the SC03 and US06 and cold start FTP. It is also important to note that for the BEV case, these results are for the on vehicle use of electricity for motor power (termed DC Wh/mile) and the conversion of Wh/mile to GGE is done using a conversion factor of 33.7 kw-hr/gallon of gasoline (which is accounted for in the GREET analysis taking into account EV charger efficiency). The EPA applies additional correction factors to adjust the raw BEV fuel economies to the 5-cycle test and such these results are above the “City” and “Highway” fuel economy numbers on the EPA vehicle fuel economy sticker. These results do allow for a most direct comparison to the vehicle systems simulation fuel economies for the non-electrified PFI, CDC and RCCI powertrains.

3.4 GREET modeling using fuel economy simulation results

The GREET model used for this study is designed for WTW analysis for transportation systems and as such has a backbone of stationary power calculations to accurately account for electricity’s role in transportation, including upstream emissions for electrical power generation. GREET is a Microsoft Excel-based calculation tool that has simulation values for emissions factors and energy use for stationary power generation to more accurately determine life-cycle criteria and GHG emissions and energy use for mobile applications. For both stationary and transportation use there are default electricity generation mixes for the US regions as well as user-defined mixes. The mixes allow inputs for percent of electricity generated by residual oil, natural gas, coal, nuclear, biomass, and others. The latter category is broken down into: hydroelectric, wind, solar photovoltaic, and undefined others.

Autonomie [41] which was used to provide the default values in GREET over the city and highway federal driving cycles [42]. EPA fuel economy data assume a split of 45% city driving and 55% highway driving. It should be noted that the driving schedule, the particular vehicle used and driver behavior all have a significant impact on fuel economy and can result in real world driving fuel economy that differ as much as 40% from the EPA estimate [43].

For the BEV, a charger efficiency of 88 % is assumed [44]. For conventional gasoline vehicles in GREET, the fuel is assumed to be a US specification E10, the diesel is assumed to be a US diesel fuel. The fuels for RCCI have both fuels that match the fuel used while conventional diesel combustion uses the diesel fuel used (either ULSD or B20).

Table 31 shows fuel economies in units of miles per gasoline gallon equivalent (mpgge) which assumes gasoline has an energy content of 31,270 kJ/L and diesel fuel has an energy content of 35,801 kJ/L. Electricity generation has an assumed 8% T&D loss [45].

GREET accounts for the EV charger efficiency by applying the efficiency to per-mile fuel consumption of vehicle operations giving an EV with charger value. For this analysis, an EV charger efficiency of 88 % is assumed. In practice, the EV charger efficiency depends greatly on the type of charger in place. Since EVs can charge through a slow charger using 120V, a LEV II charger supplied by 220V up to DC fast chargers. The driver would not see any difference on the TTW fuel economy on the EV but would notice a difference in the electricity use which would result in very different upstream emissions as shown on the WTP analysis. This accounting methodology cuts off the WTP portion at the input to the EV charger meaning that T&D losses are accounted for to the point of the charger.

3.5 Electricity generation in GREET including future CO₂ regulations

Three BEV charging scenarios are examined. Charging via the US electrical generation mix, current coal fired plants and a case assuming new EPA regulations on reducing CO₂ from fossil fuel-fired plants. A US electrical generation mix is assumed as shown in Figure 58 along with a scenario with only coal generation. For the current coal generation scenario, the GREET default assumptions for a steam turbine generation plant with an energy conversion efficiency of 34.7% is assumed. Additionally, an EV scenario taking into account the proposed EPA new source performance standard to limit CO₂ emissions fossil fuel-fired power plants is also considered. The proposed emissions limits would be 1,000lb CO₂/MWh (454 g/KWh) for large plants and 1,100lb CO₂/MWh for smaller units. It should be noted that the EPA assumes three possible scenarios, highly efficient with partial carbon capture and sequestration (CCS),

high efficient with full CCS and highly efficient with no CCS scenario [47]. In order to meet the large plant standard without CCS, an integrated gasification combined cycle (IGCC) coal plant would need to have on the order of 75.2% electrical generating efficiency as measured at the power plant gate. The highest efficiency natural gas combined cycle GE Flex Efficiency plants have only a 61% baseload efficiency [48]. GREET has a CCS energy use assumption for CO₂ capture in Coal-based liquids of 336 kWh/ton C and 357 kWh/ton for gaseous hydrogen plants. A 20 - 30% de-rating factor is assumed with an 80% efficient CCS method and a recent report from the National Energy Technology Laboratory (NETL) [49] which reported a higher heating value efficiency for IGCC of 40.3% with a resulting net efficiency of 31.6% w/CO₂ capture. According to the NETL report, the reductions in net electrical generation efficiency were greater with pulverized coal technologies than for the IGCC plants. For this analysis, a lower heating value efficiency of 38.01% was assumed for the base case of highly efficient fossil fuel-fired coal plant with a net efficiency with CO₂ capture of 29.81% which is 14% lower than the current steam turbine generation plant used for this analysis.

3.6 Modifying GREET for dual fuel operation

With the exception of the plug-in electric hybrid vehicles (PHEV) which use electricity only in a charge depleting mode while a combination of electricity and fuel in charge sustaining mode, GREET is only designed for single fuel analysis. To perform WTW energy use analysis, GREET had to be modified. For this analysis, the PFI and DI fuel usage for the two RCCI multimode maps were separated out and a fuel economy for each fuel was determined. The total fuel of each type was converted to GGE over the cycle distance and the EPA split of 45% highway and 55% city driving was used to determine PFI fuel economy and DI fuel economy. These fuel economies were put into the correct fuel type in GREET with gasoline and E30 being put into a gasoline vehicle while ULSD and B20 were put in a CIDI vehicle and the energy use and emissions results were added as shown in Table 32.

4. Results

Using GREET, key assumptions were modified in accordance with the references discussed in the assumptions section. Vehicle fuel economies were normalized to the energy content of gasoline using mpgge. GHG emissions are presented in grams of CO₂ equivalent as described previously.

The total WTW energy use and vehicle energy use in kJ/km are shown in Figure 59. The WTW and vehicle petroleum use are shown in Figure 60. As compared to the 2.7L PFI baseline, the RCCI enabled vehicles were found to provide a 28% and 26% reduction in vehicle petroleum use for the E30 and B20

RCCI cases respectively. It should be noted that the addition of the CO₂ capture technology to the BEV coal fired case increased the total energy use by 24%.

The WTW and vehicle GHG emissions are shown in Figure 61. As has been shown in previous research, the zero tailpipe emissions with BEVs illustrates the importance of comparing advanced vehicle technologies on a well-to-wheels basis as energy for transportation is further diversified to include more associated upstream emissions. The CO₂ capture reduced the BEV charging scenario by ~50%.

It should be noted that the GREET derived upstream CO₂ emissions that are calculated on Fuel economy.gov show a 49% reduction with a Nissan Leaf as compared to a Chevy Cruze Diesel (124 and 243 g/km respectively). The results from Autonomie provide a 51% reduction in WTW GHG gases compared to CDC vehicle based on the 1.9 L GM ZDTH CIDI vehicle. .

Further comparison of that the role of the renewable fuels has on the WTW GHG reductions was examined by assuming replacing the biofuel portions B20 and E30 RCCI cases with conventional gasoline (E0) and ULSD assuming no change in drive-cycle fuel economy. The petroleum energy use and GHG emissions for the 2.7L PFI gasoline baseline with conventional gasoline and E15 (15%ethanol/ 85% gasoline), the CIDI case with ULSD and B20, the RCCI cases with and without biofuels and the BEV with the future EPA proposed restrictions on GHG emissions from coal fired power plants are shown in Figure 62 Figure 63 respectively.

5. Discussion

The DOE VTP Advanced Combustion Engine research and development program's strategic goals are to reduce petroleum dependence by removing critical technical barriers to mass commercialization of high-efficiency, emissions-compliant internal combustion engine powertrains in passenger and commercial vehicles [34]. Improvements in engine efficiency and engine systems efficiency through advanced combustion strategies is an important pathway to this goal. For advanced combustion strategies to be able to meet these goals [3], their effectiveness over different driving cycles on real vehicles with emission compliance will have to be determined.

The addition of exhaust aftertreatments will most likely result in increasing the total energy use of the RCCI vehicles as the calibration would need to be adjusted for emissions compliance. This initial analysis of WTW energy, GHG and petroleum usage for RCCI enabled vehicles has shown significant benefits as compared to a comparable PFI baseline. These improvements were seen despite the lack of complete drive cycle coverage with engine hardware that was primarily designed for conventional diesel combustion.

This analysis did not attempt to adjust simulations to the 5-cycle averages with the EPA adjustment factors. Instead, the comparison was carried out with an assumed split of city and highway driving using the UDDS and HWFET drive cycles on the same vehicle size and weight.

The analysis of the RCCI cases assumed no WTW benefit from renewable fuel usage still shows a significant decrease in petroleum use and GHG emissions compared to the gasoline baseline but not as significant with as with BEV which would be expected with the high powertrain efficiency of the current BEVs. Analysis of proposed future regulations on BEV scenarios showed that CO₂ capture offers significant GHG reduction potential at the cost of reduced energy efficiency. This scenario could also make the WTW energy use and GHG reduction potentials of RCCI plug-in hybrid more attractive. .

6. Conclusions

Unprecedented advances in fuel economy and emissions control standards are driving the need for significantly higher engine efficiency than current stoichiometric PFI gasoline technology prevalent in LD market. The WTW analysis of an RCCI enabled vehicle demonstrated significant petroleum and GHG reductions. The unique properties of renewable fuels not only allowed to better cover the drive-cycle in RCCI mode but made a difference in WTW GHG emissions.

There are further improvements possible as the RCCI concept is further refined and optimized for drive-cycle concerns and should be able to offer further reductions in petroleum and GHG emissions on not only conventional vehicles but hybrid vehicle powertrains. The analysis presented here does not address potential hybrid vehicle integration. However, initial simulations results with a RCCI/CDC multimode engine in a series hybrid configuration show the potential for even further improvements in fuel economy.

7. Disclaimer

This manuscript has been authored by a contractor for the U.S. Government under contract number DE-AC05-000R22725. Accordingly, the U.S. Government retains a nonexclusive, royalty-free license to publish or reproduce the published form of this contribution, or allow others to do so, for the U.S. Government.

8. Acknowledgments

The authors wish to thank their colleagues at the University of Wisconsin, Prof. Rolf Reitz, Reed Hanson, Prof. Sage Kokjohn and Derek Splitter (now at ORNL) for their modeling guidance, piston design and input on RCCI operation. Portions of this work were supported by the U.S. Department of Energy (DOE), Vehicle Technologies Office. The authors gratefully acknowledge the support and

guidance of Gurpreet Singh, Ken Howden, Leo Breton, Kevin Stork, Steve Przesmitzki, Lee Slezak and David Anderson at DOE. The authors would also like to acknowledge the Bredesen Center for Interdisciplinary Graduate Research and Education at the University of Tennessee including Prof. Lee Riedinger and Prof. Mike Simpson as well as Prof. Claudia Rawn.

References

1. "Worldwide Emissions Standards: Passenger Cars and Light Duty Vehicles," Delphi Automotive: <http://delphi.com/pdf/emissions/Delphi-Passenger-Car-Light-Duty-Truck-Emissions-Brochure-2013-2014.pdf>.
2. "Average Fuel Economy Standards," Title 49 U.S. Code, Sec. 32902 et seq, 2001 ed.
3. "Control of Air Pollution From Motor Vehicles: Tier 3 Motor Vehicle Emission and Fuel Standards; Proposed Rule," 78 Federal Register [98], 21 May 2013, pp. 29816-30191.
4. Review of the Research Program of the FreedomCAR and Fuel Partnership: 3rd Report, NRC 2010
5. DOE Quadrennial Technology Review 2011
6. Energy Information Agency, Annual Energy Outlook, 2011
7. US Department of Energy, Office of Vehicle Technologies http://www1.eere.energy.gov/vehiclesandfuels/pdfs/pir/vtp_goals-strategies-accomp.pdf
8. "Emissions Standards for Light-Duty Vehicles, Light-Duty Trucks, and Medium-Duty Passenger Vehicles," Code of Federal Regulations, Part 86, Protection of the Environment. Subpart 1811-04, Office of the Federal Register, 2001.
9. US Environmental Protection Agency, Testing and Measuring Emissions, www.epa.gov/nvfe/testing/dynamometer.htm.
10. Curran, S., Hanson, R., Wagner, R., and Reitz, R., "Efficiency and Emissions Mapping of RCCI in a Light-Duty Diesel Engine," SAE Technical Paper 2013-01-0289, 2013
11. Sluder, C., Wagner, R., Storey, J., and Lewis, S., 2005, "Implications of Particulate and Precursor Compounds Formed During High-Efficiency Clean Combustion in a Diesel Engine," SAE 2005-01-3844.
12. Wagner, R., Green, J., Dam, T., Edwards, K., and Storey, J., 2003, "Simultaneous Low Engine-Out NOX and Particulate Matter with Highly Diluted Diesel Combustion," SAE 2003-01-0262.
13. Sluder C., Wagner R., Lewis, S., Storey, J., 2006, "Fuel Property Effects on Emissions From High Efficiency Clean Combustion in a Diesel Engine," SAE Technical Paper 2006-01-0080.
14. Sluder, C. Wagner, R., 2006, "An Estimate of Diesel High-Efficiency Clean Combustion Impacts on FTP-75 Aftertreatment Requirements," SAE 2006-01-3311

15. Kokjohn, S., Hanson, R., Splitter, D., and Reitz, R., 2009, "Experiments and Modeling of Dual-Fuel HCCI and PCCI Combustion Using In-Cylinder Fuel Blending," SAE 2009-01-2647.
16. Inagaki, K., Fuyuto, T., Nishikawa, K., and Nakakita, K., 2006, "Dual-Fuel PCCI Combustion Controlled by In-Cylinder Stratification of Ignitability," SAE paper 2006-01-0028.
17. Manente, V., Johansson, B., and Tunestal, P., 2009, "Partially Premixed Combustion at High Load using Gasoline and Ethanol, a Comparison with Diesel," SAE 04-20-2009.
18. Chadwell, C., Alger, T., Roberts, C., and Arnold, S., 2011, "Boosting Simulation of High Efficiency Alternative Combustion Mode Engines," SAE 04-12-2011.
19. Hanson, R., Kokjohn, S., Splitter, D., and Reitz, R., 2010 "An Experimental Investigation of Fuel Reactivity Controlled PCCI Combustion in a Heavy-Duty Engine," SAE 2010-01-0864
20. Cho, C., Han, M., Wagner, R., and Sluder, S., 2008, "Mixed-Source EGR for Enabling High-Efficiency Clean Combustion Modes in a Light-Duty Diesel Engine," SAE 2008-01-0645
21. Curran, S., Prikhodko, V., Cho, C., Sluder, C., Parks, J., Wagner, R., and Kokjohn, S., 2010, "In-Cylinder Fuel Blending of Gasoline/Diesel for Improved Efficiency and Lowest Possible Emissions on a Multi-Cylinder Light-Duty Diesel Engine," SAE 2010-01-2206
22. Curran, S., Cho, C., Briggs, T., and Wagner, R., 2011, "Drive Cycle Efficiency and Emissions Estimates for Reactivity Controlled Compression Ignition in a Multi-Cylinder Light-Duty Diesel Engine," Proceedings of the 2011 Internal Combustion Engine Division Fall Technical Conference, ICEF2011, Morgantown Wv.
23. Splitter, D., Hanson, R., Kokjohn, S., and Reitz, R., 2011, "Reactivity Controlled Compression Ignition (RCCI) Heavy-Duty Engine Operation at Mid-and High-Loads with Conventional and Alternative Fuels," SAE 2011-01-0363
24. Curran, S., Hanson, R., and Wagner, R., 2012, "Reactivity controlled compression ignition (RCCI) combustion on a multi-cylinder light-duty diesel engine", International Journal of Engine Research, 2012
25. US Environmental Protection Agency, 2011. *Climate Change*, <http://www.epa.gov/climatechange/index.html>.
26. The International Council on Clean Transportation, 2012. *Global Comparison of Light-Duty Vehicle Fuel Economy/GHG Emissions Standards*, <http://www.theicct.org>.

27. 2017 and Later Model Year Light-Duty Vehicle Greenhouse Gas Emissions and Corporate Average Fuel Economy Standards Fed Reg Vol. 77 Monday, No. 199 October 15, 2012
28. Intergovernmental Panel on Climate Change, 2007. *Fourth Assessment Report*, <http://www.ipcc.ch/pdf/assessment-report/ar4/wg1/ar4-wg1-chapter2.pdf>.
29. Atkins, M., and Koch, C., "A Well-to-Wheel Comparison of Several Powertrain Technologies," SAE Technical Paper 2003-01-0081, 2003, doi:10.4271/2003-01-0081.
30. Heywood, J., et al., "The Performance of Future ICE and Fuel Cell Powered Vehicles and Their Potential Fleet Impact," SAE Technical Paper 2004-01-1011, 2004, doi:10.4271/2004-01-1011.
31. Meyer, P., et al., "Total Fuel-Cycle Analysis of Heavy-Duty Vehicles Using Biofuels and Natural Gas-Based Alternative Fuels," *Journal of the Air & Waste Management Association*, V 61, 2011.
32. Wang, M., and Huang, H., 1999. A Full Fuel-Cycle Analysis of Energy and Emissions Impacts of Transportation Fuels Produced from Natural Gas, ANL/ESD-40, Argonne National Laboratory.
33. Argonne GREET Model, <http://greet.es.anl.gov/>.
34. Curran S, Gao Z, Wagner, R., "Reactivity Controlled Compression Ignition Drive Cycle Emissions and Fuel Economy Estimations Using Vehicle Systems Simulations with E30 and ULSD", SAE Technical Paper 2014-01-1324, 2014.
35. Curran, S., Gao, Z., and Wagner, R., "Reactivity controlled compression ignition drive cycle emissions and fuel economy estimations using vehicle systems simulations", *International Journal of Engine Research* (Article in press 2014)
36. Curran S, Hanson R, and Wagner R. Reactivity controlled compression ignition (RCCI) combustion on a multi-cylinder light-duty diesel engine, *International Journal of Engine Research* 2012; 13(3): 216–225.
37. Autonomie website, <http://www.autonomie.net/>
38. Vehicle Technologies Office. Advanced Combustion Engines, www1.eere.energy.gov/vehiclesandfuels/technologies/engines/index.html.
39. US Department of Energy and EPA, Fuel Economy.gov website
40. ANL AVPRF data – Henning Louche Busch
41. Gopal, R., and Rousseau, A. "System Analysis Using Multiple Expert Tools," SAE Paper 2011-01-0754, 2011.
42. Burnham, A., 2012. *Updated Vehicle Specifications in the GREET Vehicle-Cycle Model*, Argonne National Laboratory, <http://greet.es.anl.gov/publication-update-veh-specs>.

43. "Final Technical Support Document, Fuel Economy Labeling of Motor Vehicle Revisions to Improve Calculation of Fuel Economy Estimates", US EPA EPA420-R-06-017, 2006
44. Chae, H., et al., "3.3kW On Board Charger for Electric vehicle," 8th International Conference on Power Electronics—ECCE Asia, May 30–June 3, 2011, The Shilla Jeju, Korea, 2011.
45. US Department of Energy, 2008. *Combined Heat and Power: Effective Energy Solutions for a Sustainable Future*,
<http://info.ornl.gov/sites/publications/files/Pub13655.pdf>.
46. US Department of Energy, 2008. *Combined Heat and Power: Effective Energy Solutions for a Sustainable Future*,
<http://info.ornl.gov/sites/publications/files/Pub13655.pdf>.
47. The Federal Register, Vol 79, No.5, Part II 2014, "Standards of Performance for Greenhouse Gas Emissions From New Stationary Sources: Electric Utility Generating Units; Proposed", Rule <http://www.gpo.gov/fdsys/pkg/FR-2014-01-08/pdf/2013-28668.pdf>
48. GE flexefficiency_50_combined_cycle_power_plant, 2014
http://www.geenergy.com/products_and_services/products/gas_turbines_heavy_duty/flexefficiency_50_combined_cycle_power_plant.jsp
49. NTEL CCS roadmap
<http://www.netl.doe.gov/File%20Library/Research/Carbon%20Seq/Reference%20Shelf/CCSRoadmap.pdf>

Appendix 4.1

Table 27. IPCC GWP potentials [24].

Greenhouse gas	Common sources	GWP
Carbon dioxide	Combustion	1
Methane	CH ₄ slip	21
Nitrous oxide	Combustion	310

Table 28. E30/ULD RCCI Multi-Mode Results

FE/Emissions	FE %	%RCCI Distance	%Total Diesel	%Diesel for RCCI
UDDS	39.35	51.8%	64.2%	42.4%
HWFET	60.90	74.3%	54.7%	38.9%

Table 29. Gasoline/B20 RCCI Multi-mode Results

FE/Emissions	FE %	%RCCI Distance	%Total B20	%B20 for RCCI
UDDS	37.62	72.3%	56.1%	40.9%
HWFET	57.08	88.2%	44.4%	36.9%

Table 30. Benchmarking UDDS and HWFET fuel economy with vehicle weight corrections and % difference from vehicle system simulation fuel economy (in actual MPG)

Type	Vehicle Weight (kg)	Weight Correction (MPG)	UDDS raw (MPG)	UDDS Corrected (MPG)	HWFET raw (MPG)	HWFET Corrected (MPG)	Combined Corrected (MPG)	% Diff
1.8L PFI	1382	-2.02	33.90	31.88	48.10	46.08	38.27	7.5%
2.4L PFI	1690	1.12	28.28	29.40	44.03	45.15	36.49	- 0.1%
2.7L PFI	1700	1.22	25.11	26.33	38.30	39.52	32.27	- 4.1%
4.0L PFI	1896	3.22	22.00	25.22	33.80	37.02	30.53	- 2.2%
1.9L CIDI	1360	-2.24	36.56	34.31	57.61	55.37	43.79	- 1.7%

Table 31. Vehicle Systems simulation mpgge fuel economies used for WTW analysis

	UDDS MPGGE	HWFET MPGGE	Combined MPGGE
1.8L PFI	29.57	43.00	35.61
2.4L PFI	30.02	44.51	36.54
2.7L PFI	26.98	41.81	33.65
4.0L PFI	24.71	39.19	31.23
1.9L CIDI	31.22	48.31	38.60
RCCI (UTG/B20)	32.86	49.86	40.18
RCCI (E30/ULSD)	34.37	53.19	42.50
BEV	189.4	149.8	171.5

Table 32. Dual fuel PFI and DI fuel economies used in GREET for analysis

	PFI MPGGE	DI MPGGE	Combined MPGGE
E30 RCCI	104.9	81.23	42.50
B20 RCCI	90.7	93.6	40.18

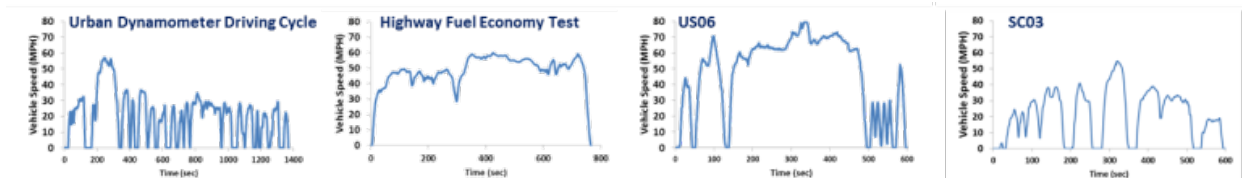


Figure 53. US EPA light-duty dynamometer driving cycles

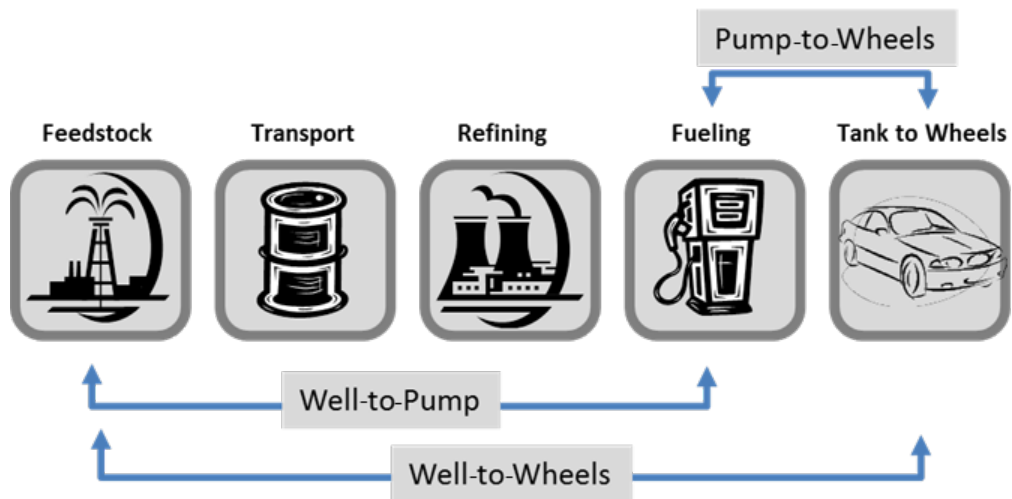


Figure 54. WTW fuel pathway.

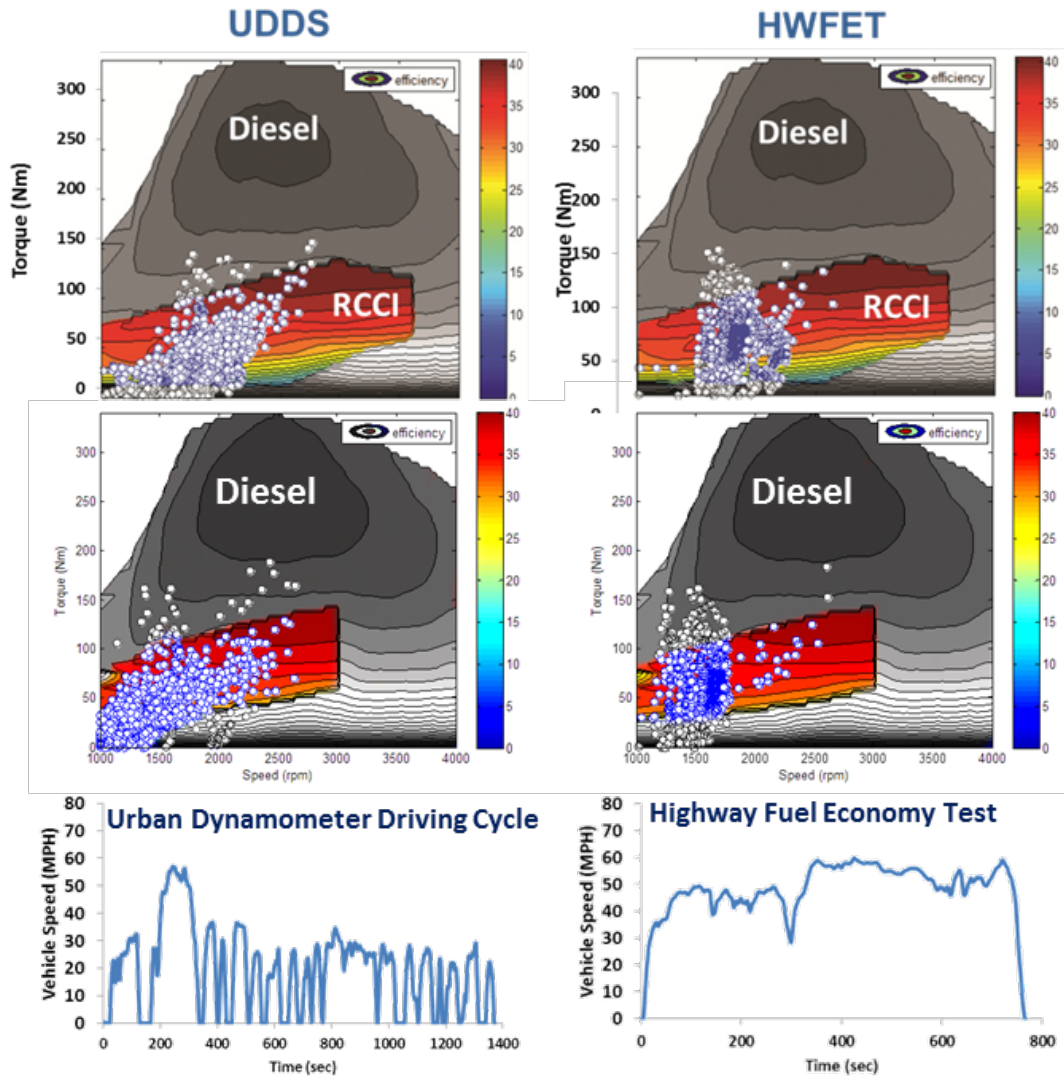


Figure 55. Drive cycle coverage in terms of engine speed and load plots for RCCI multi-mode map

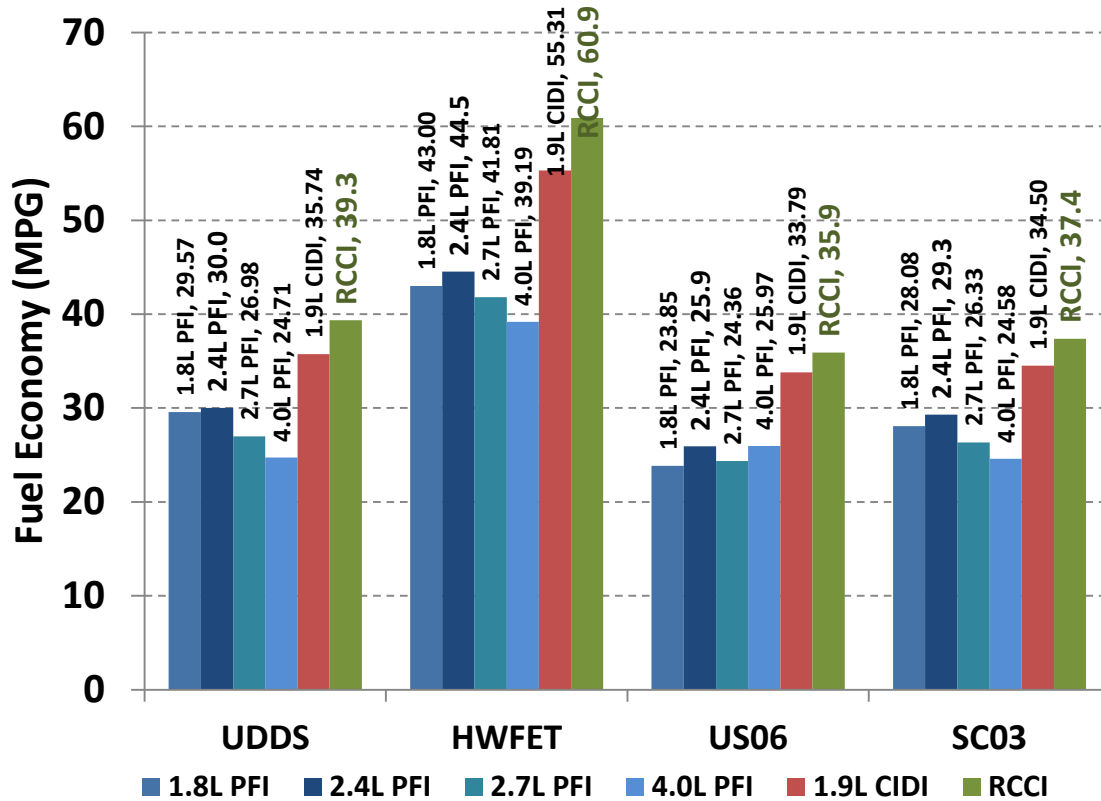


Figure 56. Vehicle Systems simulations for PFI, CDC and RCCI multi-mode

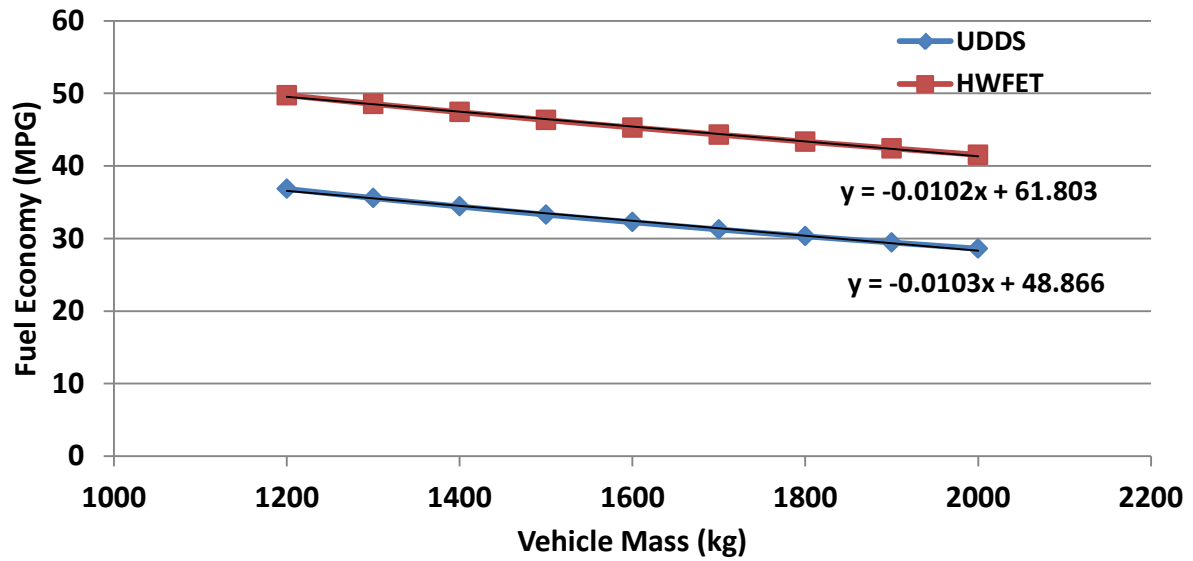


Figure 57. Fuel economy penalty for vehicle mass using a 2.2L SIDI engine conventional gasoline baseline

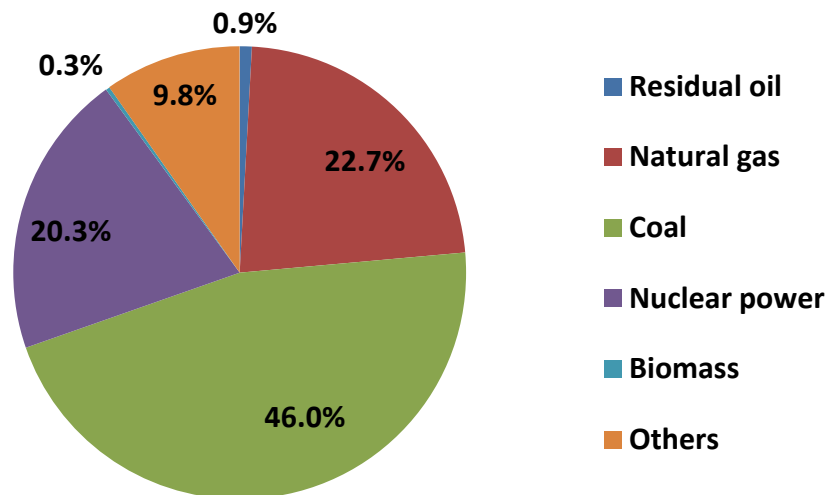


Figure 58. US Electrical Generation Mix

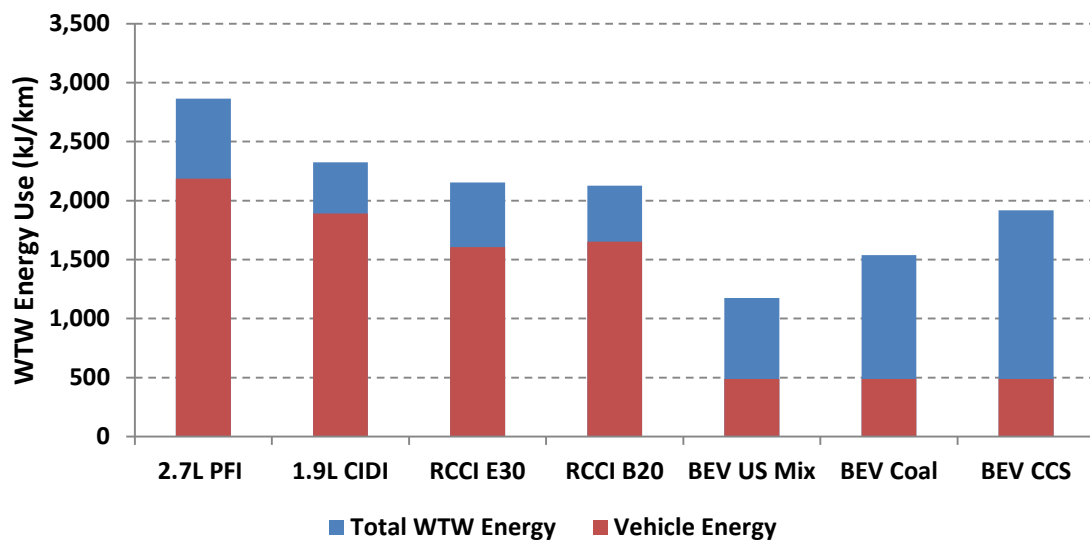


Figure 59. Total and vehicle energy use

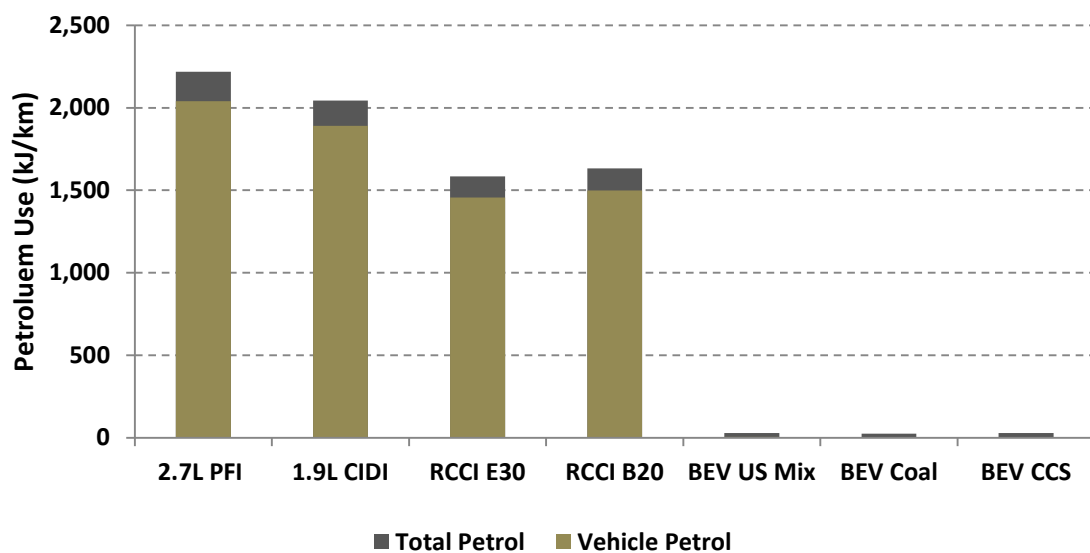


Figure 60. Total and vehicle petroleum use

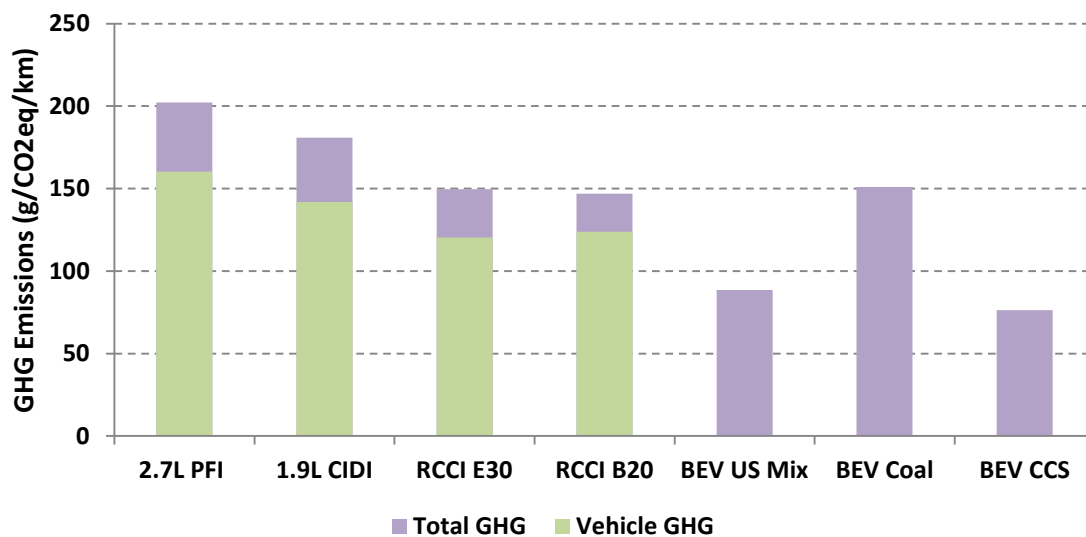


Figure 61. Total and vehicle GHG emissions

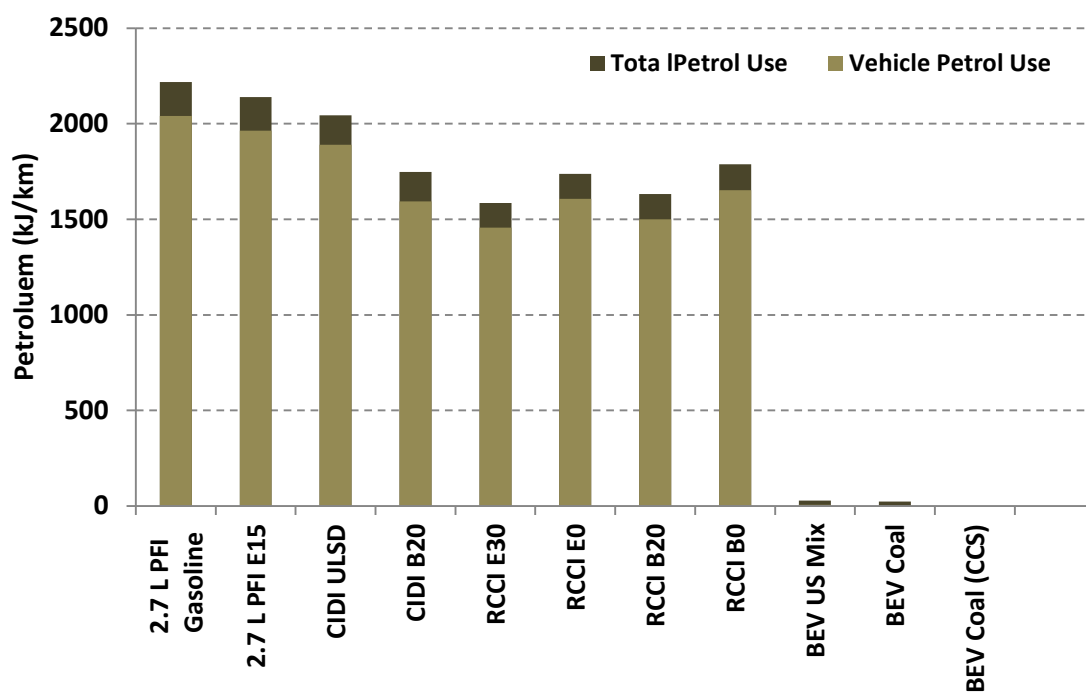


Figure 62. Petroleum energy use, with and without biofuels

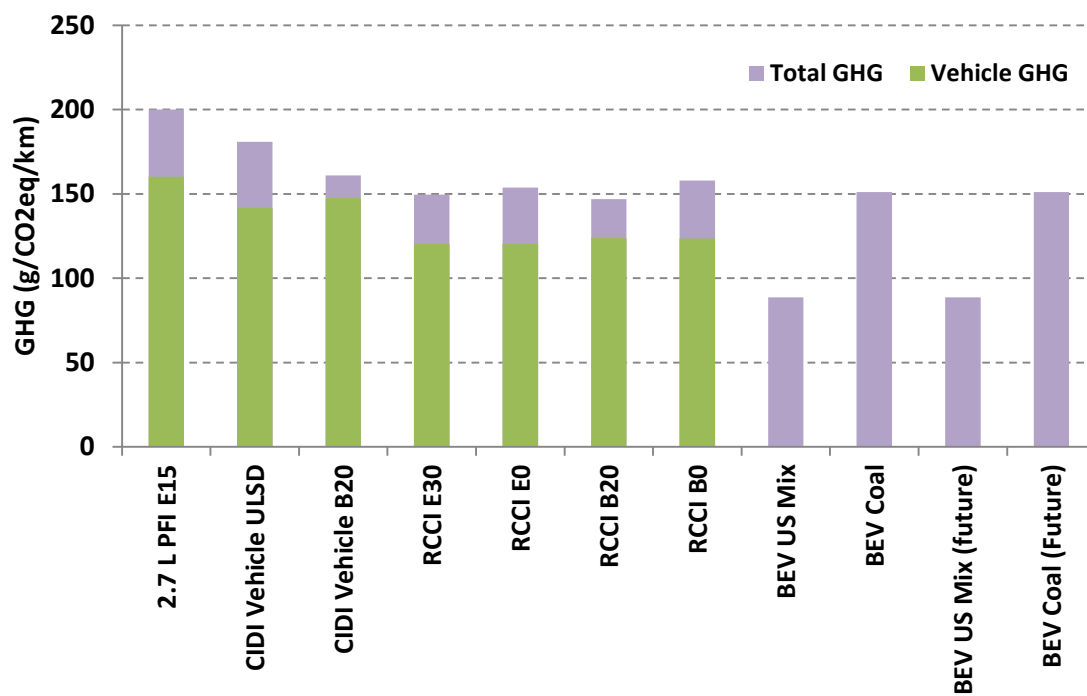


Figure 63 GHG emissions, with and without biofuels

Appendix 4.2

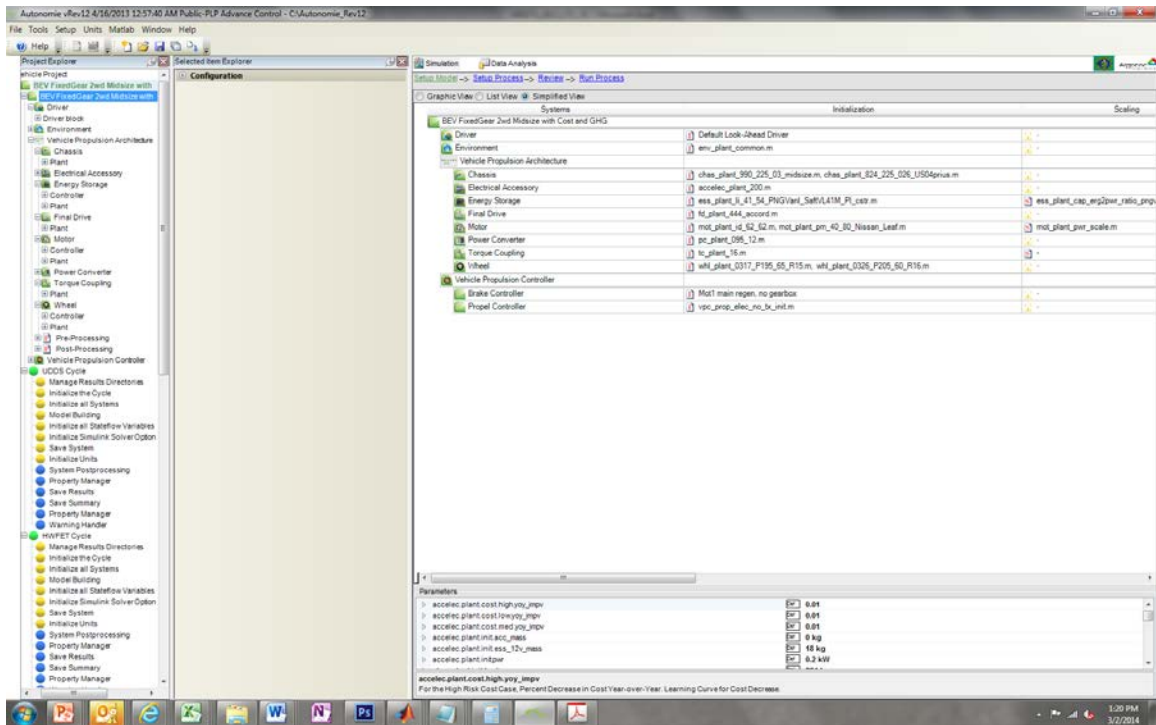


Figure 64. Nissan Leaf Model

Table 33. Nissan Leaf Modeling Results

Name	Unit	leaf_udds_cycle	leaf_hwfet_cycle
System Name		bev_fixedgear_2wd_mids ize	bev_fixedgear_2wd_mids ize
Simulation Folder		2014_0301_1927_54_62 9	2014_0301_1928_58_75 2
Process Name		UDDS Cycle	HWFET Cycle
Cycle Name		UDDS	HWFET
Distance Traveled	mile	7.44	10.25
Cycle Distance	mile	7.45	10.26
Start Time	s	0	0
End Time	s	1369	764
Percent Time Trace Missed by 2mph	%	0	0
Electrical Consumption	W.h/mile	178.85	225.49
Initial SOC	%	90	90
Final SOC	%	87.3	85.31
Delta SOC	%	-2.7	-4.69
Percent Regen Braking at Battery	%	81.53	80.4
Percent Regen Braking at Wheel	%	97.17	99.49
Regen Braking Energy Recovered at Battery	W.h	-527.52	-155.75
Regen Braking Energy Available at Wheel	W.h	-636.62	-192.37
Total Braking Energy at Wheel	W.h	-655.13	-193.37
Energy Storage			
Bidirectional Efficiency	%	100	99.99
Unidirectional Energy In	W.h	1331.24	2312.16
Unidirectional Energy Out	W.h	1331.13	2311.97
Motor			
Bidirectional Efficiency	%	89.4	84.18
Unidirectional Energy In	W.h	1251.07	2267.29
Unidirectional Energy Out	W.h	996.81	1854.32
Torque Coupling			

Table 33. Continued

Name	Unit	leaf_udds_cycle	leaf_hwfet_cycle
Bidirectional Efficiency	%	97.03	97.01
Unidirectional Energy In	W.h	996.81	1854.32
Unidirectional Energy Out	W.h	930.82	1787.75
Final Drive			
Bidirectional Efficiency	%	97.03	97.01
Unidirectional Energy In	W.h	930.82	1787.75
Unidirectional Energy Out	W.h	865.74	1722.86
Wheel			
Bidirectional Efficiency	%	73.86	59.66
Unidirectional Energy In	W.h	865.74	1722.86
Unidirectional Energy Out	W.h	254.99	830.87
Chassis			
Bidirectional Efficiency	%	87.36	49.51
Unidirectional Energy In	W.h	254.99	830.87
Unidirectional Energy Out	W.h	-0.36	-0.07
Power Converter			
Bidirectional Efficiency	%	95	95
Unidirectional Energy In	W.h	80.06	44.68
Unidirectional Energy Out	W.h	76.06	42.44
Electrical Accessory			
Bidirectional Efficiency	%	0	0
Unidirectional Energy In	W.h	76.06	42.44
Unidirectional Energy Out	W.h	0	0
Energy			
Vehicle Propulsion Architecture			
Energy Storage			
Unidirectional Energy In	W.h	1331.24	2312.16
Unidirectional Energy Out	W.h	1331.13	2311.97
Motor			
Unidirectional Energy In	W.h	1251.07	2267.29
Unidirectional Energy Out	W.h	996.81	1854.32
Torque Coupling			
Unidirectional Energy In	W.h	996.81	1854.32
Unidirectional Energy Out	W.h	930.82	1787.75
Final Drive			

Table 33.Continued

Name	Unit	leaf_udds_cycle	leaf_hwfet_cycle
Unidirectional Energy In	W.h	930.82	1787.75
Unidirectional Energy Out	W.h	865.74	1722.86
Wheel			
Unidirectional Energy In	W.h	865.74	1722.86
Unidirectional Energy Out	W.h	254.99	830.87
Chassis			
Unidirectional Energy In	W.h	254.99	830.87
Unidirectional Energy Out	W.h	-0.36	-0.07
Power Converter			
Unidirectional Energy In	W.h	80.06	44.68
Unidirectional Energy Out	W.h	76.06	42.44
Electrical Accessory			
Unidirectional Energy In	W.h	76.06	42.44
Unidirectional Energy Out	W.h	0	0

CONCLUSION AND FUTURE STUDIES

RCCI was demonstrated on a multi-cylinder engine with diesel-like BTE or higher with reductions in NO_x and soot. The robustness of the RCCI strategy was demonstrated over a wide speed and load range. The ability of RCCI to be mapped allowed RCCI engine maps to be integrated with a CDC engine map for a multi-mode strategy that was implemented in vehicle systems simulations to model fuel economy potential of the multi-mode concept as compared to a PFI gasoline and CDC baseline on the same base vehicle platform. The modeled drive cycle results allowed for a WTW analysis to estimate WTW energy and GHG emissions with the RCCI multi-mode strategy.

Multi-mode operation was shown through vehicle system simulations using experimental engine data to have the potential to offer greater than 15% fuel economy improvement over a 2009 gasoline PFI baseline over many light-duty driving cycles. RCCI fuel economy improvements were observed despite lack of complete drive cycle coverage. The results showed how much of an effect multi-mode operation can have on engine-out NO_x emissions depending on the amount of the drive cycle coverage that RCCI operation can allow. Modeled drive cycle emissions results showed between 17 and 21% reduction in NO_x with multi-mode RCCI compared with diesel-only operation. If an engine has to switch to CDC operation during high engine loads, the engine out NO_x will be very high and quickly can degrade the NO_x reduction potential of a multi-mode RCCI strategy.

RCCI fuel economy improvements were demonstrated despite lack of complete drive cycle coverage. The use of E30 for the low-reactivity fuel shifted the drive cycle coverage to a higher load. Increasing the RCCI drive cycle coverage is possible and being investigated through changes in engine hardware and fuel choices. The high HC and CO shown in the simulations along with the decreased exhaust temperature will pose a challenge for meeting federal emissions regulations and may require a modification the low load operating strategy or advancements in catalysts. Limitations of the study include the use of a multi-mode operating map that switched between piston types; a follow up study is planned to create a multi-mode RCCI operating map using only the RCCI modified pistons. Other limitations included the lack of transient engine efficiency and emissions validation.

The WTW analysis of an RCCI enabled vehicle demonstrated significant petroleum and GHG reductions. The unique properties of renewable fuels not only allowed to better cover the drive-cycle in RCCI mode but made a difference in WTW GHG emissions.

There are further improvement possible as the RCCI concept is further refined and optimized for drive-cycle concerns and should be able to offer further reductions in petroleum and GHG emissions on not only conventional vehicles but hybrid vehicle powertrains. The analysis presented here does not address potential hybrid vehicle integration, however initial simulations results with a RCCI/CDC multimode engine in a series hybrid configuration show the potential for even further improvements in fuel economy.

VITA

Scott received his B.S. in mechanical engineering in 2007 and his M.S. in mechanical engineering in 2009 from the University of Tennessee. While attending graduate school for his M.S. degree, he was awarded a DOE Graduate Automotive Education Fellow (GATE) award to pursue automotive related research. He was the team leader for a DOE hybrid design competition (Challenge X) as well as the team lead for a biodiesel production pilot plant on the UT campus (UT Biodiesel Pilot Plant). Scott is now pursuing his PhD degree at the UT with multidisciplinary aspects from the mechanical engineering and environmental engineering departments at UT and in collaboration with ORNL researchers. His PhD focus area is related to life-cycle analysis of advanced energy technologies. This topic is considerably different than his on-going research at ORNL, further demonstrating his breadth and depth of interests and expertise.

Scott joined Oak Ridge National Laboratory (ORNL) as a post-master research fellow in 2009 following an internship in the Fuels, Engines and Emissions Research Center (FEERC). He became a member of the ORNL Research and Development staff in early 2012. Scott has been a critical team member and/or lead for meeting numerous Department of Energy (DOE) high-level milestones. As a research fellow, he supported a critical milestone to demonstrate 45% brake thermal efficiency on a light-duty passenger engine and received an ORNL significant event award for his contributions. He is now the Principal Investigator (PI) for two advanced combustion engine programs where he leads a research team and has responsibility for several high-level DOE milestones as mentioned earlier. This research is focused on transitioning fundamental progress in RCCI combustion to near-production multi-cylinder engine hardware and controls to demonstrate the potential of this approach on impacting real-world fuel economy and emissions. This is an important area of research for the DOE Vehicle Technologies Program and directly supports the DOE mission of reducing the nation's dependence on foreign oil. Scott is also active in supporting the ORNL Sustainable Campus Initiative, research on combined heat and power, and a sought after expert in bio-fuel production and end-use opportunities and challenges. This research has led to more than 4 archived journal, 20 conference publications, and many invited presentations on the topics of high efficiency combustion, combined heat and power, and bio-fuel opportunities. Besides being active in ASME technical conferences as a session co-organizer and associate member of the Internal Combustion Engine Division, he is also an active participant in SAE International as a super-session organizer and a member of the combustion committee. Scott is also an active participant in other technical conferences such as the National Biodiesel Board (NBB) Biodiesel Conference, the NBB Biodiesel Technical meeting and the DOE Directions in Engine-Efficiency and Emissions Research meeting, International Energy

Agency's combustion task leaders meeting. He also has active participation in invitation only government-industry meetings supporting USDRIVE and DOE interests including being a member of VSATT team. Scott is a member of the American Association for the Advancement of Science (AAS). Scott is a registered Engineer-in-Training in the state of Tennessee.

Scott maintains a zero-cost staff appointment with the Mechanical, Aerospace and Biomedical Engineering department and serves as the EcoCAR 2 team Outreach Advisor strictly on a voluntary basis. Under this role, Scott mentors students, provides training and instruction on successful public outreach and K-12 Science, Technology, Engineering and Mathematics (STEM) recruiting. Over the past three years, Scott has supervised three different Communication Managers which were funded by the competition to manage the hybrid vehicle design team's public outreach and STEM program. During this time some of the outreach program highlights include the publication of a peer-reviewed conference paper in the American Society of Mechanical Engineers Congress detailing the outreach and STEM Activities during Year 2 of the competition, dozens of outreach event in East Tennessee and success getting media coverage for the team. The teams involvement in outreach events over the past three years helps highlight the high quality of student projects that the University of Tennessee is known for. Scott has been able to leverage outreach resources not only with the University of Tennessee but those of Oak Ridge National Laboratory (ORNL) and the local Department of Energy Clean Cities program. To help prepare for the future of hybrid vehicle design competitions at the University of Tennessee, he assisted in obtaining support from the College of Communications and Information to have a faculty member committed to be on the EcoCAR 3 proposal and contributed to the proposal.

Scott has remained dedicated to K-12 STEM recruiting since being involved in the Challenge X hybrid design competition at UTK and serving as coordinator of the UT Biodiesel pilot biodiesel production plant. Scott continues to work with ORNL, UT, Oak Ridge Associated Universities, the Oak Ridge Institute for Science Education and the regional DOE Clean Cities organizations to get younger students excited about the science of alternative fuels, hybrid vehicles and engine efficiency. Scott has been a long time participant with the local DOE Clean Cities organization (ET Clean Fuels) going to public outreach events to help East Tennesseans understand the benefits and challenges of alternative fuels. Scott is a committee member of the annual Run for Clean Air; a 5K run/walk that serves to educate the community and showcase alternative fuel vehicles. All of which have enabled him to leverage successful outreach partnerships for the UTK EcoCAR team.